Real scale simulation of ballistic test for soft armor

by

Mario Michael Dippolito

B.S., Kansas State University, 2000
M.S., Kansas State University, 2011

AN ABSTRACT OF A DISSERTATION

submitted in partial fulfillment of the requirements for the degree

DOCTOR OF PHILOSOPHY

Department of Mechanical and Nuclear Engineering
College of Engineering

KANSAS STATE UNIVERSITY
Manhattan, Kansas

2017

Abstract

The strength of the fabric system is based on fiber strength and fabric mechanics. Modeling a fabric system accurately requires research into fiber behavior within the yarn and yarn behavior within the fabric. Limited computer resources require new approaches to yarn modeling and fabric modeling especially in regards to ballistic impact. The fabric is discontinuous. There are many factors which require modeling the physics in order to accurately simulate and design fabric systems.

Weaving yarns into fabrics can introduce fiber level damages such as surface defects and crimps through sliding friction and bending and thus add variance to the tensile strength of the fibered yarn. A Weibull distribution is an often used method to develop a statistical model and is developed to calculate the strength of the yarn. It is necessary to carefully remove the fibers from the as woven fabric and use a standard ASTM single fiber tensile test to create a Weibull distribution of tensile strength.

In general in Kevlar systems the edge radius for laboratory projectiles is much larger than the actual dimeter of the fiber; however, the yarn itself can be sheared, and this fibered yarn system requires modeling. There is no direct measurement of Kevlar fiber shear strength, so combined tensile-twist test data is used to develop equations to determined shear strength.

DFMA is modeling software developed to create digital fabrics in a method that accurately models yarn shape with limited computer resources using a concept of a digital fiber. The digital fiber represents multiple real fibers, so it is necessary to use the digital yarn effective bending rigidity developed with numerical simulation of experimental results. Since the yarn is composed of hundreds to thousands of fibers, the physical yarn cannot be modeled in full scale fabrics.

The yarn composed of digital fibers is structurally similar to real yarns and is capable of representing the real fabric mechanics. In the process of impact, within the relatively short time frame, the distribution of stress is mostly in principal yarns at a time when the event is considered complete through penetration or projectile rebound. The hybrid mesh method represents the small number of principal yarns with high density mesh and the rest of the fabric (the non-principal yarns) with coarse mesh. With hybrid mesh, the full scale simulation of actual fabrics is possible.

The projectile geometry for real threats is variant depending on the types of projectiles in use (projectiles for maximum energy transfer to the target or projectiles for high shear). The laboratory projectiles are therefore variant in order to represent threats. In this research the RCC is the threat and two standard weights are modeled with local geometry. The local laboratory projectile geometry is controlled however it is bounded by a tolerance much larger than the Kevlar fibers studied here. It does act against the fibered yarn which will shear mechanically dependent on fiber to fiber interactions and possibly fiber shear strength.

Real scale simulation of ballistic test for soft armor

by

Mario Michael Dippolito

B.S., Kansas State University, 2000
M.S., Kansas State University, 2011

A DISSERTATION

submitted in partial fulfillment of the requirements for the degree

DOCTOR OF PHILOSOPHY

Department of Mechanical and Nuclear Engineering
College of Engineering

KANSAS STATE UNIVERSITY
Manhattan, Kansas

2017

Approved by:

Major Professor
Youqi Wang

Copyright

Abstract

The strength of the fabric system is based on fiber strength and fabric mechanics. Modeling a fabric system accurately requires research into fiber behavior within the yarn and yarn behavior within the fabric. Limited computer resources require new approaches to yarn modeling and fabric modeling especially in regards to ballistic impact. The fabric is discontinuous. There are many factors which require modeling the physics in order to accurately simulate and design fabric systems.

Weaving yarns into fabrics can introduce fiber level damages such as surface defects and crimps through sliding friction and bending and thus add variance to the tensile strength of the fibered yarn. A Weibull distribution is an often used method to develop a statistical model and is developed to calculate the strength of the yarn. It is necessary to carefully remove the fibers from the as woven fabric and use a standard ASTM single fiber tensile test to create a Weibull distribution of tensile strength.

In general in Kevlar systems the edge radius for laboratory projectiles is much larger than the actual dimeter of the fiber; however, the yarn itself can be sheared, and this fibered yarn system requires modeling. There is no direct measurement of Kevlar fiber shear strength, so combined tensile-twist test data is used to develop equations to determined shear strength.

DFMA is modeling software developed to create digital fabrics in a method that accurately models yarn shape with limited computer resources using a concept of a digital fiber. The digital fiber represents multiple real fibers, so it is necessary to use the digital yarn effective bending rigidity developed with numerical simulation of experimental results. Since the yarn is composed of hundreds to thousands of fibers, the physical yarn cannot be modeled in full scale fabrics.

The yarn composed of digital fibers is structurally similar to real yarns and is capable of representing the real fabric mechanics. In the process of impact, within the relatively short time frame, the distribution of stress is mostly in principal yarns at a time when the event is considered complete through penetration or projectile rebound. The hybrid mesh method represents the small number of principal yarns with high density mesh and the rest of the fabric (the non-principal yarns) with coarse mesh. With hybrid mesh, the full scale simulation of actual fabrics is possible.

The projectile geometry for real threats is variant depending on the types of projectiles in use (projectiles for maximum energy transfer to the target or projectiles for high shear). The laboratory projectiles are therefore variant in order to represent threats. In this research the RCC is the threat and two standard weights are modeled with local geometry. The local laboratory projectile geometry is controlled however it is bounded by a tolerance much larger than the Kevlar fibers studied here. It does act against the fibered yarn which will shear mechanically dependent on fiber to fiber interactions and possibly fiber shear strength.

Table of Contents

List of Figures x
List of Tables xiii
Acknowledgements xiv
Dedication xv
Chapter 1 - Introduction 1
Chapter 2 - Review of impact loading and model scaling 10
2.1 Yarn level micro-mechanics model 11
2.1.1 Yarn properties 11
2.1.2 Single yarn tests 13
2.1.3 Numerical simulation 17
2.2 Yarn micro-dynamics 22
2.2.1 Fiber to fiber interactions 23
2.2.2 Yarn impact observations 23
2.2.3 Effect of shear strain on fiber tensile strength 25
2.2.4 Fiber level model 26
2.2.4.1 Fiber level fabrics ballistics impact simulation 29
2.3 Model sizing importance and effects 30
2.4 Multi-layered fabric 32
2.4.1 Geometry effects in low areal density layered fabric 35
2.4.2 Other modeling approaches 38
2.4.3 Remarks 42
Chapter 3 - Numerical simulation of full scale ballistics 44
3.1 DFMA fabric modeling 44
3.1.1 Weibull distributed damage related to gage length 47
3.1.2 Shear added to the fabric modeling process 51
3.1.3 Failure criteria of fiber 53
3.1.3.1 Modeling projectile radius of curvature 57
3.1.3.2 Effect of shear strength on V_{50} 66
3.1.3.3 Fiber coefficient of friction and moment of inertia 68

3.2 DEA ballistic testing 70
Chapter 4 - Hybrid mesh development 72
4.1 Area based mesh 76
4.2 Yarn based mesh 79
4.2.1 Yarn based numerical simulations 81
4.2.1.1 Part 1: Comparison group 1 82
4.2.1.2 Part 1: Comparison group 2 86
4.2.1.3 Part 1: Comparison group 3 88
4.2.1.4 Part 2: Comparison group 1 - 7 91
4.3 Summary 94
Chapter 5 - Numerical simulation 95
Chapter 6 - Numerical results 102
6.1 Numerical and experimental 4 grain projectile impact 102
6.2 Numerical and experimental 16 grain projectile impact 108
6.3 Conclusion 111
References 114

List of Figures

Figure 1-1: Digital fabric elements 5
Figure 2-1: Wave propagation in transversely impacted fiber [9]. 14
Figure 2-2: Air drag effect on polyester yarn [10]. 15
Figure 2-3: High speed impact against Dyneema yarn [12]. 17
Figure 2-4: The schematic of numerical approach for fabric impact [14]. 18
Figure 2-5: Improved yarn model [20]. 19
Figure 2-6: Yarn level FE model [22] 20
Figure 2-7: Song and Lu early impact compression of yarn [29]. 23
Figure 2-8: Twist effect on strength [29]. 24
Figure 2-9: Shear-tension model [30] 25
Figure 2-10: Fiber before and after yarn discretization [34] 28
Figure 2-11: Base numerical modeling for layered system [1] 34
Figure 2-12: Projectiles used in the laboratory testing. 35
Figure 2-13: Sharp nosed projectile FE simulation details [36] 36
Figure 2-14: Ballistic limit for 12x12-14 vs ply [37]. 38
Figure 2-15: Zohdi and Powell sub yarn model [38] 39
Figure 2-16: FEM fiber level yarns [39] 40
Figure 2-17: Projected and actual energy absorption at full areal density [40]. 41
Figure 3-1: Digital fabric 44
Figure 3-2: RCC projectile 45
Figure 3-3: Length scales of KM2 fabric and local 64 Gr. RCC projectile geometry 46
Figure 3-4: Warp Weibull distribution for 10 mm and 25 mm 50
Figure 3-5: Fiber bending moment [34] 51
Figure 3-6: Saturated strength ratio at fiber failure. 55
Figure 3-7: Curve fit to static combined shear tensile test 57
Figure 3-8: The Leica Microsystem: scope and electronic control and interface [45]. 59
Figure 3-9: 4 grain projectile microscopic radius of curvature and radius profile. 60
Figure 3-10: 16 grain projectile microscopic radius of curvature and radius profile. 60
Figure 3-11: 64 grain projectile microscopic radius of curvature and radius profile 60

Figure 3-12: A single Kevlar 49 fiber on the edge of a 64 grain RCC projectile. 61
Figure 3-13: Experimental V_{50} compared to numerical simulation 63
Figure 3-14: Radius of curvature effects on V_{50} 65
Figure 3-15: RCC early impact analysis. 67
Figure 3-16: RCC early impact fiber failure under projectile. 68
Figure 4-1 Panel layer side veiw detail directly stacked. 74
Figure 4-2: Random staggered layered fabric. 74
Figure 4-3: Staggered fabric layers 75
Figure 4-4: Area detail of area based mesh [37]. 76
Figure 4-5 Area based mesh unit cell detail [37]. 77
Figure 4-6: Hybrid cells [37]. 79
Figure 4-7: Hybrid fabric assembly [37]. 80
Figure 4-8: Center portion of hybrid mesh with 3 different numbers of principal yarns [37] 83
Figure 4-9: Graphical results from Part1 Group 1 [37] 83
Figure 4-10: Local fabric geometry contrasted against projectile dimensions 84
Figure 4-11: V_{50} comparison of hybrid mesh and uniform mesh [37] 85
Figure 4-12: Graphical results for impact force [37] 86
Figure 4-13: V_{50} comparison of layered hybrid mesh and uniform mesh [37] 87
Figure 4-14: Small portion of the center of the standard sized hybrid mesh [37] 89
Figure 4-15: Impact force between fabric and projectile for standard single layer tests [37] 89
Figure 4-16: V_{50} comparison standard test hybrid mesh and uniform mesh [37] 90
Figure 4-17: V_{50} comparison standard layered test hybrid mesh and experimental [37] 92
Figure 4-18: V_{50} of layered fabric [37] 93
Figure 5-1: Digital and physical yarn cross-section 96
Figure 5-2: Friction related to moment of inertia 97
Figure 5-3: Single yarn test results 99
Figure 5-4: Close detail top and front view of the fabric 100
Figure 5-5: Effective digital fiber bending rigidity determination 101
Figure 6-1: 4 grain bullet over lay on single layer hybrid fabric 103
Figure 6-2: 4 grain projectile numerical vs experimental 104
Figure 6-3: Original 4 grain impact data compared to experimental results 107

Figure 6-4: 16 grain bullet over lay on single layer hybrid fabric 108
Figure 6-5: 16 grain projectile numerical vs experimental 109
Figure 6-6: Original 16 grain impact data compared to experimental results 110

List of Tables

Table 2-1: Twist-angle data [30]..... 25
Table 2-2: ARL-TR_6403 pre-twist data for Kevlar KM2 single fiber [30]..... 26
Table 2-3: Armor level and threat comparison [35] 33
Table 3-1: Warp strength distribution with gage length 48
Table 3-2: Weft strength distribution and with length..... 49
Table 3-3: Combined tensile shear strength ratio vs strain [30]..... 56
Table 3-4: Radius of curvature for various projectiles given in μm 61
Table 3-5: Fabric and projectile for DEA and physical ballistic simulation 63
Table 3-6: Variance table for above figure 64
Table 3-7: Radius of curvature effects on V_{50} 65
Table 3-8: Fabric and projectile for shear test 66
Table 3-9: List of V_{50} over a range of shear strength layers for the fabric and projectile. 67
Table 4-1: Area based mesh properties and projectile information..... 77
Table 4-2: Validation of hybrid mesh DEA ballistics 81
Table 4-3: DEA input data..... 82
Table 4-4: V_{50} data single layer uniform and hybrid comparison tests [37]..... 85
Table 4-5: V_{50} data multi-layer uniform and hybrid comparison tests [37] 88
Table 4-6: V_{50}: Standard test uniform and hybrid mesh comparison [37]..... 91
Table 4-7: V_{50} data for layered fabric [37] 93
Table 5-1: Single yarn cross-sectional shapes (internal research at KSU) 98
Table 5-2: Development of moment equation 101
Table 6-1: Modified DFMA 4 grain projectile impact data..... 103
Table 6-2: V_{50} of square bounded fabric..... 104
Table 6-3: Original DFMA 4 grain projectile impact data 106
Table 6-4: 16 grain impact data 109
Table 6-5: Original 16 grain impact data vs experimental 110

Acknowledgements

I am grateful to Dr Wang my major professor and academic advisor for her guidance in this research and for all that I have learned throughout my Ph.D studies.

I would like to also thank Dr. Chian-Fong Yen, Dr. William Hsu, Dr. Jack Xin and Dr. Anil Pahwa for serving on my supervisory committee.

This research work is made possible by funding from the U.S. Army Research Laboratory (ARL) and PEO-Soldier. I would like to thank Dr. Chian-Fong Yen from ARL and James Q Zheng from PEO-Soldier for their help and guidance in completing the projects for this thesis.

I would also like to thank the members of my team Dr. Ying Ma, Dr. Xiaoyan Yang and Dr. Habib Ahmadi for their helpful inputs to my research and career.

Dedication

To the men and women of the US armed forces

Chapter 1 - Introduction

The true to scale simulation is important to modeling in the design of ballistic fabrics since boundary clamp spacing effects changes in the ballistic strength for the same piece of fabric. Scaled modeling is inaccurate since fixed boundaries reflect stress waves back to impact site and free boundaries allow bulk fabric movement; both distort fabric failure dynamics thus preventing scaled modeling of full scale experimental results. Limited detail modeling such as yarn level modeling eliminates fiber interactions which limits generalized numerical modeling while homogeneous modeling additionally eliminates yarn to yarn interactions. It is impossible for real scale simulation of fabrics modeled down to the fiber level due to current computer resources which cannot model the true path of the many thousands of fibers at full scale. While in general the area near projectile impact is subject to compression and shear and while the far away areas are subject to in plane tension, shear is important to ballistic performance near the area of impact especially for sharp projectiles and lower number of fabric layers. The edge of the projectile varies in sharpness and shear must be calculated at the fiber level to account for energy loss differences by sharp and dull edges.

Real scale ballistic analysis of fabrics is mostly experimental. High speed camera observation enabled analytical model proofing even from early research. However early research and current research modeling is limited to high predictability in single fiber and single yarn tests and becomes for the most part intractable in fabric due to the complexity of ballistic fabric modeling. Fixed boundaries are necessary to hold the soft fabrics in place for ballistic testing; however they do not represent how the fabric will be used once it is in service. Boundary conditions will enhance the stress concentrations by reflecting the faster longitudinal and the slower transverse waves back to the impact site. In an individual yarn or fiber the

longitudinal waves will begin arriving back at the impact site after a time period of twice the length to the boundary divided by the root of the ratio of the bulk modulus to the density of the fabric. In fabrics however this effect is much more complicated as lesser reflections will travel out from both sides of a yarn crossing. Due to the very large number of yarn crossings and for that matter parallel yarns absorbing energy the problem becomes much more complicated.

The term V_{50} is terminology used to describe a statistical speed of projectile which has a 50 percent chance to defeat the fabric. The experimental V_{50} stabilizes as the dimensions approach 12x12 inches. When the penetration of the bullet occurs simultaneously with the arrival of the longitudinal wave back to the impact site, the reflected stress does not change the ballistic performance.

Cepuš and Poursartip found that these two equations describe the rebound time for the longitudinal wave in a particular weave of fabric:

$$t_{rebound} = \frac{2L}{C_{weave}} \tag{1.1}$$

$$C_{weave} = \sqrt{\frac{E_{fiber}}{\alpha\rho}} = \frac{C_{fiber}}{\sqrt{\alpha}} \tag{1.2}$$

where C_{weave} is the fabric panel strain wave velocity and L is the distance from the impact point to the boundary and where E_{fibre}, ρ and C_{fibre} are the fiber elastic modulus, mass density and longitudinal wave speed, respectively, and α>1 is a single parameter that encompasses the weave effect [1]. For the particular weave of Kevlar the value of α is not given here, however if it is greater than unity it reduces the speed of the wave within the fabric and therefore increases

rebound time. Behind these reflected waves is a tensile strain that is double that of the original longitudinal wave [2]. It is almost unavoidable that these reflected waves will superpose upon the stress wave at the impact site causing an artificial higher stress and therefore early fiber failure. If the boundaries are spaced far enough, the bullet will pass through the fabric before the time required for the waves to return, and the correct strength of the fabric will show in the test results. Standard sizes of ballistic tests are given by military and National Institute of Justice (NIJ) which are usually around 12”x12”. This requirement for correct sizing has its challenges when modeling yarns at the micro-level and attempting to simulate numerically; the main challenge is computer resources.

Comprehensive experimental testing would be required to design fabrics so researchers made attempts to better the design process using material parameters and fabric mechanics. Research into fabrics has led to analytical modeling and many limited detail numerical modeling techniques in attempts to predict the mechanics of the real scale model to overcome computer resource limitations. In the analytical modeling the generalized assumption that the fabric will conically deform after impact is used to determine equations for the mechanics of the fabric using parameters such as fiber material properties, projectile shape, projectile speed, and energy absorption of the fabric. Finite Element Method (FEM) modeling of fabrics at yarn level is much more difficult than modeling continuous material. The relative size differences of the parts and variable shapes of yarn cross-section prohibit modeling efficiency and ballistic modeling accuracy. FEM Fiber level modeling is impossible even for scaled modeling. These particular methods would hamper any creative computer design and simulation without having first created a physical fabric and analyzed this fabric to determine its yarn shape as it traces through the unit cell. A far more complex problem is the dynamic shape of the yarn at the impact site during the

course of a ballistic event; which as one can surmise, is completely neglected by modeling a solid yarn with a fixed albeit it variable cross-section. The changes in shape and inter yarn to yarn and fiber to fiber friction would not be modeled, and it would be unknown if this has an effect on the output data from the simulation.

A bullet which does not have a spherical nose such as Fragment Simulating Projectile (FSP) and Right Circular Cylinder (RCC) need special considerations for simulating numerically. The edge where the side wall meets the face will have variable sharpness as both edges will meet with a radius of curvature. This needs to be considered numerically in shear calculations of the edge of the bullet against the fiber. The shearing process between sharp and more rounded edges would be different with the more rounded edge absorbing more energy from the projectile. In experimental tests the bullet must impact perpendicular for the data to be accepted so it is not necessary to consider angle of impact unless it is part of the testing.

The digital element approach (DEA) for modeling ballistic impact at the fiber level is developed by Wang and Miao [3] established in 2009. The numerical tool digital fabric mechanics analyzer DFMA was introduced by Huang and Wang [4] in 2009 to model the relaxation process to create a digital fabric. The numerical fabric created by this process models the yarn at the fiber level. The fibers are made up of same length digital rod elements connected by frictionless pins and as the length of the rod elements approach zero the fiber becomes fully flexible. The fiber strength, friction, fiber to fiber contact and yarn to yarn interactions can be modeled. Figure 1-1 shows the elements of the digital fabric and the final fabric assembly created with these elements.

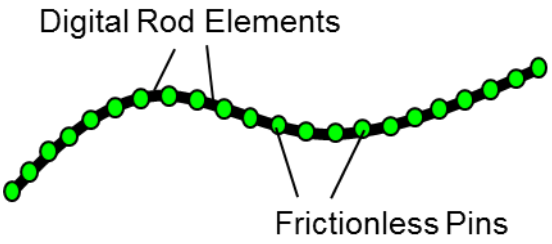

Fig (1-a)

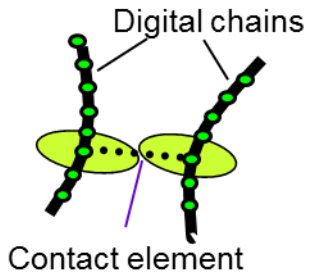

Fig(1-b)

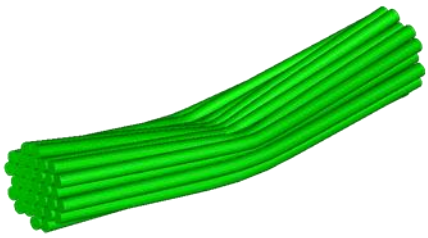

Fig(1-c): Digital yarn

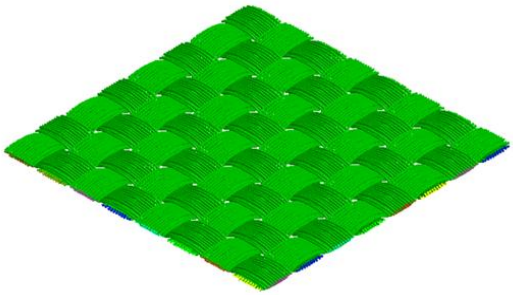

Fig(1-d): Digital fabric

Figure 1-1: Digital fabric elements

In the previous simulations of fabric modeled with the digital element method (DEM) the fiber is considered fully flexible which eliminates shear stress development. One of the ways the fabric absorbs energy is through fiber failure. Without shear the digital fiber will fail in tension only. Physical observations of spherical projectile impact show a dominate mode of fiber failure from tension while observations of the RCC shows failure through shear of the upper layers of the fabric. When Cheng and Chen studied the mechanical properties of a single Kevlar KM2 fiber they discovered that it is linear elastic in the transverse direction and non-liner elasto-plastic in the transverse direction [5] and they also developed the stress strain curve for its behavior under transverse compression [6]. Using this information Wang and Miao developed an elasto-plastic model of compression deformation to account for fabric energy absorption in ballistic analysis of

digital fabrics. They noticed divergence in the fabric displacement during the rebound process where projectile residual velocities and rebound velocities were higher than experimental. With elasto-plastic modeling the agreement of residual and rebound velocities was closer however there was still discrepancies requiring further investigation in to energy loss, fiber stress distribution and penetration resistance through the effects of fiber transverse properties. When moment is added to the pin joints then shear calculations can be introduced to the model. The introduction of the moment of inertia to the calculations requires the development of a tension shear modeling of digital fibers.

DFMA fabrics have been developed and DEA has been verified against experimental results for small scale models and single panel full scale models. Full scale is not possible at high mesh density required for accuracy so hybrid mesh is required. Principal yarns bear nearly all of the impact loading while in contact with the bullet (the longitudinal wave through these yarns distributes the stress toward the boundary and equilibrium forces pull the fibers towards the center of impact to balance this stress). It is important that these yarns must be modeled with enough fineness (fiber count) that they capture shape changes from the displacement cross-sectional area (relative fiber movement) and capture the outward stress development. The non-principal yarns are acted upon by the sliding friction of the principal yarns and the eventually by the longitudinal wave which for most of the yarns in the fabric arrives after the event is considered complete. The required number of principal yarns in orthogonal weave is constant as the fabric dimensions increase thereby effectively solving the limitations computer resources allowing the modeling of full scale fabrics. To develop the hybrid mesh the two different configurations will be explored to determine if they adequately model the ballistic impact. Area

mesh will use fine mesh in the impact area similar to FEM modeling and principal yarn mesh will use fine mesh principal yarns and both methods will use coarse mesh in the far field fabric.

With the development of the hybrid fabric to solve full model simulation, the next step is the development of the combined tensile-shear stress model and detailed projectile edge geometry to activate the proper shear stress the geometry would cause in the fibers. Then the final step would be to perform real scale simulation detailed by NIJ and US military (standard test) and compare these numerical results to the standard experimental tests using hybrid fabrics.

The objective of this research is to simulate the actual physics of true to scale ballistic fabrics undergoing ballistic impact. It is impossible to do accurate real scale simulation of the entire model due to 1) computer resources, 2) numerical accuracy of the scaled model and limited detail model and 3) the interaction of the local geometry of the projectile against the fibers. The outline for this proposal is

1. Review of soft ballistic panel scaling modeling methods and ballistic loading
    i. Small scale modeling techniques proposed by researchers to model real scale ballistic impact are discussed in detail. Full scale modeling overview is presented showing the various methods of working with limited computer resources while attempting to model standard test fabric for accurate results. Inter-panel friction and non-linear strength enhancement of layering on the ballistic protection system will be discussed.
    ii. A small percentage of the yarns in the fabric bear almost all of the ballistic loading while the rest of the yarns see very little. This concept of principal (load bearing) yarns is a key in the development of variable mesh density fabric in this research.

2. Development of combined tension-shear model

   The moment of inertia correction can be effected by the coefficient of friction for a coarse meshed yarn. If a bundle of fibers are modeled as a single yarn the moment of inertia needs to be redesigned to simulate the fiber bundle in bending. The moment of inertia is based on the coefficient of friction so that a generalized pseudo moment can be calculated to model shear induced during impact for a coarse mesh.

3. Incorporate the details of the local projectile geometry into shear calculations

   For proper consideration DEA is modified with calculations added for shear stress. Then the geometry of the bullet is observed under a microscope and along with the manufacture data on the projectile this is used to model local projectile geometry in DEA. Modeled local projectile geometry now produces a shear stress in the fibers and contributes to fabric energy absorption from the projectile. Due to its small size the radius of curvature is given a tolerance by the manufacture. This tolerance is large enough to cause large variations in ballistic performance of fabrics. Variations in the radius of curvature will be explored to generate data as to how the variations in radius of curvature affect the V_{50}. These measurements will be used in to model variance in ballistic performance and this will be modeled in DEA.

4. Develop the hybrid mesh approach

   In FEM analysis the approach is to use high density mesh in high stress areas and low density mesh in low stress areas to accomplish the goal to reduce model size and enable efficient numerical calculation while retaining acceptable accuracy. In the digital element method (DEM) the fiber level modeling requires an approach with the goal of retaining accuracy with a reduced model size in order to model standard experimental

tests. In the first approach which is similar to FEM, the impact area is modeled with fine mesh (more fibers per yarn) and coarse mesh in the area away from impact. In the second approach which is more unique to fabric mechanics, the primary yarns (yarns intersecting the impact area) are fine meshed and the secondary yarns are coarse meshed. It was known in early experimental research of ballistic fabrics that principal yarns bear almost 100% of the loading. In earlier research with elastic full field mesh modeling using DEM, 19 fibers per yarn were shown to capture fabric displacement, energy loss in the projectile and V_{50} with high accuracy. In both approaches the fine mesh would be at this fiber density and the coarse mesh which is the majority of yarns (around 98% of the yarns for full scale fabrics) would be meshed at two-four fibers per yarn. Preliminary tests show that the area mesh is not able to capture stress wave development in the yarns due to yarn discontinuity so the yarn based mesh is adopted. The yarn based hybrid mesh numerical results are validated against full field mesh results and the results of this validation are presented.

5. Numerical simulation of real scale standard tests

Standard test multiple layer sub yarn modeling is made possible with hybrid fabrics and compared to experimental results. The deviations in the results generated from RCC projectiles will be examined and compared to the modified tension-shear model for standard tests.

Chapter 2 - Review of impact loading and model scaling

The dimensions for standard test fabric for ballistic tests allow enough time for a complete penetration of the fabric by projectile before reflected stress waves arrive back to the impact site so the relationship of material properties, velocity and projectile geometry to fabric impact strength can be studied. Testing small scale fabrics experimentally and modeling them numerically is complicated by unknown stress wave reflection variations influenced by factors such as fabric slip and clamp behavior. Fabrics are complex with a multi-scale nature with a base fiber unit a few microns in diameter, the yarn in millimeters and the fabric in centimeters, all of which presents challenges to engineering design. Impact experiments involving a single yarn are simulated analytically with a high degree of predictability and this enables study into the mechanical behavior. Fiber is studied using various novel methods to determine both longitudinal and transverse material properties with a high degree of accuracy. Additional studies into fiber statistical strength from spool and from woven fabric were also studied. The individual behavior of fibers and yarns are compounded with friction effects when they are part of a fabric and the weaving sets them into various shapes which also influences the strength of the fabric. Accurate numerical modeling of the physics of fabrics in ballistic simulations must be based on fiber material properties, fiber level interaction and yarn level interaction based on weave, projectile geometry and boundary conditions. Early on, computer resource constraints prevented fiber level modeling so yarn level or fabric level model were used to simulate fabric impact experiments using the numerical models developed from individual fiber and yarn experiments and assumptions for friction and weave. After advances in computer resources a limited fiber level approach with coarse mesh density was developed for small scale modeling. This requires building detailed geometry down to the fiber level which was still impossible to do

at full dimensioned fabric with the computer resources. When using fiber level modeling, the approach was to model a specimen as large as practical for computing purposes surrounding the area of impact and containing enough mesh density to capture the physics of the impact event. To begin the discussion it is important that the approach first attempt to understand the yarn dynamic behavior and even more specifically the single fiber behavior under ballistic loading then review the assumptions and methods used to model fabric yarn scale and then fabric scale and finally fiber level scale.

2.1 Yarn level micro-mechanics model

It is difficult to capture fiber level impact since it is on the micron scale. Yarn impact has been studied early on to develop behavior characteristics and physical properties for use in fabric modeling. The fiber interactions make the yarn behavior complex so research continues to develop newer models and yarn behavior is unique when it is part of a fabric so this continues to be a research topic. Physical impact studies are still modeled at the yarn level because of computer limitations and earlier yarn level models still have relevance in yarn level mechanics.

2.1.1 Yarn properties

A yarn is a bundle of fibers with a denier number and tenacity with fiber counts in hundreds up to 10,000. Yang assembled a comprehensive study of Kevlar (aramid) fibers [7] and his book details the chemical and physical properties, structure and morphology of fibers, fabrics and Kevlar products. The denier number of a yarn is established as weight in grams per 9000 m as defined by Industrial Fabrics Association International and another notation is Tex which is g/km. In other yarn level research the breaking strength or tenacity of the yarn is force in grams to break the yarn normalized with respect to the denier as g/denier [8].

Assembling a yarn from twisted fiber often happens however efforts are made to keep this to the minimum since it will influence the yarn tenacity. As a general rule the twist should be derogatory to overall yarn strength since it introduces shear. The works of different researchers are presented below. Fibers twisted about the yarn axis have been claimed to modify the fiber properties as there is a variation with overall strength with rate of twist. This is also discussed below.

The discontinuous nature of a fabric and the small area of impact allow specific yarn loading during high velocity impact. In an impact the principal yarns are the intersecting yarns under the projectile and also those very near to the impact interacting with the projectile through friction. The principal yarns bear the load and usually break if projectile penetration occurs while the other yarns in the fabric are not severely loaded and do not break. An additional yarn terminology for non-principal yarn is orthogonal yarn which intersects the principal yarn. The orthogonal yarn is pulled by the principal yarn at the intersection making it undergo deformation and experience strain like the principal yarn and in plane bowing motion towards the center. The transvers wave naturally pulls the orthogonal yarn transversely as well. This motion is transferred to the other yarns in the fabric through each crossover.

The stress wave in a yarn moves at the speed of sound of the material through the yarn along the longitudinal axis of the fiber. As an example, KM2 yarns are low density and therefore a high sound speed. This helps disperse energy away from the impact site increasing the ballistic strength of the yarn and fabric system. Studies into yarn density (controlled by denier number) have been made and layered systems have been tested to determine how density effects a layered system.

The friction between yarns in a fabric is accurately modeled by developing a model that generates the correct cross-sectional shapes and relaxation state for the yarn of a fabric with a certain weave pattern. The yarn cross-sectional shape cannot be easily determined unless the yarn is modeled as a digital element model composed of fibers and allowed to relax into its correct shape from forces within the fabric itself. Yarn modeled down to the fiber level will be discussed in the next section. Orthogonal yarns touch the principal yarns and through friction at their contact points along their cross-section perimeter forces are transferred through to the rest of the non-principal yarns.

An important shape that will affect the ballistic event is the crimp or undulations of the yarn as it is traced through the fabric. The yarn must first stretch axially enough that the stress in the yarn exceeds its maximum strength before it will break. The undulations allow the projectile to pull the yarn through the fabric stretching the yarn until it is straight, a process that allows energy dissipation through friction and stretching. In light ballistic protection systems the transverse fabric movement allowed through yarn straightening would absorb much less projectile energy than the actual tensioning of the fibers.

2.1.2 Single yarn tests

In earlier research in the 1970s David Roylance presents the point that the phenomena of wave reflections at boundaries, longitudinal and transverse wave interactions, unloading wave interactions along with cross over yarn interactions would make the problem of analyzing the fabric of the yarn analytically intractable. However, he adds to this discussion that "any understanding of the textile structure ballistics must be [preceded] by an understanding of single fiber response" [9]. The figure below describes the dynamics of the transversely impacted stand-alone fiber. This figure describes a rate independent fiber originally straight in the horizontal

direction prior to impact. The variable w is the speed of the material flow in the direction of impact brought about by the longitudinal wave and its speed is measured in reference to a Lagrangian coordinate system from a perspective point of the unstrained fiber. The variable Ut with an over bar represents the outward speed of the transverse wave measured with reference to fixed laboratory coordinate system. At the head of the longitudinal wave front the material is stress free; when it reaches a fixed boundary the material movement w caused by the longitudinal wave is restricted which forces a doubling of the stress in the reflected longitudinal stress wave. Since the material has momentum and is already under strain it continues to move behind the longitudinal stress wave towards the impact point when the stress wave reaches the boundary. The material now is double stretched by the reflected stress wave which is also traveling towards the impact point. In a free boundary configuration the material speed w is doubled and the stress vanishes at the unrestrained end as this stress reaches the boundary.

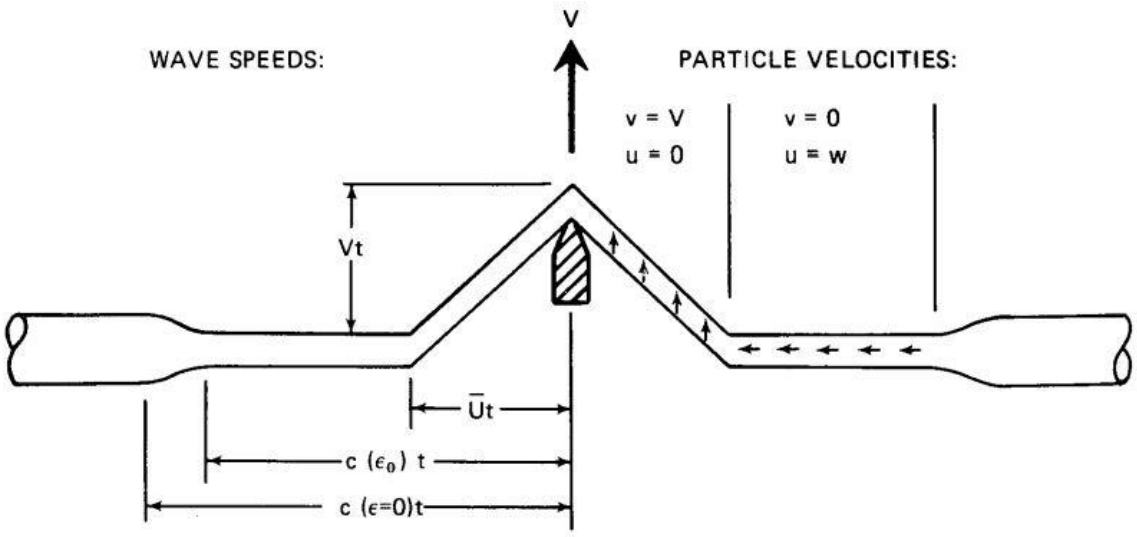

Figure 2-1: Wave propagation in transversely impacted fiber [9].

This figure is backed up by pervious research completed with high speed camera system. J. C. Smith et al. [10] were determined to explore the physical effects of the surrounding air on the

fabric material. They started with a yarn held straight and perpendicular to a projectile. They recorded the ballistic event with a series of photographs through the course of the bullet impact against the single yarn shown in Figure 2-2. This is however an experiment with a yarn rather than fiber. It is still not a practice today to use a single fiber in these tests since they are too small in diameter to get anything useful for observation when impacted with an actual projectile. Single fiber observations can however be completed with a Hopkinson bar impact against a yarn and close up high speed imagery produced for very early impact to observe individual fiber behavior. This will be discussed later in this chapter for the transverse compression effects on yarn.

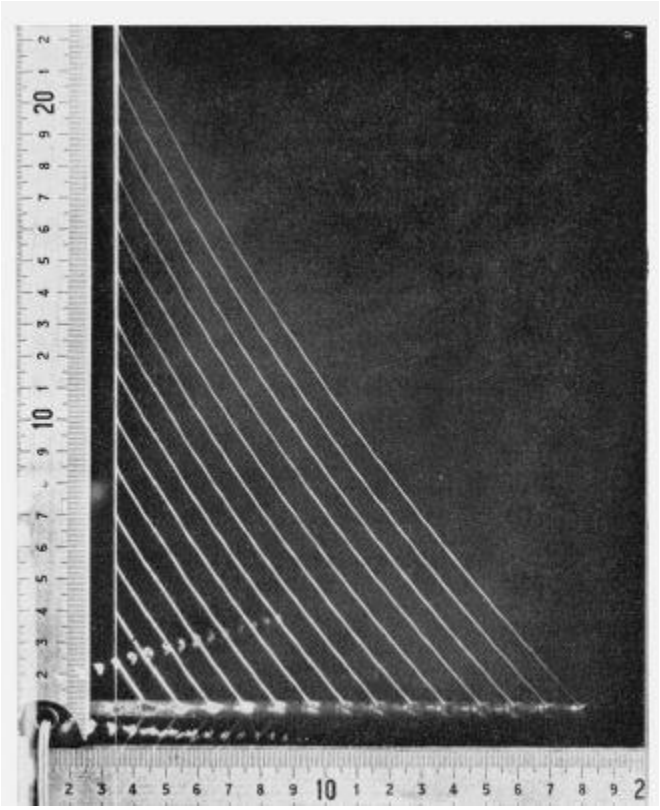

Figure 2-2: Air drag effect on polyester yarn [10].

Figure 2-2 is a set of composite images showing a yarn struck and pulled by a high velocity projectile over time. This clearly shows the details of the development of the longitudinal wave

over this time period. Although the figure was supposed to be observed for its air drag effect or lack of significance of air drag we are interested in the profile over time and how it shows the particular motion of the yarn transition from longitudinal to transverse mode at the head of the transverse wave front. The interesting part of the wave is that it travels throughout its whole length in only the longitudinal direction at the speed of the projectile as schematically represented in Figure 2-1. Observations of the angle for each time frame show that the angle is constant; this shows that the yarn section within the transverse wave is behaving as a rod with one degree of motion (no rotation about its axis) at the speed of the projectile. Now this is true for sharp nosed projectiles. For round nosed bending is observed in this same test. For the sharp nose, this means that the particle speed completely stops in the longitudinal direction and changes to the transverse direction at the transverse wave front. As such the wave front can be considered a shock boundary. These tests form the basis for later models of a tension only yarn model under transverse fabric impact. It will be beneficial to revisit this later in this research to discuss how this information can be used to defend the concept of the fiber modeled as a collection of rod elements connected with frictionless pins as a useful and accurate approach to simulate a yarn fiber system to create a fabric model. This concept will be further useful to the research into a hybrid fabric model which is desired due to limited computer resources to calculate a ballistic event within full scale fabric system. More recent high speed camera research into this topic was completed by Chocron et al. with state of the art cameras and a new technique using nickel-chromium wires to measure fabric level interactions [11]. More visible curvature and bending of the material is observed near projectile impact in their high speed images shown in Figure 2-3. The material flow toward the center is clearly seen against the overlaid colored lines.

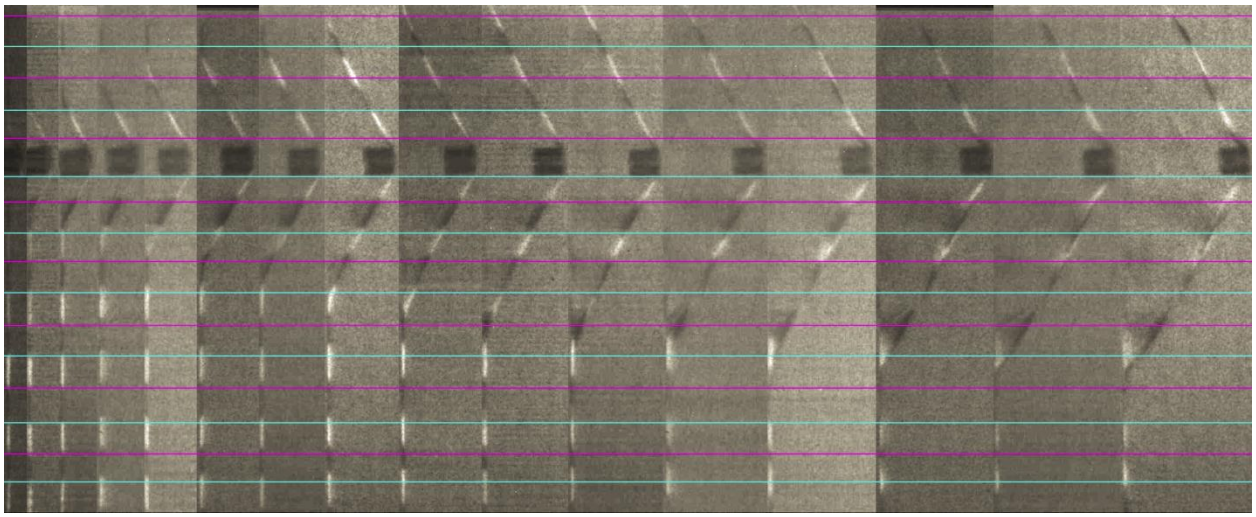

Figure 2-3: High speed impact against Dyneema yarn [12].

2.1.3 Numerical simulation

Throughout the history of development of the yarn level model the early contributors realized that the fiber level was elemental in numerically modeling a fabric and realized the intractability of the analytical problem as discussed above and discussed the necessity of fiber modeling to realize any high numerical accuracy. Roylance goal was a unified analytical and experimental model [13] and extended the work of other researchers into the first micro-mechanics model using pins joined at nodes to form a grid pattern to study viscoelastic fibre impact and impact on fabric panels [14]. This pin-joint model introduced the elemental model for capturing the physics of the fabric material at the yarn level. Keeping with the idea to unify experimental with his work, Roylance proofed his numerical model referencing much of Jack Smiths work at the National Bureau of Standards and Smiths use of high speed camera recording physical behavior of single yarn impact. A schematic of his numerical model given in Figure 2-4 is an assembly of pin jointed flexible yarn elements each with mass and is capable of capturing areal density of a fabric.

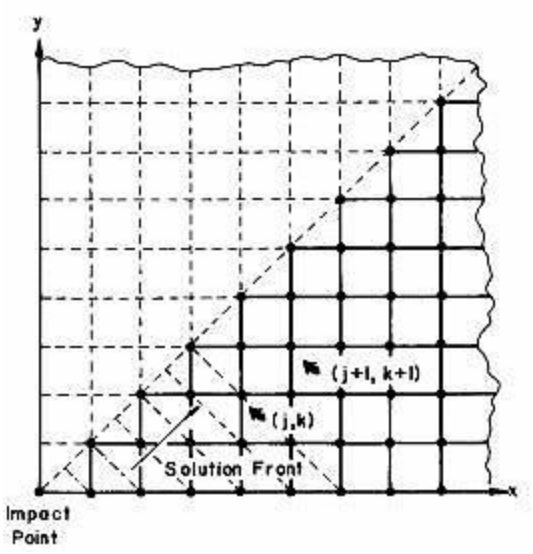

Figure 2-4: The schematic of numerical approach for fabric impact [14].

Instead of varying parameters and running tests he compared his simulations directly to actual fabric tests and based his weave on actual fabrics. This approach and his model enabled studies into yarn cross-over interactions, strain and tension histories, ability to incorporate failure, tension wave propagation. His hope for this numerical code was that it would provide incentive for experimental work aimed at obtaining numerical properties needed to model fabric. This basic model proved to be a useful building block capable of accepting additions and modifications: Cunniff [15] determined projectile geometry effects ballistic performance and a single layer model cannot capture layered panel behavior as Roylance originally thought; Shim and his colleagues [16] incorporated viscoelastic parameters and identified crimp (crimp interchange studied by Dent [17] and Prevorsek [18]) as an important factor. The model was reconstructed by researchers under the guidance from Roylance [19] with an attempt to add yarn slippage and friction and a detailed model was created by Ting, Carina, Joseph Ting, Cunnif and Roylance [20] which modeled out of plane yarn undulations, crossovers with spring coupling,

and subdivision near impact zone crossovers. The model is shown in Figure 2-5 showing the warp and fill fibers, crossover connectors and projectile impact point.

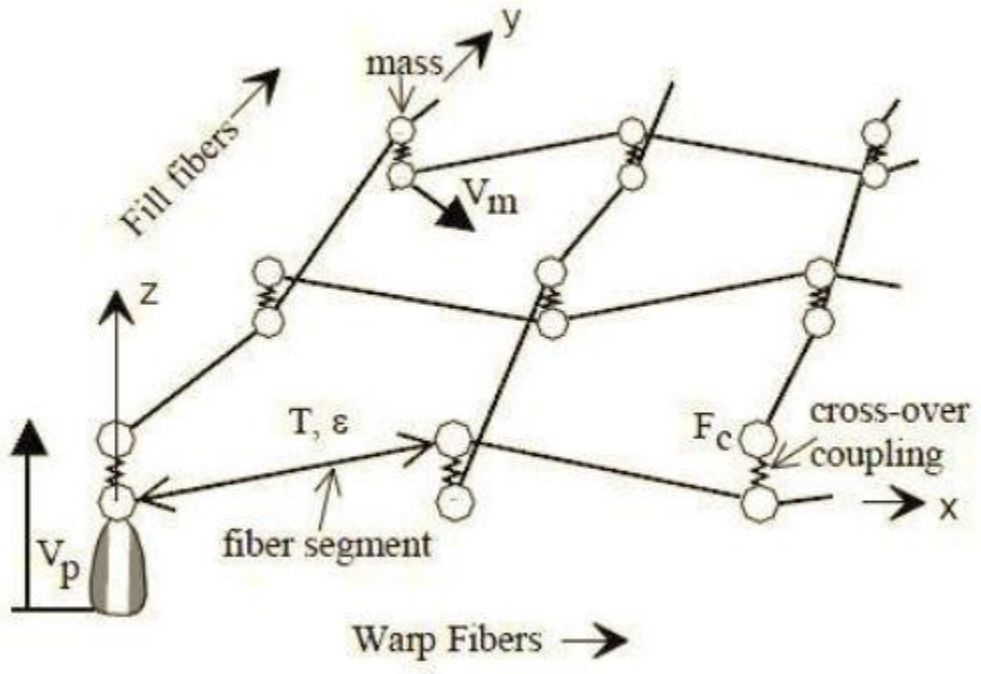

Figure 2-5: Improved yarn model [20].

This new model enabled better modeling of yarn weaves energy transfer during impact and decrimping analysis as additional capabilities to the previous model. In critique model was considered quite capable to model yarn level fabric impact and showed signs of narrowing the gap of a generalized numerical approach to predicting experimental results. The details of micro yarn geometry and those interactions at the fiber level are not taken into account.

The event is very high speed, the yarns are very small let alone the fibers that make up the yarn and there is large transverse and extremely small longitudinal deflections; all of these tax any imaginative breakthrough physical measurement devices to prove analytical or numerical models. With more computing capability FEM research came into higher usage and various yarn models were presented in literature. In 1997 Shockey [21] used a Tied Node with Failure

(TNWF) algorithm using a membrane to model the fabric with yarns modeled discretely in the continuum and solid elements to model a projectile for Zylon engine containment shroud. Three dimensional yarn modeling which included crimp friction between yarns, and compression/deformation was pioneered in the work of Duan, Keefe, Bogetti, Cheeseman and Powers [22] [2] [23]. They used commercially available LS-DYNA to model a small patch of fabric and varied the boundary conditions from fixed, fixed/free and free to study the yarn crossover interactions, projectile friction and sliding friction effects on energy absorption. Their motivation was to model yarn motion which was prevented in the previous pin jointed and continuum models. Their model is given in Figure 2-6.

Figure 2-6: Yarn level FE model [22]

The numerical analysis with specific bullet parameters and Kevlar material performed by Cheeseman et al. of two different cases where yarn friction was 0 and 0.5 revealed a difference in the number yarns contributing to stress absorption. For the friction free case there were 3 principal yarns (three weft and three warp) severely stressed during impact while during the same test with friction there were 5 principal yarns (five weft and five warp) stressed by the same amount as the friction free case. One of the observations for the development of the numerical analysis is that the intersecting principal weft and warp yarns are the main contributors to the energy absorption of the fabric. The drop off in loading from principal to non-principal yarns is so drastic such that the principal yarn which breaks under impact stress can be touching a non-principal yarn which is under such a small percentage of the load of the principal yarn that it appears not loaded at all when represented in a von-misses load graphic.

A further observation is that the change in the friction coefficient of the yarns does not greatly increase the number of principal yarns. So the parallel non-principal yarn cross-sectional shape accuracy is not of much importance and not as critically important as the principal yarns. Friction is one of the factors that influence the strength of the fabric. Yarn to yarn friction is generated mainly between intersection yarns (the majority of influence between the principal weft yarns and the principal warp yarns they intersect) as they are pulled by the force of the impacting projectile. Friction restricts the lateral mobility of the principal yarns in the fabric which in turn delays the yarn breakage by distributing the maximum stress [23].

While this energy dissipation transfers energy from the bullet, the longitudinal wave front has more time to move the fabric further into the protection zone before penetration occurs. Too much movement into the protection zone allows the fabric to cause blunt force trauma. In light ballistic protection systems the transverse fabric movement allowed through yarn straightening

would absorb much less projectile energy than the actual tensioning of the fibers. The design criteria of light ballistic protective systems are to have a tight weave with the least spacing between the yarns since this provides the most effective protection as such. It makes sense since the actual strength is only realized once the yarns are straightened and they are subjected to axial tensioning.

2.2 Yarn micro-dynamics

Aromatic polyamide (aramid) Kevlar fibers provided a novel boost to the strength of soft ballistic protection systems. Soon after their arrival research and modeling of the foundational makeup of the material were presented. The Kevlar fibers crystalline lattice was proposed by Northolt and Van Aartsen [24], Northolt [25] and Tashiro et al [26] and from their work anisotropic behavior due to its bonding along the crystalline plans can be deduced. The fibers crystals are the base unit for the formation of fibrils which are oriented along the longitudinal direction of the fiber giving superior strength along its axis. Kevlar also has high decomposition temperature due to aromatic high structure stability and this is optimal during high speed impact where local heating between projectile and fabric must be higher in order to cause decomposition failure of melting. Another soft armor ballistic fiber included in the group of aramid is Twaron and in another group polyethylene there is Spectra and Dyneema which are discussed in more recent publications [27], [28]. The polyethylene group behavior is noted for its characteristic of becoming highly oriented along the fiber axis during deformation during tension compression or shear and that polyethylene materials come with three different unit cell structures and also for its lower melt temperature.

2.2.1 Fiber to fiber interactions

When discussing this topic the important effects of realizing yarn in a truer to form shape as a part composed of representative fibers modeled to a density required to capture the true physics of the event. The computer would not have the capability to model all the fibers actually present in all the yarns in a full scale fabric system so the number of representative fibers would be high enough to actually capture the physics of the event. Solo fiber level experiments provide invaluable information to incorporate into a fiber inserted into a fabric; there is a limit to interpretations from these results used directly to model fabric performance or behavior.

2.2.2 Yarn impact observations

Song and Lu [29] completed twisted yarn impact tests against a single yarn using Hopkinson barn apparatus. This apparatus allows very precise control of the speed of the impactor allowing uniform testing. They were able to create a close up of the cross-section during very early impact and noted yarn flattening due to possible fiber compression and or spreading of the fibers.

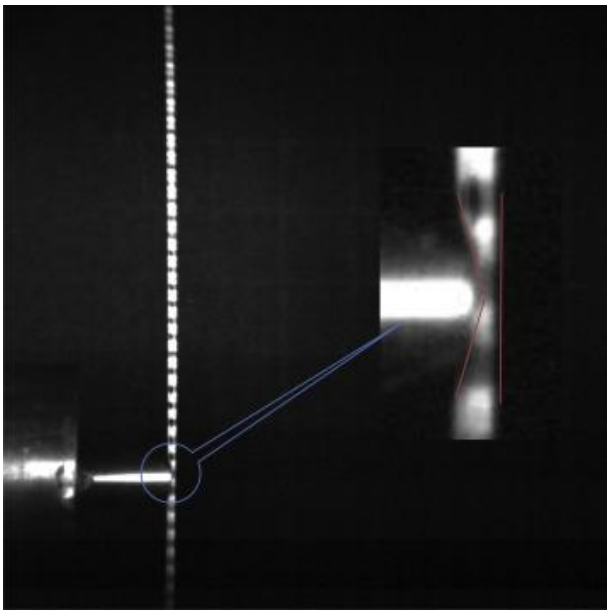

Figure 2-7: Song and Lu early impact compression of yarn [29].

Figure 2-7 shows the struck yarn and the early impact results through the use of high speed camera. Song and Lu noted that the yarn behaves as a bundle of fibers rather than a homogenous unit. They did a comprehensive analysis on twisting effects of the yarn on its toughness. Twist more effectively holds the yarn linear density by holding the fibers together during impact. Their conclusions were that slight twist increases the tensile strength of the fiber however over six turns per inch they concluded caused a significant Young's modulus decrease. They noted variance in the transverse wave angle which is directly proportional to the Euler transverse wave speed with change in twist. Higher transverse wave speed is an indication of higher ballistic performance indicating energy transferred to the fibers from the projectile.

Twist effect on Euler transverse wave speed at the same impact speed of 53 m/s.

Twist amount (twist per inch)	Angle	Euler transverse wave speed c_s(m/s)	Normalized Euler transverse wave speed, c_s/c_{s0}
0	19.7°	148.0	1
1/3	18.6°	157.5	1.064
2/3	17.6°	167.1	1.129
4/3	17.1°	172.3	1.164
8/3	16.5°	178.9	1.209

Figure 2-8: Twist effect on strength [29].

The results were put to the test later by other researchers via an experimental analysis of the effect of shear strain on individual fibers. The results led to conclusions that the properties of individual fibers were not changed and only the properties of the yarn were enhanced as discussed next.

2.2.3 Effect of shear strain on fiber tensile strength

The Army Research Laboratory (ARL) did a comprehensive study on a single fiber under tension subjected to twist angle. In a new approach they connected a single fiber between two setscrews held in place by cardboard and tested multiple axis loading. The setup and data are:

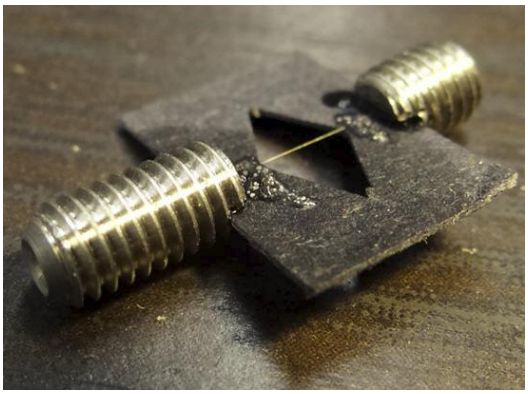

Figure 2-9: Shear-tension model [30]

Table 2-1: Twist-angle data [30]

Shear Strain	Approximate No. of 360° Rotations
0	0
0.005	<1
0.02	3
0.05	7
0.08	11
0.10	13
0.15	20
0.25	33
0.35	48
0.45	60

The results of their miniature Kolsky tension bar tests are given for three different rates of loading.

Table 2-2: ARL-TR_6403 pre-twist data for Kevlar KM2 single fiber [30].

Shear Strain	Low Rate (0.001 s^{-1})			Intermediate Rate (1 s^{-1})			High Rate (~1200 s^{-1})		
	Strength (GPa)	Stdev. (±)	(%) Untwisted	Strength (GPa)	Stdev. (±)	(%) Untwisted	Strength (GPa)	Stdev. (±)	(%) Untwisted
0	4.51	0.21	100.00	4.64	0.31	100.00	5.14	0.26	100.00
0.005	4.49	0.22	99.70	4.69	0.26	101.00	5.12	0.39	99.62
0.02	4.50	0.22	99.75	4.59	0.28	98.98	5.21	0.48	101.45
0.05	4.53	0.25	100.59	4.60	0.33	99.12	4.99	0.40	97.11
0.08	4.57	0.26	101.43	4.52	0.24	97.44	5.04	0.40	98.09
0.1	4.51	0.34	99.96	4.47	0.18	96.43	4.85	0.24	94.47
0.15	4.32	0.40	95.86	4.30	0.26	92.70	4.78	0.40	93.13
0.25	3.45	0.29	76.45	3.07	0.25	66.05	3.69	0.31	71.78
0.35	2.16	0.20	48.01	1.95	0.19	42.09	2.35	0.27	45.77
0.45	0.61	0.41	13.47	0.91	0.43	19.60	1.52	0.43	29.54

Their comparison shows that Kevlar is not rate dependent with regards to preset levels of shear strain. They concluded that the increases in strength seen by other researchers during twist tests performed on yarns were the result of single fiber interactions within the yarn such as load transfer via friction. This test is important since most yarns within the fabric have a minimal amount of twist due the weaving process and this has very noticeable enhancement and degrading effects load bearing capabilities of yarn. A curve fit of this data was completed by KSU and the results are discussed in Chapter 3.

2.2.4 Fiber level model

Wang and Sun initiated the development of fiber level representation of complete fabric [31], [32], [33]. The DFMA software was developed by Wang et al. [3] to model fabric at the sub yarn level. The most basic units are rod elements, pin joints and nodal masses to create a fiber. The rod elements connect the nodal masses at fully flexible pinned joints. This fiber unit is aptly named the digital rod element and is one of the basic units of digital yarn. The basic control unit of the digital fiber is the element length which will create a fully flexible fiber as this length approaches zero. To create a yarn a fourth element is added to the digital fiber which is the contact element. This gives the digital fiber a three dimensional shape as it will be added when

two digital fibers are closer than twice their radius somewhere along their length. Additional contact elements are added for multiple points of contact. So this enables the creation of the yarn which begins as a single digital fiber with a cross-sectional area of the real modeled yarn. As such this yarn has circular shape (a contact element will prevent penetration into its cross-sectional area) and can only represent the value of the cross sectional area of the physical yarn and not the physical variable shape. To develop the yarn a process of dividing the single fiber yarn into multiple fibers is affected, a process called fibering. Simply put the cross-sectional value of the yarn is maintained by the varying cross-sectional area of the subdivided fibers. Since the cross-sectional area is defined the basic control unit of the yarn is the numbers of fibers. As the yarns are fibered their shape is coarse due to the long element length which models the yarn fibers as straight lines connected at the nodes. To smooth the shape of the fibered yarns the fibers are elemented by selecting an element length which has a relation to the diameter of the fiber itself. A standard is usually an element length that is half the diameter of the digital fiber and will give the fiber a smooth curve shape along its length. This dimension of half the fiber diameter will enable accurate contact modeling and prevent penetration. Figure 2-10 shows the fiber (l=element length and D=fiber diameter) that we could consider as a having just been created by the fibering process within a yarn and the smoothing process that it undergoes along its length after it has been elemented.

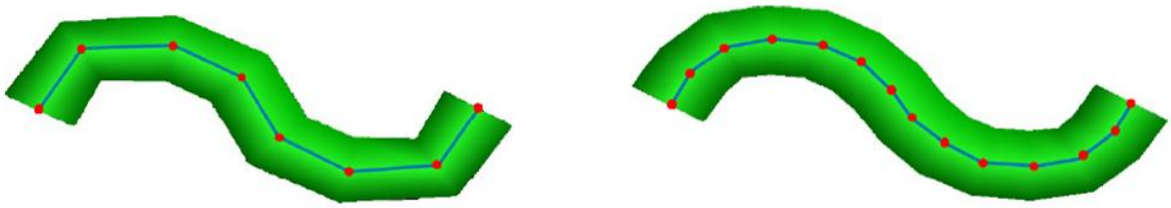

(a) A fiber with $l/D = 1$ (b) A fiber with $l/D = 0.5$

Figure 2-10: Fiber before and after yarn discretization [34].

The definition of the yarn is complete however it cannot take shape on its own and is only modeled as part of a fabric. The fabric can be considered as a collection of unit cells when it is first created and has not undergone any shape changes. The unit cell is a two dimensional repeatable unit of fabric weave. The modeler will determine this basic unit from examination of the fabric to be modeled and start the process of modeling the particular fabric. The numbers of weft and warp yarns are input into the software as well as the weave pattern and DFMA creates the unit cell with single fiber yarns. With this process in mind it is now time to step back and describe how the yarn cross-sectional area forms within the unit fabric cell. There are two methods of simulating the creation of digital fabric; one is by simulating the weaving process and the second is by adding latent tension measured from the weaving process, applying this to the yarns and then allowing these forces to shape the yarn into a low potential energy shape in relation to other yarns in the system. The second method will be described here. The single fibered yarns are tensioned longitudinally to simulate weaving forces and relaxation calculations are repeated by DFMA until the unit cell is at a lower potential energy state. Then the yarns are fibered in a compressed state (fibers are compressed along their lengths against each other) to

seed the formation of the yarn cross-sectional shape development; and then the fibers are elemented to half the length of their diameter. The concept is to model the fabric with yarns of true to scale variable cross sectional area. The yarns are modeled with a required number of fibers to accurately model the yarn under forces within the fabric and allow it to be formed within the fabric. The fibers which are modeled using iso length digital rod elements connected by frictionless pins or node elements allow the formation of the cross-sectional area of the yarn from forces within the fabric. In the relaxation procedure, a search is conducted at each time step to determine contact between adjacent fibers and compressive and frictional forces are determined at each point of contact based on contact stiffness and the frictional coefficient [3]. So the basic unit of control of the unit cell is the weave pattern since the length and width are input and it follows that the basic control unit of the fabric is the number of unit cells to create the required size of fabric.

2.2.4.1 Fiber level fabrics ballistics impact simulation

Wang et al. introduced fiber level ballistic simulation [3] using fiber level fabrics and rigid projectiles. This development combined the latest research of all the individual mechanics of fabrics into the interactions of the fabric system as a whole. The fabric generated in the relaxation process is used by the software to simulate ballistic tests performed on fabrics. Various mesh density fabrics (yarns modeled using varying numbers of fibers) are simulated. The physical yarns in fabrics consist of hundreds of fibers and the first step in the simulation process was to generate data to determine the number of fibers required to generate accurate models of physical tests. Wang et al. [3] determined that for Kevlar KM2 fabric the mesh density of 1 fiber per yarn generates different results for energy loss by projectile as compared to 7 fibers per yarn and 14 fibers per yarn generates almost the same curves for energy loss for the

projectile as compared to 19 fibers per yarn. So, the yarn mesh density threshold to properly capture results from ballistic tests on Kevlar is around 19 fibers per yarn. Compared to actual Kevlar fiber numbers of around 600 fibers per yarn this is a significant reduction in mesh density for a numerical model.

There are considerations that need to be addressed when combining fibers in the yarn model to make it numerically feasible; accurate cross-sectional area, bending which is tied to cross-sectional area, friction between fibers in the yarn and its relation to bending moment (when a group of fibers are replaced by a single numerical fiber) and the additional modes of vibration within the yarn such as yarn separation (flexural) during a single yarn test with full fiber count. The cross-sectional shape of the yarn will be more accurately determined as the numbers of the fibers in the yarn is increased.

2.3 Model sizing importance and effects

Boundary effects play an important role in the outcome of the ballistic event if they are close enough to allow a reflected wave enough time to travel back to the impact site before the ballistic process is considered complete. When a projectile strikes a single fiber, two mechanical waves are generated in the material; longitudinal and transverse waves. The longitudinal wave is propagated at the speed of sound of the material and the material of the medium (the fiber) moves longitudinally towards the impact site directly behind the longitudinal wave front [2]. The equation for speed of sound, which is also the speed of the wave, in the material is given by

$$c = \sqrt{\frac{E}{\rho}} \tag{2.1}$$

Due to this movement, a tensile stress is therefore developed behind the longitudinal wave front. It will be noted here that ahead of the longitudinal wave front there is no stress generated

in the material as a result of the material movement since it has not been yet acted upon by the longitudinal wave. This tensile strain developed in the material is given by

$$2\varepsilon\sqrt{\varepsilon(1+\varepsilon)} - \varepsilon^2 = \frac{\rho v^2}{E} \tag{2.2}$$

The other mechanical wave generated in the fiber is a transverse wave. Its speed is lower than the longitudinal wave and this speed is given by

$$u = c\sqrt{\frac{\varepsilon}{1+\varepsilon}} \tag{2.3}$$

Across the transverse wave the strain of the yarn stress does not change, however behind the transverse wave the motion of the yarn material changes abruptly to the direction of impact [2].

When the longitudinal wave reaches the boundary it is reflected back to the impact point. Behind the longitudinal reflected wave the material movement is stopped (the yarn end is fixed) and the tensile yarn stress is doubled (the reflected wave has the same sign as the incident wave). If the boundary was free the wave speed would double (the reflected speed amplitude is the same as the incident) and the wave stress would drop to zero (reverse amplitude). Once the longitudinal wave reaches the impact site the tensile stresses are superimposed on each other [2]. This is the process that will cause the fiber to break earlier than if it were free or the clamps were spaced further apart. As the boundaries are spaced further and further apart, the fiber breakage will begin occur at the expected V_{50} projectile speed.

The results from a single fiber test above are applicable to a fabric. Any data from a physical fabric model after the stress wave has been reflected back to the impact site will have enhanced stress concentrations there. These results are similar but not the same as the single fiber results for enhanced stress at the impact site since there are additional mechanisms of friction and

interactions of the yarn components within the fabric. The simulated model which captures the true physics of the fabric will also show the boundary effects. A clamped model and a free edge model will produce different V_{50} results just as the physical model. In the analysis of high speed projectiles, the higher the projectile speed will allow it to penetrate the fabric before the reflected wave has time to cause any enhancements so the V_{50} values will be true while the analysis of bullets near the V-50 speed will not be at expected V_{50} requiring the fabric model to be of larger physical size to simulate real world strength of the fabric in service. Almost all soft body armor in a ballistic system is larger than 5 or 6 inches and is not clamped at the edges.

2.4 Multi-layered fabric

Ballistic effectiveness of fabrics is presented as V_{50} and is meaningful in terms of the protection that a fabric system provides against a specific projectile. The V_{50} is specific to a projectile of a given geometry and mass. The National Institute of Justice has developed guidance for the selection of body armor for the threat level which is presented in Table 2-3.

Table 2-3: Armor level and threat comparison [35]

	0101.04	0101.06	0101.04	0101.06	0101.04	0101.06	0101.06 (Conditioned)
Armor Type	Test Bullet	Test Bullet	Bullet Weight (grains)	Bullet Weight (grains)	Reference Velocity (ft/s)	Reference Velocity (ft/s)	Reference Velocity (ft/s)
I	.22 caliber LR LRN	N/A	30	N/A	1080	N/A	N/A
	.380 ACP FMJ RN	N/A	95	N/A	1055	N/A	N/A
IIA	9 mm FMJ RN	9 mm FMJ RN	124	124	1120	1225	1165
	40 S&W FMJ	40 S&W FMJ	180	180	1055	1155	1065
II	9mm FMJ RN	9mm FMJ RN	124	124	1205	1305	1245
	.357 Mag JSP	.357 Mag JSP	158	158	1430	–	1340
IIIA	9 mm FMJ RN	.357 SIG FMJ FN	127	125	1430	1470	1410
	.44 Mag JHP	.44 Mag SJHP	240	240	1430	1430	1340
III	7.62 mm NATO FMJ (M80)	7.62mm NATO FMJ (M80)	148	147	2780	–	2780
IV	.30 Caliber M2 AP	.30 Caliber M2 AP	166	166	2880	–	2880
Acronyms / Abbreviations							
	AP	Armor Piercing			LR	Long Rifle	
	FMJ	Full Metal Jacket			LRN	Lead Round Nose	
	FN	Flat Nose			NATO	North Atlantic Treaty Organization	
	JHP	Jacketed Hollow Point			RN	Round Nose	
	JSP	Jacketed Soft Point			SIG	Sig Sauer	

Table 2-3 shows the particular capability to defeat a threat level of the type of armor is dependent on the mass and geometry of the projectile. For armor I there are two different V_{50} values given for the .22 caliber and the .380 Automatic Colt Pistol (ACP) rounds. These threats in this table represent existing bullets while the tests performed in the laboratory are involving gas guns with steel rounds of different geometries to represent manufactured ammunition and fragmentation. The geometry is important because of shear capability of the geometry of the nose of the projectile can lower the value of the V_{50} as it increases in sharpness. The flat

projectile also has shear capability along the circumference of its edge and the sharpness of this edge is very capable to cause early shear failure of the fibers in the yarns.

The improved yarn level numerical model developed by Roylance was designed to directly model panel systems. In experimental ballistic analysis Cunniff [1] noticed that he could increase the energy absorption as he lowered the denier of single piles but also increased system effects of the multiply ply systems constructed with lower denier plies. This effect varied with the material used and in some materials was not observable. Novotny [1] and his colleagues numerically modeled the ballistic efficiency or system effects in multilayered systems using a model shown in Figure 2-11 similar to the original model developed by Roylance.

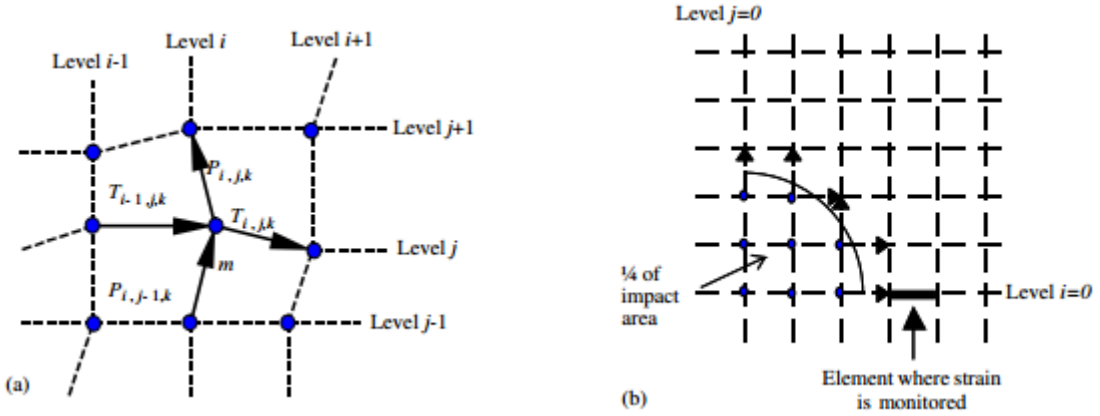

Figure 2-11: Base numerical modeling for layered system [1].

They revisited Cunniffs experimental data with variable denier and confirmed that areal density was the factor which changed the ballistic strength at least in the early stage of impact. They varied the denier number and kept the areal density constant by additional layering and noticed that the ballistic strength was exactly the same as any other system with different denier number having the same areal density. There are a few research papers that address this issue for numerical modeling the effects of allowing an air gap in layers and how it has a very noticeable

effect on the ballistic properties of the fabric. Novotny concluded that the gap has influence for the early stages of impact and is a factor with layer numbers above 10 for Kevlar 29. From their numerical analysis they developed a comparison of layers and gap distances for a few different cases. The take away from this research is the importance when modeling layered fabrics that the numerical fabrics are properly interlaced at each layer so as not to introduce efficiency losses in the ballistic performance.

2.4.1 Geometry effects in low areal density layered fabric

In this discussion of multi layered fabrics this topic of shear is visited once again and examined as to how as the number of layers increase the shear failure becomes less of an issue. The goal of numerical simulation is to present a method to model laboratory projectiles and capture all their parameters that will influence the performance of the fabric model. In ballistic testing there is not a practice of using actual firearms or actual ammunition in every case (9mm full metal jacket is a common case of the use of real bullet used in testing) rather, gas guns and specially shaped projectiles are used to simulate types of projectiles and fragments.

Figure 2-12: Projectiles used in the laboratory testing.

Figure 2-12 shows the various geometries that are used to represent projectile threats. These various geometries are used to simulate the range of projectiles and fragmentation that may be encountered in the service life of armor. From left to right in Figure 2-12 the projectile depicted

is spherical, RCC, FSP and 9mm. Numerical simulations of these models will incorporate the geometry of these projectiles and then create a ballistic event to compare to laboratory testing. Talebi, Wong and Hamouda [36] evaluated the nose angle effect of the projectile on the fabric using a FE LS-DYNA simulation with a rigid projectile with 8 node solid elements to model each yarn. They varied the angle of the nose in their simulation and recorded the von-Mises stress and energy absorption and size of hole left by projectile. Their model is given in Figure 2-13.

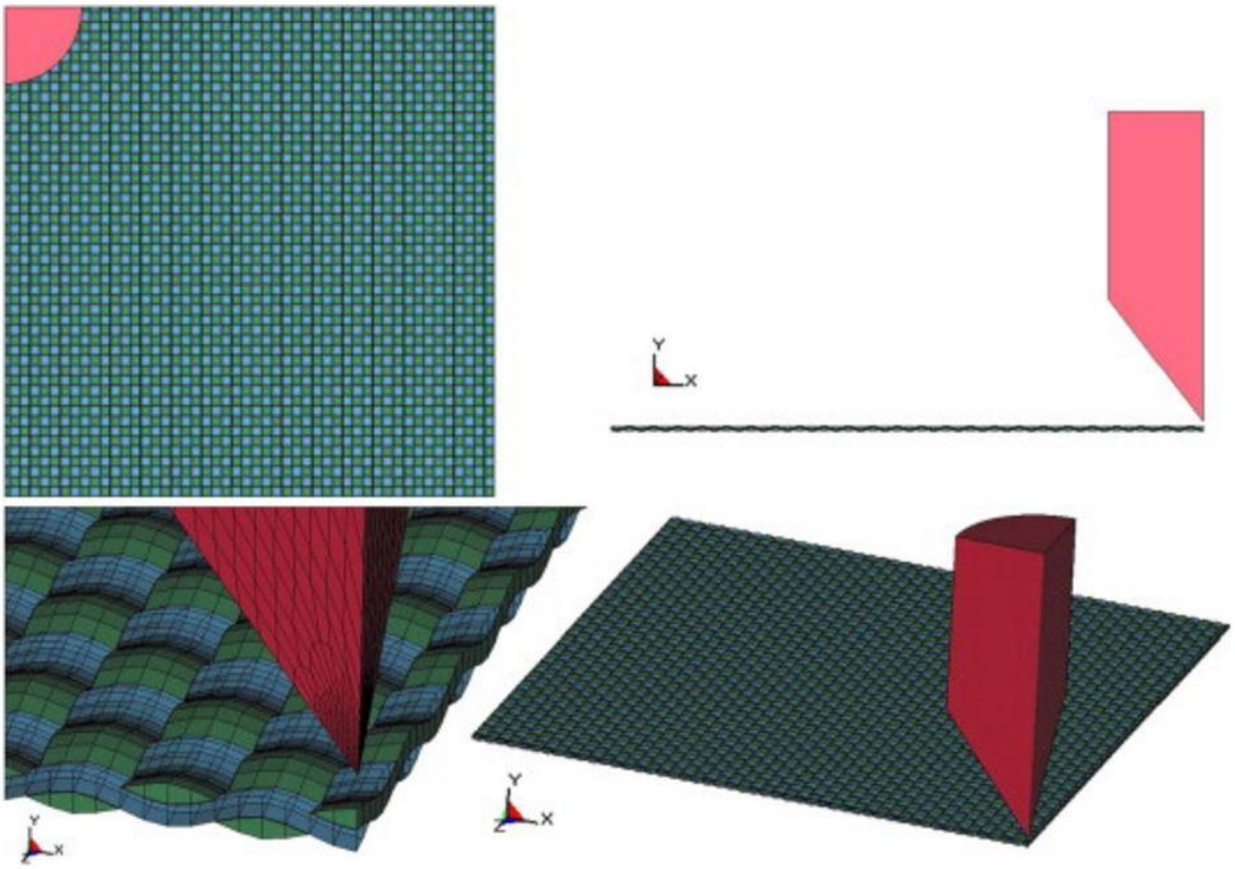

Figure 2-13: Sharp nosed projectile FE simulation details [36]

The round ball ammunition and the round nose ammunition are simulated by capturing the radius of the nose and mass while the RCC and the FSP can be more difficult. The edges of these projectiles are assumed to meet at 90 degree angles which would make them very sharp.

Some researchers have included a radius of curvature where the faces meet, an assumed number that is considered representative of an edge radius. Incorporating radius of curvature in numerical research is not a standard practice because of the small scale required modeling the edges of these projectiles. For this research these projectiles (RCC) were examined under a microscope and the actual radius of curvature was determined. With this information DEA was used to model these projectiles with improved accuracy as the original work with RCC involved no shear. This work will be presented in Chapter 3. The question at hand is how the number of layers interacts with a sharp edged projectile capable of producing a shearing action on the fibers it encounters. It is desirable to build on the idea that the fabric layers below the surface layer will experience a more diluted form of shearing respectively until at a depth where the layers will simply experience tension failure before they are contacted by the edge of projectile. Figure 2-14 shows the ballistic limit V_{50} versus the number of piles of both experimental and numerical DEA. The complete data set is modeled without including shear and bending moment which may be the cause of the separation of the experimental versus the numerical on the lower end of areal density. To test this theory the numerical data is modified to include shear and then the lower areal density models are completed again numerically and presented in Chapter 3.

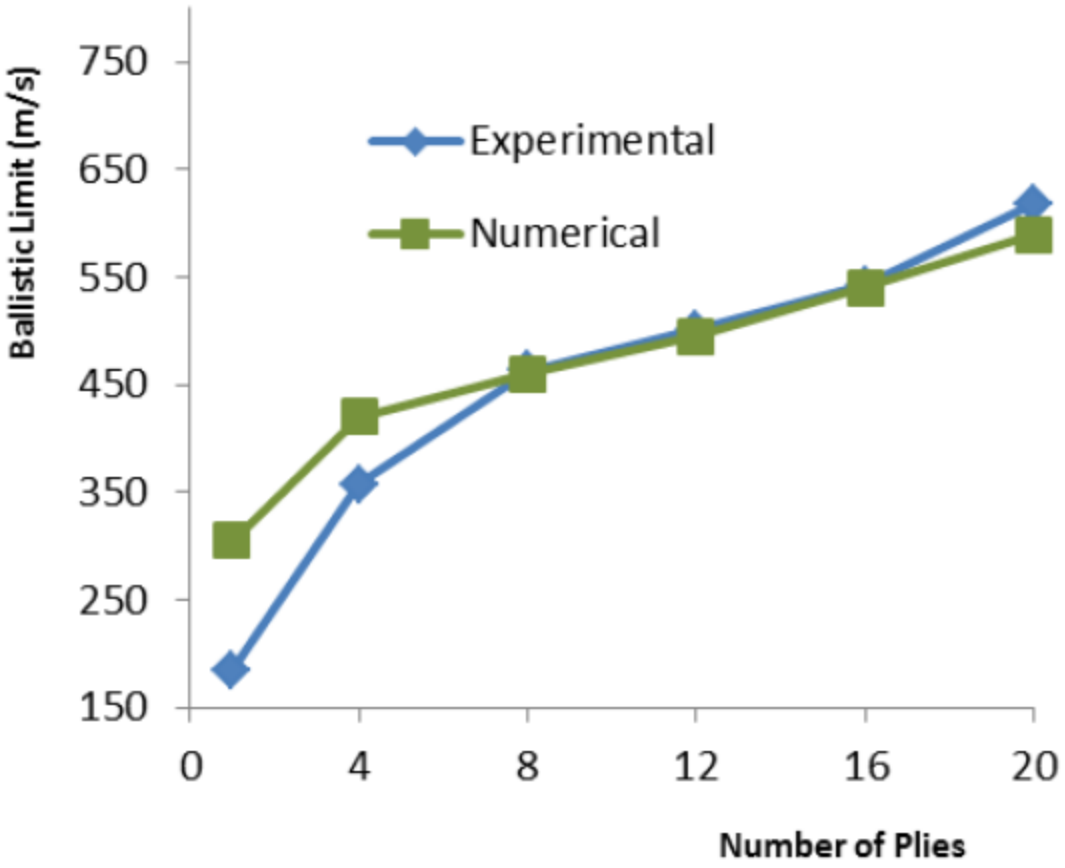

Figure 2-14: Ballistic limit for 12x12-14 vs ply [37].

The projectile for this test is 4 grain RCC and the fabric is KM2 Kevlar. The 1 ply and the 4 ply systems show that there is a discrepancy between experimental and numerical.

2.4.2 Other modeling approaches

Zohdi and Powell [38] proposed a fabric model with the yarns modeled with microscale fibrils and each yarn connected at crossover points to create a network. Their approach is shown in Figure 2-15.

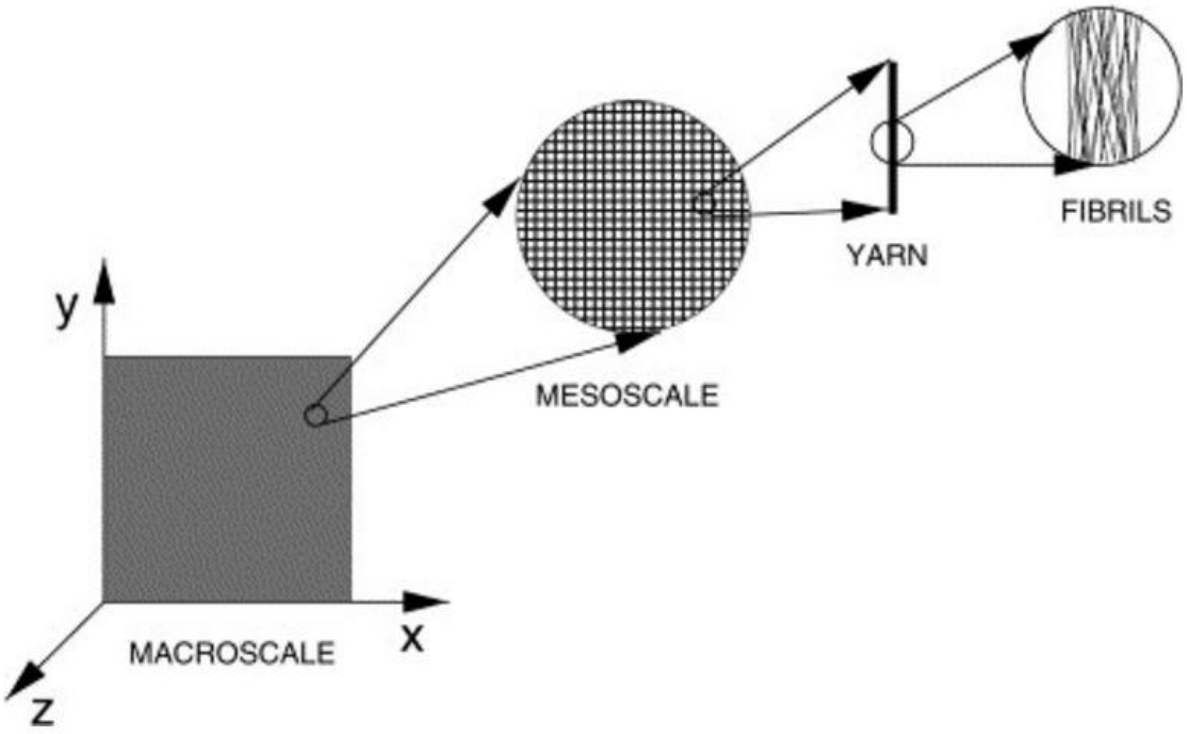

Figure 2-15: Zohdi and Powell sub yarn model [38]

Their goal was a rapid computational model to overcome cost associated with experimental work and realistic modeling with large-scale modeling and a realistic fiber count.

Guric et al. [39] modeled the fabric at the fiber level using FEM framework. The body of the work consisted of modeling spherical projectiles to determine the impact resistance of fabric and deflection and deformation damage using DEA to validate the outcomes. The parameters under close observation included fiber transverse properties, inter fiber friction and fiber fracture. Their fiber models are given in Figure 2-16.

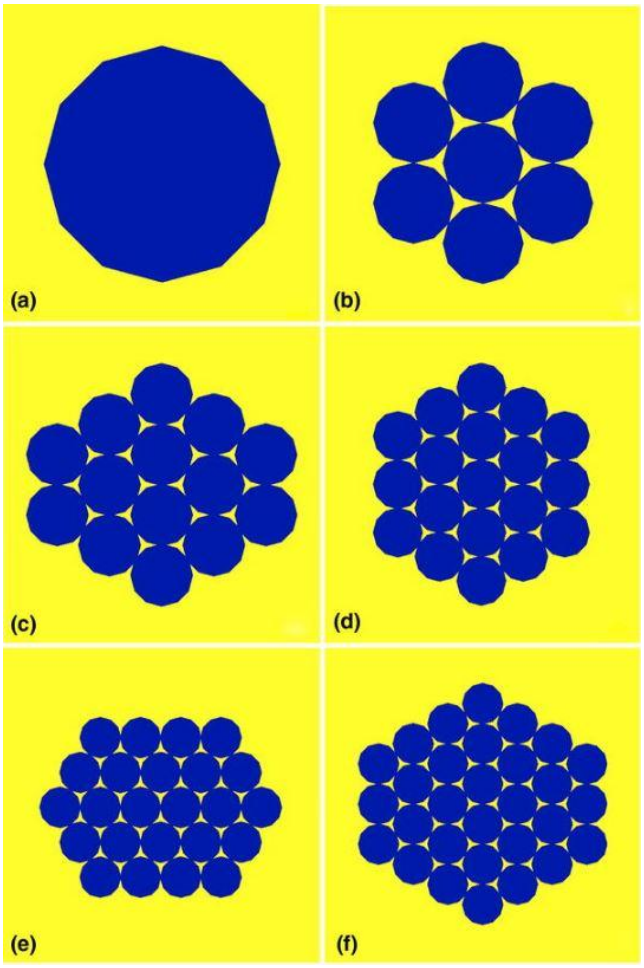

Figure 2-16: FEM fiber level yarns [39]

In earlier research the use of ballistic performance indicator (BPI) was discussed as a way to predict the V_{50} of layers of fabric necessary to defeat a threat. The BPI was based on using areal density of the fabric and initial V_{50} values from low velocity test and to then extrapolate data to predict the V_{50} as more panels were added (ie increase the areal density of the fabric). The researchers reasoned that the V_{50} and the areal density for low velocity testing had a linear relationship and therefore they could be extrapolated further to predict the ballistic resistance of more layers of fabric.

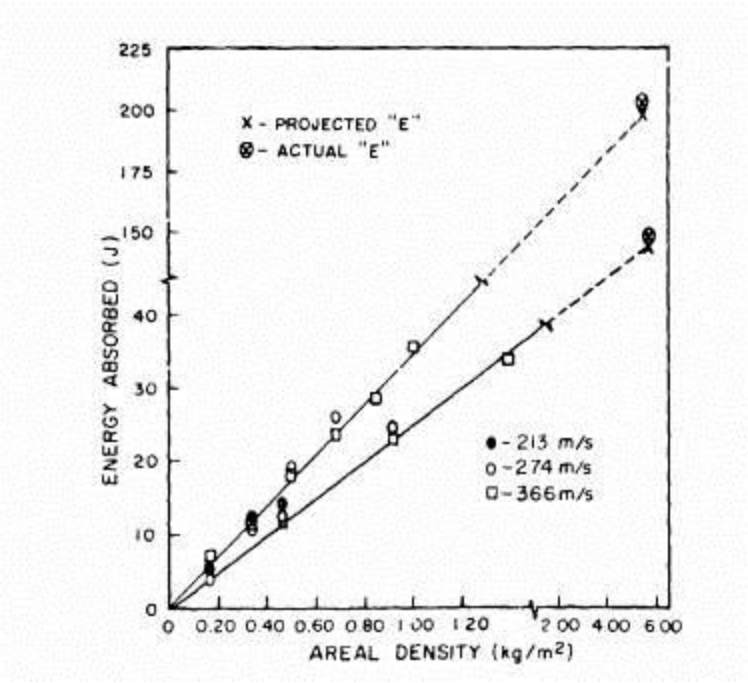

Figure 2-17: Projected and actual energy absorption at full areal density [40].

Figure 2-17 shows the initial testing performed by Figucia which became the BPI after a least squares curve fit was assigned as well as what he extrapolated to predict higher levels of areal density. One of the reasons is that at speeds close to V_{50} the dwell time of the bullet in contact is much longer which means that the reflected waves will have more time to affect the stress concentrations at the impact point. As speed increases more and more beyond the V_{50} of a layered fabric system strain develops quicker and there is a shorter time period for the stress to reach ultimate strength and so there is less and less energy absorbed and as a consequence the residual speed increases relatively more sharply up to a point that there is little difference between the strike speed and the residual speed.

2.4.3 Remarks

This chapter provides an overview of the methods used to model ballistic impact of soft fabrics. It is not possible to model the fabric to full scale down to the fiber level due to limited computer resources. However fiber level modeling is needed and cannot be simulated with higher scale methods due to: numerical inaccuracy of yarn level model which excludes fiber to fiber interaction and inability to create accurate yarn cross-section; area level modeling which excludes all fiber and yarn interactions; requirement of fiber level detail to model the radius of curvature interaction of a projectile against the fiber. Projectiles defeat yarns by pushing them aside, shear the fibers or break the yarns in tension. So, all interactions down to the lowest level are important to designing a fabric.

Small scaled modeling introduces boundary effects into the model so the results cannot be directly used to predict larger scale model. Experimental single yarn tests are very useful in validating numerical yarn behavior to be assembled into a fabric. However, constraints on the single yarn in a fabric will not be predictable by a single yarn test. A single numerical yarn correctly modeled at the micro level with correct fiber behavior and fiber interactions and at the macro level with correct cross-sectional area and mesh density should be able to predict fabric ballistics when woven into a fabric. This is only limited by computer resources. This is especially true when the numerical fabric layers are themselves assembled into a layered ballistic panel.

The object of this research is to develop a hybrid mesh for variable density fabric that accurately predicts the fabric behavior while at the same time overcoming the limitation of computer resources which prevent full scale modeling and full mesh density. The behavior of fabric is such that it has two classifications of yarns with a fabric. Primary yarns are the primary

conductors of stress waves and support almost all of the ballistic loading when the projectile is in contact with the fabric. Accurate cross sectional area is necessary when modeling these yarns in order get true physical interactions within the yarn and to get correct interactions with other yarns and capture areal density of the fabric.

Shapes of projectiles with sharp edges will require the development of a tension shear numerical solver. Introducing shear requires development the moment of inertia that simulates full mesh density using coarse density yarns. Multiple sized and weighted RCC projectiles are used in experimental calculations and there are multiple manufactures. The radius of curvature is not included as a parameter of the projectile so there may be variability as it is not a controlled parameter.

Chapter 3 - Numerical simulation of full scale ballistics

3.1 DFMA fabric modeling

Only the yarns impacted by the projectile support nearly 100% of the stress loading and on small diameter projectiles this would only be 6 to 14 yarns in a KM2 fabric. A standard test size aperture is 12”x12” and a 12”x12” Kevlar fabric contains nearly 816 yarns which means that less than 2% of the total yarns bear stress loading. Modeling fabrics numerically is a challenge due to the orders of magnitude difference of the different length scales from fiber to fabric. Up to this point there are no numerical models of standard size tests with fiber detail due to the limitations in computer resources. DFMA established by Wang et al. [33] [4] [41] [42] [43] is capable of modeling fabrics for ballistic impact on sub yarn level. Figure 3-1 is a digital fabric with 19 fibers per yarn generated from DFMA.

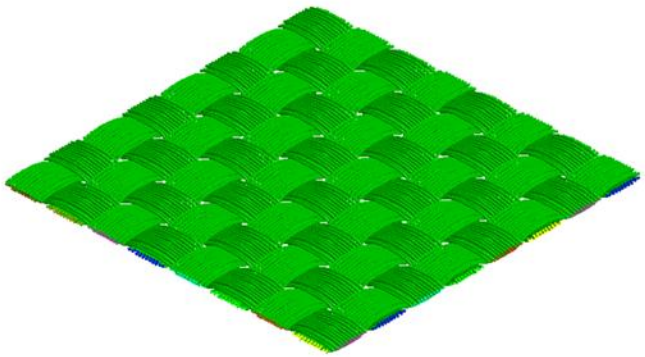

Figure 3-1: Digital fabric

The fabric is composed of unit cells with each unit cell composed of fibered yarns. The fibers are fully flexible rod elements connected by frictionless pins enabling the fabric system full flexibility under ballistic impact. Contact elements enable the fiber to fiber contact under compression and friction. Fiber is assigned material properties such as fiber stiffness, modulus, density and strength and a friction coefficient is assigned during a DEA ballistic simulation.

Once the unit cell is meshed and relaxed it is assembled into fabric so mesh control is based on one unit cell. It is a goal of this research to change the level of control of the mesh to allow relaxation of base unit cells of varying mesh prior to assembly and allow control of assembly of each mesh level to create large hybrid mesh fabrics.

Currently RCC and spherical non deformable projectiles are used in DEA ballistic simulations. The RCC is modeled as a cylinder with disks on each end and as such the RCC cannot incorporate local projectile geometry contact with the fabric. Figure 3-2 shows the geometry of the RCC projectile parameters which also includes a mass and friction coefficient.

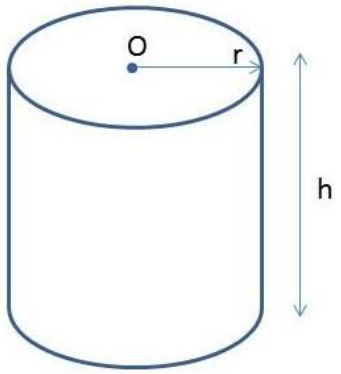

Figure 3-2: RCC projectile

The goal for the RCC is to incorporate local geometry contact in the ballistic event and then run simulations as discussed in Chapter 2 for low areal density impact.

Figure 3-3 shows the length scales of KM2 fabric and impactors 9mm and 64, 16, and 4 grain RCC with local geometry of a 64 grain RCC compared to KM2 fiber. This model will be used to create proper geometry for the numerical model RCC.

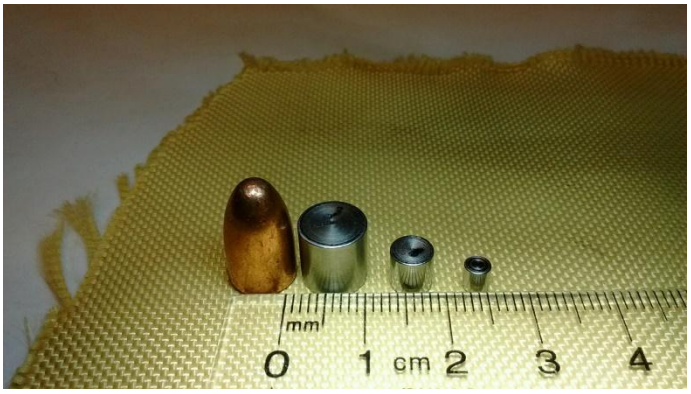

Fig(3-a) Fabric (cm) projectile (mm)

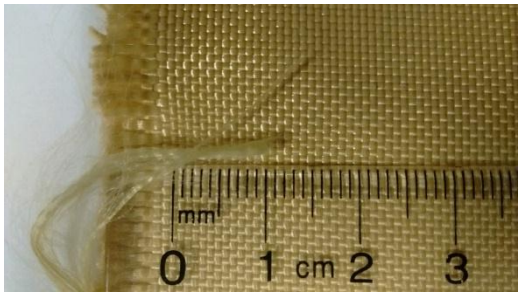

Fig(3-b) Yarn (mm)

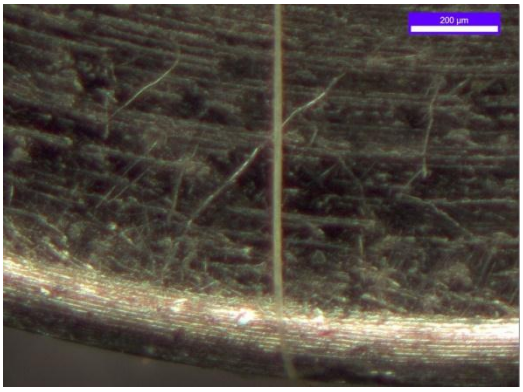

Fig(3-c) Projectile edge and fiber (200 µm)

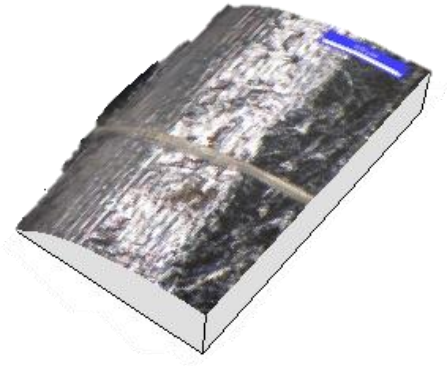

Fig(3-d) Edge and fiber (100 µm)

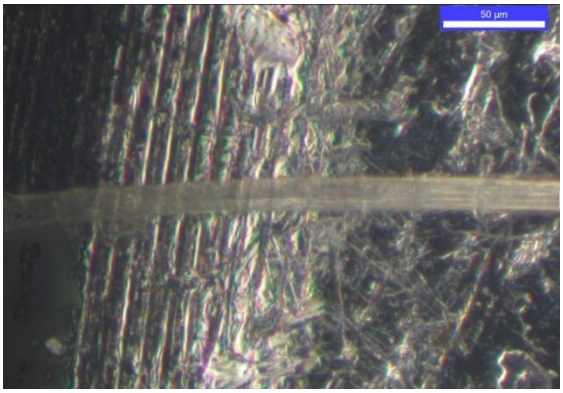

Fig(3-e) Edge and fiber (50 µm)

Figure 3-3: Length scales of KM2 fabric and local 64 Gr. RCC projectile geometry

Through internal communication the manufacture data on the RCC was obtained. The RCC requirements for local projectile geometry are r = 177 µm ± 76 µm (254-102 µm). As seen in Figure 3-3 c-e the local geometry appears very blunt if it were to act to shear the fiber. The

examination of the effects on the fiber and yarn will include varying the numerical local projectile geometry along the manufactures tolerance range (254-102 μm) and record the changes in ballistic performance of the fabric. As discussed above this data will be generated for the low areal density tests and the results will be again compared to the experimental for a discrepancy check.

3.1.1 Weibull distributed damage related to gage length

In research into woven fabrics there are tables of measured weft and warp yarn strengths which indicate much stronger weft than warp. The weaving process is considered the step in fabric manufacturing where the fibers in the yarn are weakened. The warp undergoes higher amplitude undulations than the weft which causes more bending stress. This is one of the reasons given to explain the testing results. Introducing variables while testing the small fibers is also an area of concern. The process of removing and testing the yarns then the fibers is tedious and delicate and also requires novel approaches to test without introducing any modifying factors. The following strength measurements were completed on both weft and warp to create a test data sample for Weibull analysis. This test will also be used to compare the strength of weft and warp to validate the other tests completed in literature.

When modeling the damage mechanisms it is common practice to use Weibull statistical distribution on the recorded test samples. For the following test samples the fibers were taken from a carefully manufactured fabric. The manufactures made an attempt to protect the fibers in the fabric in order to reduce strength reduction in warp. These tests are a sample of two different gage lengths. The gage length measurements in Table 3-1 and Table 3-2 will allow a Weibull statistical analysis of defect distribution within the fibers.

Table 3-1: Warp strength distribution with gage length

10mm			25mm	
Sample #	Strength		Sample#	Strength
1	2.61E+09		1	2.97E+09
2	3.30E+09		2	2.98E+09
3	3.32E+09		3	3.08E+09
4	3.32E+09		4	3.24E+09
5	3.33E+09		5	3.25E+09
6	3.43E+09		6	3.35E+09
7	3.49E+09		7	3.39E+09
8	3.49E+09		8	3.49E+09
9	3.61E+09		9	3.55E+09
10	3.69E+09		10	3.56E+09
11	3.71E+09		11	3.56E+09
12	3.77E+09		12	3.62E+09
13	3.81E+09		13	3.62E+09
14	3.84E+09		14	3.63E+09
15	3.86E+09		15	3.63E+09
16	3.87E+09		16	3.66E+09
17	3.88E+09		17	3.72E+09
18	3.90E+09		18	3.74E+09
19	3.92E+09		19	3.77E+09
20	3.95E+09		20	3.78E+09
21	3.97E+09		21	3.80E+09
22	3.98E+09		22	3.86E+09
23	4.03E+09		23	3.90E+09
24	4.04E+09		24	3.95E+09
25	4.06E+09		25	3.95E+09
26	4.09E+09		26	3.97E+09
27	4.13E+09		27	3.99E+09
28	4.14E+09		28	4.01E+09
29	4.17E+09		29	4.02E+09
30	4.22E+09		30	4.05E+09
31	4.37E+09		31	4.06E+09
32	4.41E+09		32	4.17E+09
33	4.43E+09		33	4.52E+09
Average	3.82E+09		Average	3.69E+09

Table 3-2: Weft strength distribution and with length

10mm			25mm	
Sample #	Strength		Sample#	Strength
1	2.72E+09		1	2.62E+09
2	2.75E+09		2	2.76E+09
3	2.75E+09		3	2.82E+09
4	2.86E+09		4	2.96E+09
5	3.30E+09		5	2.98E+09
6	3.44E+09		6	3.03E+09
7	3.45E+09		7	3.04E+09
8	3.49E+09		8	3.14E+09
9	3.50E+09		9	3.17E+09
10	3.55E+09		10	3.17E+09
11	3.56E+09		11	3.28E+09
12	3.59E+09		12	3.51E+09
13	3.59E+09		13	3.56E+09
14	3.81E+09		14	3.58E+09
15	3.85E+09		15	3.58E+09
16	3.95E+09		16	3.58E+09
17	4.07E+09		17	3.69E+09
18	4.08E+09		18	3.78E+09
19	4.12E+09		19	3.91E+09
20	4.15E+09		20	3.96E+09
21	4.39E+09		21	3.97E+09
22	4.40E+09		22	4.06E+09
23	4.41E+09		23	4.10E+09
24	4.44E+09		24	4.19E+09
25	4.45E+09		25	4.23E+09
26	4.45E+09		26	4.37E+09
27	4.47E+09		27	4.41E+09
28	4.51E+09		28	4.44E+09
29	4.52E+09		29	4.45E+09
30	4.53E+09		30	4.68E+09
31	4.54E+09		31	4.71E+09
32	4.59E+09		32	4.86E+09
33	4.97E+09			
Average	3.92E+09		Average	3.71E+09

Comparing 10 mm weft to warp there is not the 30% difference in strength that is posted in other literature. This also applies the 25 mm samples. This test insured that the causes for

manufacturing damages were not present and carefully removing and testing the fibers eliminated the large discrepancies and variability in strength. A bimodal Weibull strength distribution solution for these data tables is created. The derivation of parameters from data for the Weibull distribution is described by Goda and Fukunaga [44]. The following bimodal Weibull strength distribution equation is given below for the 25 mm weft where the parameter F(σ) is the failure probability, σ is the stress level and l is the fiber length.

$$F(\sigma) = 1 - Exp\left(-\frac{l}{0.025} \times \left[\left(\frac{\sigma}{3.866e9}\right)^{10.6593} - \left(\frac{\sigma}{4.033e9}\right)^{10.6598}\right]\right) \quad (3.1)$$

With the small variability in strength between weft and warp it is not necessary to have two equations if the plan is to simulate a well manufactured fabric. So this analytical solution is added to the numerical calculations to characterize all fiber strength in a ballistic simulation. Figure 3-4 is the graphical depiction of the bimodal strength distribution for the weft.

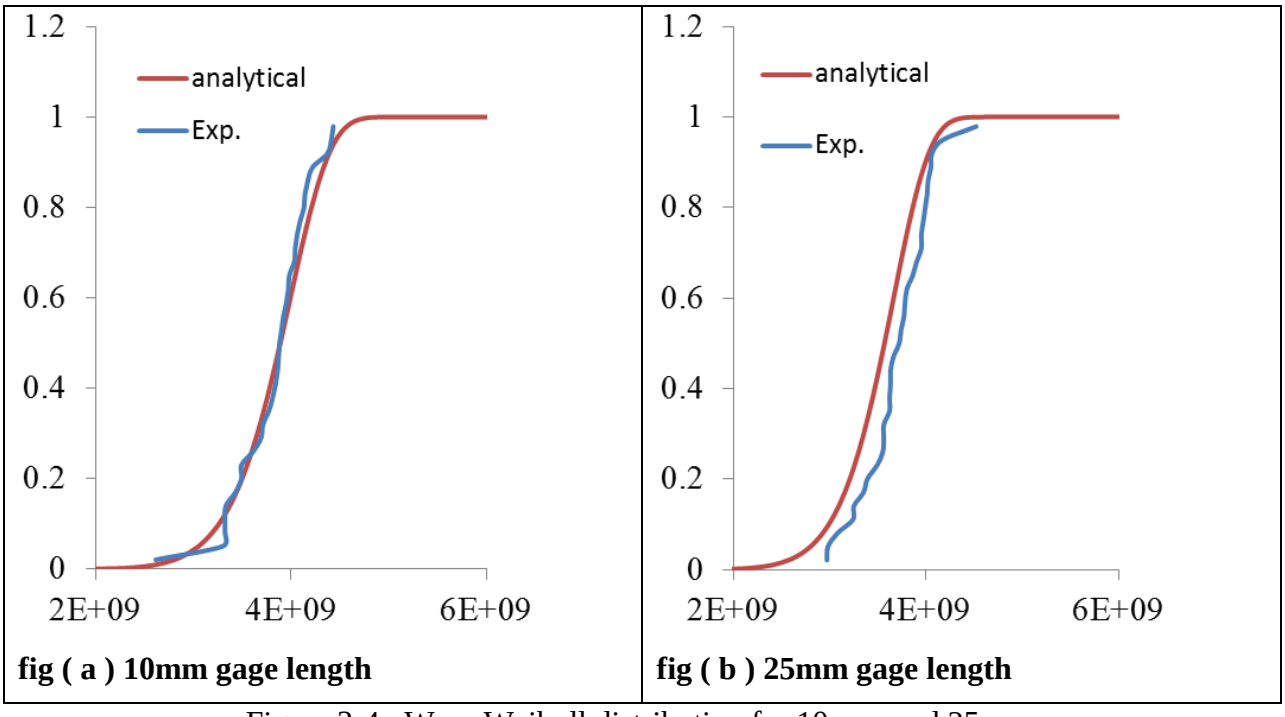

Figure 3-4: Warp Weibull distribution for 10 mm and 25 mm

3.1.2 Shear added to the fabric modeling process

DEA has the capability to model bending within the fibers. The pinned joint of the fabric is modeled with a spring system to simulate fiber bending. Figure 3-5 shows the digital fiber with two elements each of length l_0 connecting at node i and bent at angle θ with a torsional spring added at the nodal joint to simulate fiber bending where M is the induced moment at the joint and Q is the induced force at the node.

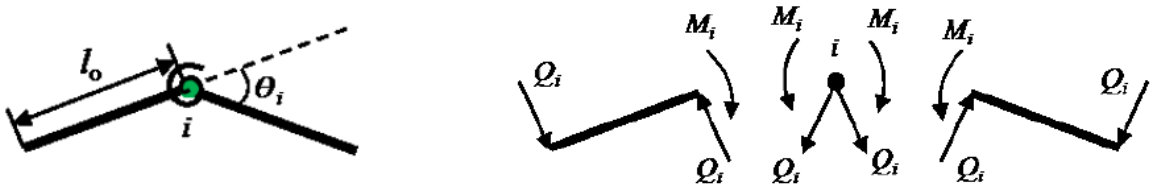

Figure 3-5: Fiber bending moment **[34]**.

The equation governing bending k of the fiber is given in terms of θ and element length.

$$\kappa_i = \frac{\theta_i}{l_0} \tag{3.2}$$

The area moment of inertia is given for a circular cross-sectional area element where N_a is the actual number of fibers in the yarn and N_d is the number of digital fibers to represent the physical yarn.

$$I = \frac{\pi r^4}{4}\frac{N_d}{N_a} \tag{3.3}$$

Moment is given for the digital fiber given in terms of the actual fabric young's modulus.

$$M = E_L I\kappa_i = \frac{E_L I\theta_i}{l_0} \tag{3.4}$$

Nodal forces at the node i are given in terms of the physical fabric and digital element moment of inertia.

$$Q_i = \frac{M_i}{l_0} = \frac{E_L I\theta_i}{{l_0}^2} \tag{3.5}$$

Shear force F is defined as the slope of the bending moment.

$$F = \frac{dM}{dx} \tag{3.6}$$

In earlier papers written for the development of DEA the spherical nosed projectile and the RCC projectile shear and bending was neglected in the digital fabrics. The reason is that it can be neglected due to the circumstances of the ballistic loading. Shear will defeat the fibers in a yarn and cause earlier failure however the layered system will minimize the effects of the shearing action once the top layers are sacrificed and the projectile behaves as normal as it travels through the next layers of the fabric. If there are more than 8 layers, shearing does not continue through all layers of the fabric. In this case the V_{50} is predominantly dependent on the tensile strength and the effects of shearing become less apparent and are overshadowed by the much higher tensile strength with more layers. This topic of layering and shear is discussed in Chapter 2 - . The shear simulations will be simulated with the RCC projectile in this paper. There are multiple geometries that make up real bullets as well as laboratory projectiles however they will not be discussed here. The first attempt of incorporating shear in the simulations for DEA was to activate bending moment in the fiber and add shear calculations for a RCC projectile edge. If the friction coefficient is 0 or infinity the moment of inertia equations are given as

$$I = \frac{\pi {d_f}^4}{64}\frac{N_d}{N_a} for\ \mu = 0 \tag{3.7}$$

$$I = \frac{\pi {d_f}^4}{64} for\ \mu = \infty \tag{3.8}$$

In the DEA code this equation is used to calculate a moment of inertia for the fabric where n is 2.

$$I = \frac{\pi {d_f}^4}{64} + (1 - \mu^n)\frac{N_d}{N_a}\frac{\pi {d_f}^4}{64} \tag{3.9}$$

If shearing is to be considered for the digital simulation in addition to the already included tensile strength the material is classified with actual shear strength and a criterion is need for the combination of the shear and tensile failure. The shear strength value must be determined for a single fiber.

3.1.3 Failure criteria of fiber

There are two situations to consider when judging fibers for their properties; a fiber tested when it comes from the spool and is in an unused state and a fiber tested when it is gently removed from the fabric. It has been accepted that weft fibers as tested are significantly stronger than their counter part warp fibers. Newer research with more novel approaches is beginning to eliminate the variables from testing these small fibers and in this research the results are showing that there is no significant strength difference between the warp and weft yarns. In section 3.1.1 of this paper fibers were tested and analysis of the test data shows that the variance between weft and warp is insignificant for well manufactured fabrics. The novel approach using rate loading also indicates that there is much less variance in the strengths of fibers over large rate ranges than originally thought.

The following equation is the von Mises criterion for failure which will be used for the fiber for a combined shear and tension loading.

$$\left(\frac{\sigma}{\sigma_u}\right)^2 + \left(\frac{\tau}{\tau_u}\right)^2 = 1 \tag{3.10}$$

The value σ_u is the fiber tensile strength and τ_u is the fiber shear strength. In this example the fiber tensile strength for KM2 is determined by tensioning the fiber under different frequency loadings as discussed in Chapter 2. The army research laboratory ARL completed testing on Kevlar KM2 single fibers to determine the effect of strain rate and pre-twist on the strength. Their goals were to determine these effects from high- mid- and low-rate specimens to determine how shear degrades the fiber which could experience a certain amount of twist during the weaving process [30]. The information from these tests will be used to determine the shear strength under combined tensile shear loading. Since the overall conclusion from the testing of twisted fibers under rate loading was that rate had little effect on the strength [30] it is only necessary to obtain one strength value which in this case will be the static test case.

The first step is to determine the saturated strength ratio and solve for the shear strength for the case where shear strain $\gamma_{max} = \gamma_s$ and the following steps would be to develop equations to determine the shear strength for other values of γ and tension. As the fiber is twisted the shear increases linearly from the center of the fiber cylinder to the edge. The following figure shows distribution of stress across the fiber cross-section under twist and tension at failure from combined loading. Figure 3-6 shows the conditions necessary to obtain the saturated strength ratio.

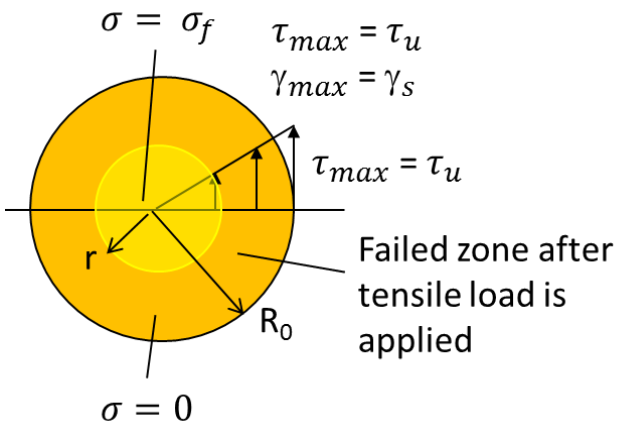

Figure 3-6: Saturated strength ratio at fiber failure.

Equation (3.10) can therefore be modified to the following equation using Figure 3-6 as a reference. The shear is linear from 0 to max shear at the perimeter under any angle of twist prior to edge failure and its ratio can be replaced by the ratio of the inner radius r to the outer radius R_0. R_0 is defined as the radius to the un-failed edge prior to tensioning, r is the radius to the un-failed edge after tensioning and R is the radius of the fiber.

$$\left(\frac{\sigma}{\sigma_u}\right)^2 + \left(\frac{r}{R_o}\right)^2 = 1 \qquad (3.11)$$

From Figure 3-6 the saturated strength ratio is a ratio of the tensile strength as $\tau_{max} = \tau_u$ to the tensile strength as $\tau_{max} = 0$. The analytical analysis will solve for the maximum ratio using Equation (3.12). This is the ratio of tensile strength with max twist to the tensile strength with no twist as depicted in Figure 3-6.

$$Saturated\ Strength\ Ratio = max\left\{\frac{\pi r^2 \sigma_f}{\pi R_0^2 \sigma_u}\right\} = max\left\{\frac{r^2}{R_0^2}\sqrt{1-\left(\frac{r}{R_0}\right)^2}\right\} \qquad (3.12)$$

Differentiating Equation (3.12) the solution for the max ratio value is given in Equation (3.13).

$$max\left\{\frac{r^2}{R_0^2}\sqrt{1-\left(\frac{r}{R_0}\right)^2}\right\} = 0.384900179 \quad \left(r = \sqrt{\frac{2}{3}}R_0\right) \tag{3.13}$$

To solve for τ_{max} the information developed from static loading will be fit to a curve and the strength ratio will be used to determine the maximum shear strain γ_{max} and this value will be used to determine the maximum shear τ_{max}. Table 3-3is the data from the twist rate test described in Chapter 2 from the static test portion of Table 2-2.

Table 3-3: Combined tensile shear strength ratio vs strain **[30]**.

Maximum Shear Strain (γmax)	**Strength Ratio (Low rate)**
0	100%
0.005	99.70%
0.02	99.75%
0.05	100.59%
0.08	101.43%
0.1	99.96%
0.15	95.86%
0.25	76.45%
0.35	48.01%
0.45	13.47%

Figure 3-7 is a curve fit to Table 3-3with a regression analysis to fit an equation to the data.

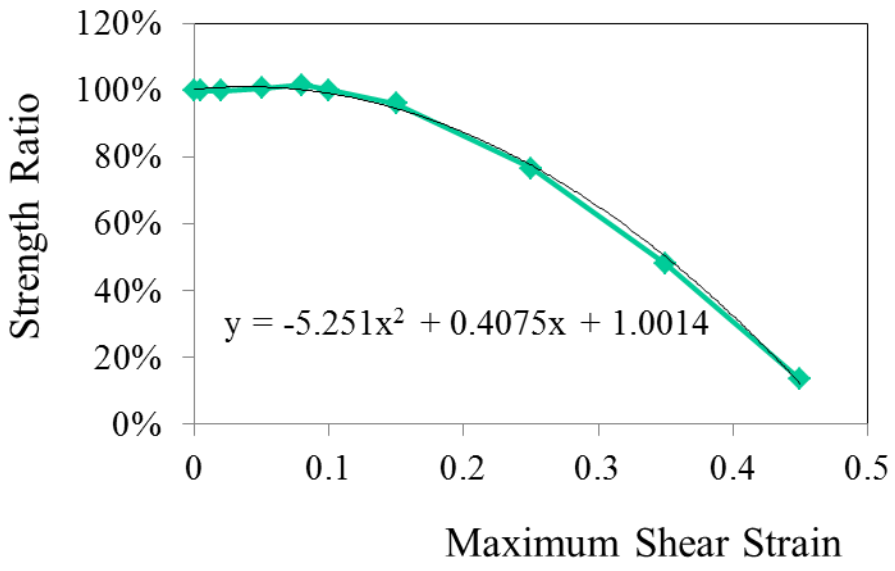

Figure 3-7: Curve fit to static combined shear tensile test

Using the curve fit equation and the quadratic equation the solution for γ_{max} is 0.3836 and solving τ = 0.3836 *G = 0.7672 GPa where G = 2 GPa and is the shear modulus of Kevlar KM2. The following analytical solutions for strength ratio are given: 1) for pretension shear failure (high twist) and 2) for saturation and lower (low twist). With pretension failure the initial applied strain is large enough to cause failure along the edge of the radius to a new diameter R_0.

(No pretension failure) $S.R. = -5.251\gamma^2 + 0.4075\gamma + 1.0014$ (3.14)

(Pretension failure) $S.R. = 0.3849\left(\frac{R_0}{R}\right)^2$ (3.15)

3.1.3.1 Modeling projectile radius of curvature

A relatively large radius of curvature along the faces of fragment simulating projectiles, usually larger than the diameters of fibers, will have a retarding effect on the shearing of the fibers and

assuming a radius would possibly leave the outcome of shearing up to validity of the assumption of the dimensions of this radius. In previous ballistic simulations the radius of curvature is modeled as a chamfer with a 26 μm dimension across its face. From internal research the manufacture is given a requirement that the radius of curvature and tolerance as r = 177 μm ± 76 μm (254-102 μm). The proper approach is to directly measure this radius to determine the variability (larger RCC projectile will most likely have larger radius of curvature than smaller RCC projectile) and conduct numerical simulations over this range to generate data for how this range affects variability in ballistic strength. New model microscopes have advanced in optics as well as measurement capability of surfaces with the help of computing augmentation. The Leica DVM 2500 model of digital microscopes has capabilities of capturing multi-zoom microscopic images and included software to assemble these images into a montage composite image to enhance viewing results of studied depth surfaces. Leica has also developed augmenting image study software which has as one of its features surface measurement along all Cartesian coordinate systems. Figure 3-8 shows the microscope with all its hardware for image capture, lighting and microscope control as well as screen interface viewing.

Figure 3-8: The Leica Microsystem: scope and electronic control and interface **[45]**.

A microscopic study was completed to determine the edge radius using the Leica system and the following images and profiles were generated RCC. The pictures list the microscopic images for the radius of curvature of the RCC projectiles and their profile curves. To help the microscope generate a montage that includes only surface (since empty space areas are out of focus and only produce noise) two projectiles were placed side by side. This way the generated montage is not out of focus on the edge. There is some image noise along the edges of the projectiles and all images below should be compared to Figure 3-11 which turned out quite nicely and shows what effect this study was trying to accomplish.

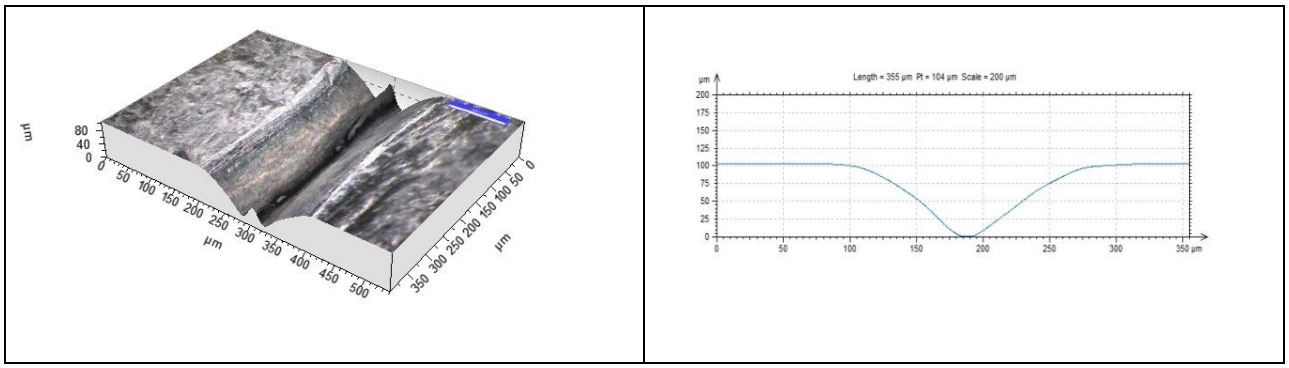

Figure 3-9: 4 grain projectile microscopic radius of curvature and radius profile.

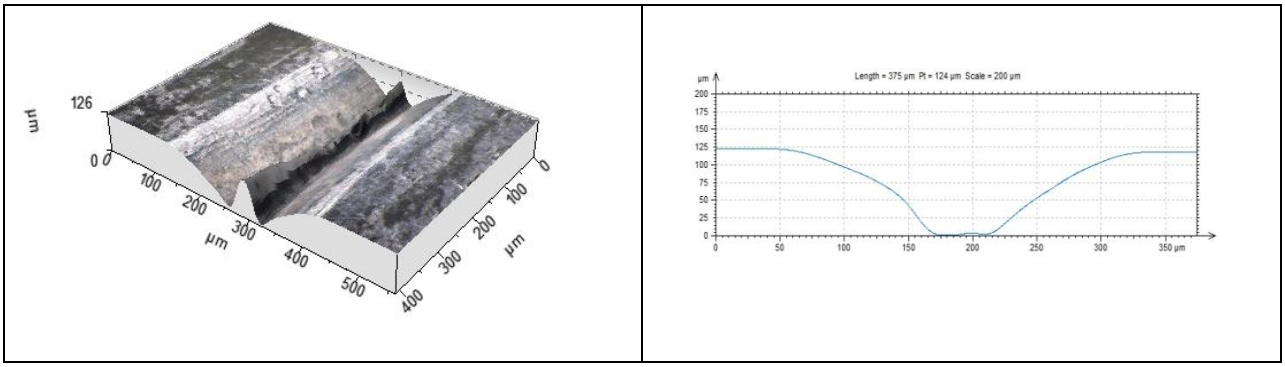

Figure 3-10: 16 grain projectile microscopic radius of curvature and radius profile.

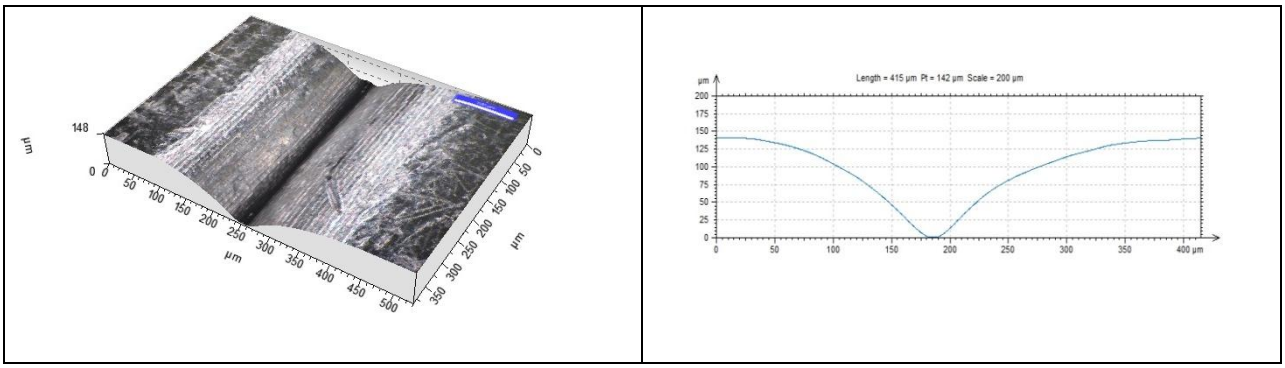

Figure 3-11: 64 grain projectile microscopic radius of curvature and radius profile

The following table is filled out with estimates of the radius of profiles for each projectile read directly from each profile shown above and it includes ball and 9mm ball ammunition.

Table 3-4: Radius of curvature for various projectiles given in μm

64 Gr RCC	**16 Gr RCC**	**4 Gr RCC**	**5.56mm Ball**	**9mm pistol**
150	125	95	2780	4500

Table 3-4 shows a clear proportional linear trend of the radius of curvature as the size of the RCC increases. It is suspected that there is variability between each RCC since the manufacture is given such a relatively large tolerance range. Comparing an example fiber against the radius of curvature brings into consideration how this edge is effectively acting as a crushing mechanism against the fiber. Since the proportions are quite large there is more blunt force causing fiber pushing and possible crushing rather than shearing. As discussed earlier this is a mode of failure for fiber causes the fibers to separate into fibrils under high dynamic loads. If there is a close proportion of the edge radius to fiber radius than there is more shearing action expected in the edge against the fiber.

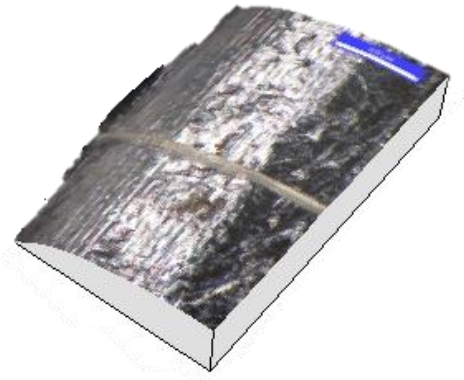

Figure 3-12: A single Kevlar 49 fiber on the edge of a 64 grain RCC projectile.

Figure 3-12 is a visual reference to the shearing of the radius of curvature as compared to a single ballistic fiber. The contrast is extreme and shows that edge of the projectile would have

most shearing effect on a fiber bundle with high friction than it would a single fiber. The roughness of the projectile would have more direct fiber surface damage than the edge as shown in the 50 μm image in Figure 3-3. As discussed earlier the dynamics of impact against a single fiber are not the same as against a yarn and single yarn impact does not represent how a yarn behaves in a fabric. It is necessary to introduce into the bullet-fiber contact the geometry calculations to account for the radius of curvature of the edge of sharp projectiles into the DEA ballistic simulation. The radius of curvature in DEA was modeled as a flat chamfer with a size of 26 μm. The contact without radius of curvature is determined if the bullet approaches within the diameter of the fiber or along the chamfer edge. Now the fiber contact along the edge of the bullet is initiated only when it touches the actual edge radius or the face of the projectile. So now the radius of curvature of the projectile is introduced to the geometry of the projectile. New calculations for low density layered fabric systems of 1, 4 and 8 layer systems are repeated to fix the separation of experimental data and numerical data. In the original blind comparison the following data for ballistic impact was higher for V_{50} speed so the conclusion was that the projectile was turning in flight. Since the experimental data was filtered to only accept flat impact the radius of curvature was explored. The manufacture data for the projectile once it was obtained showed that the radius of curvature was much larger than expected. The shearing would therefore be much less of a factor. The following numerical tests for layered ballistic panels with projectile parameters listed in Table 3-5 show a discrepancy between the data on the lower layered tests shown in Figure 3-13.

Table 3-5: Fabric and projectile for DEA and physical ballistic simulation

Fabric		**Projectile**	
Size	12x12 Multilayer	***Shape***	RCC
Strength (GPa)	Weft = Warp = 3.88	***Mass (grain)***	16
Strain Rate	Not considered	***Edge radius***	Sharp (no radius)

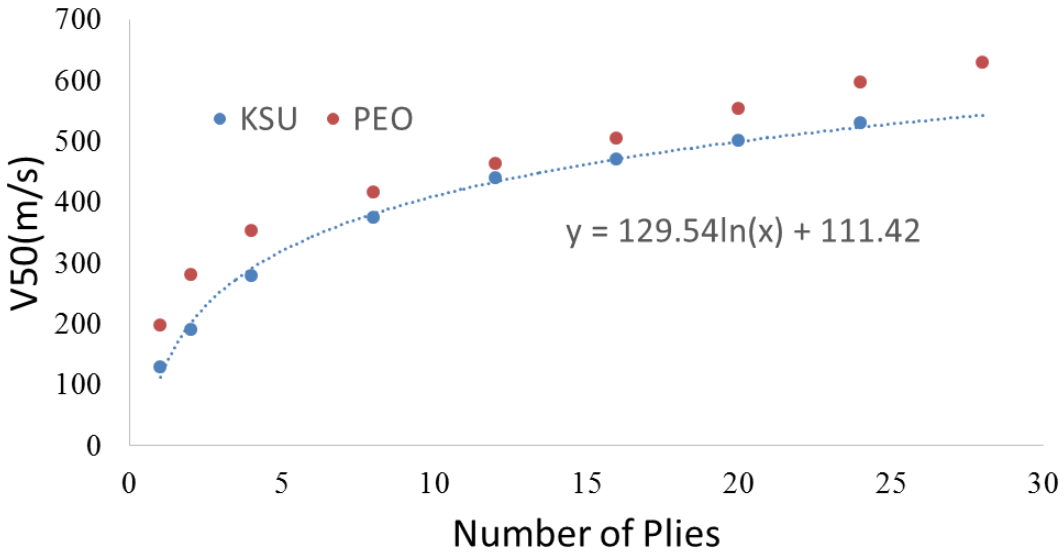

Figure 3-13: Experimental V_{50} compared to numerical simulation

Table 3-6 lists the discrepancy between experimental results and numerical simulations for number of piles and V_{50}.

Table 3-6: Variance table for above figure

Plies	KSU	PEO	Error
1	128	197	-35%
2	190	280	-32%
4	278	352	-21%
8	375	416	-10%
12	440	462	-5%
16	471	504	-7%
20	500	552	-9%
24	529	597	-11%
28		628	

The divergence for the lower areal density fabric was suspected to be caused by the radius of curvature because it showed larger divergence with fewer layers. There is a more pronounced shearing action for the top layers than the layers below. After the top layers are defeated under the projectile they are pushed through the fabric and start to isolate the edge of the projectile from the lower layers. To generate a simulation data for the radius of curvature the test above was recomputed for a single layer of fabric and the following data generated. The radius of curvature is varied to show how it changes the V_{50} of the projectile. Through internal communication the manufacture data on the RCC was obtained. The RCC requirements for local projectile geometry are r = 177 μm +/- 76 μm (254-102 μm). The tests will be conducted below this range for comparison to theoretical sharp projectiles and also within this range to generate a comparison showing what happens to ballistic limit when the local projectile geometry is not considered. A higher V_{50} is expected and shows on the numerical simulations. The test shows the amount of change effected by the correction. Now the low areal density can be recomputed to remove the variables that were responsible for the data separation.

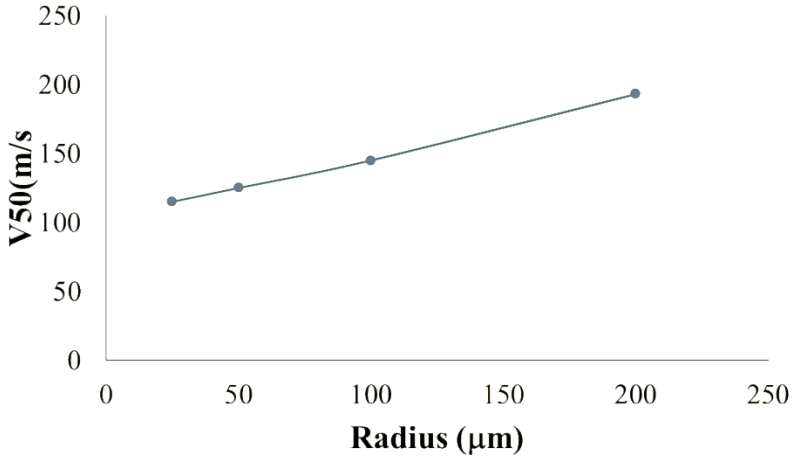

Figure 3-14: Radius of curvature effects on V_{50}

Table 3-7: Radius of curvature effects on V_{50}

Radius(μm)	V50(m/s)
25	115
50	125
100	145
200	193

As can be seen in Figure 3-14 the radius of curvature plays an important role in the calculations for the V_{50} of the fabric against RCC projectiles. Any variability would introduce statistical analysis as a valuable tool to link experimental data. If the radius of curvature is accepted as a given parameter of each projectile along with the others such as the diameter, weight and length it would remove this variability out of the Weibull analysis and leave only the variability of the defects within the fibers for Weibull analysis.

3.1.3.2 Effect of shear strength on V_{50}

The above analysis of the projectile associates the shear strength with the sharp edged projectile. Shear strength and layers have the capability to deaden the effects of the shearing through the fabric. The layers will have the capability of adding a buffer between the cutting edge of the projectile and the lower layers of the fabric. In the past numerical simulations with DEA the shear was not considered. The following tests were accomplished to determine the overall influence of shear strength on both the layering on the low density shearing. Table 3-8 lists fabric and projectile parameters used in this numerical simulation.

Table 3-8: Fabric and projectile for shear test

Fabric		**Projectile**	
Size	12x12 Multilayer	***Shape***	RCC
Strength (GPa)	Weft = Warp = 3.88	***Mass (grain)***	4
Strain Rate	Not considered	***Edge radius***	Sharp (no radius)

Numerical simulations were completed over a range of increasing shear strength and then finally a very large shear strength. With the large or infinite shear the fabric will only fail under tension. Table 3-9 lists the results for V_{50} over a range of layers and shows very clearly that the single layer is highly suspect to shear strength variations while there is much less change of strength with variance in shear in the higher layered system. This is directly related to the importance of the radius of curvature to low layered systems.

Table 3-9: List of V_{50} over a range of shear strength layers for the fabric and projectile.

Shear Stren (GPa)	**1Layer**	**4 Layers**	**8 Layers**
0.6905 (90%)	110 m/s	345 m/s	405 m/s
0.7672	185 m/s	365 m/s	425 m/s
0.9206 (120%)	220 m/s	405 m/s	445 m/s
∞	290 m/s	415 m/s	450 m/s

Using a hybrid fabric, numerical simulations of the process of the shearing action were modeled by collecting data from early impact of ballistic penetration for RCC cylinder shown in Figure 3-15 and Figure 3-16. After some elapsed time post processing of the fabric in the middle of ballistic impact was used to observe the edge of the RCC and the damages caused there.

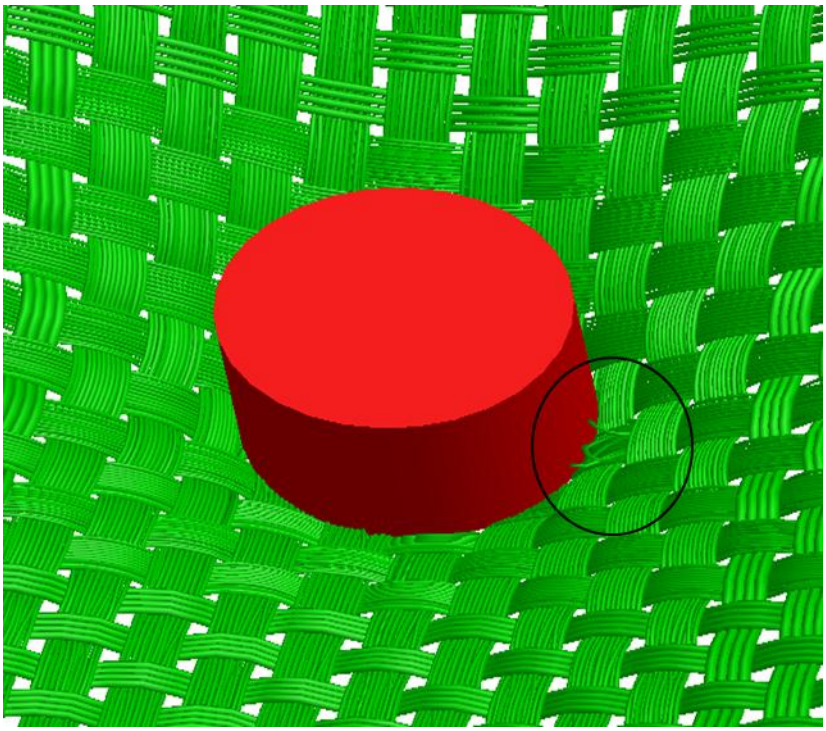

Figure 3-15: RCC early impact analysis.

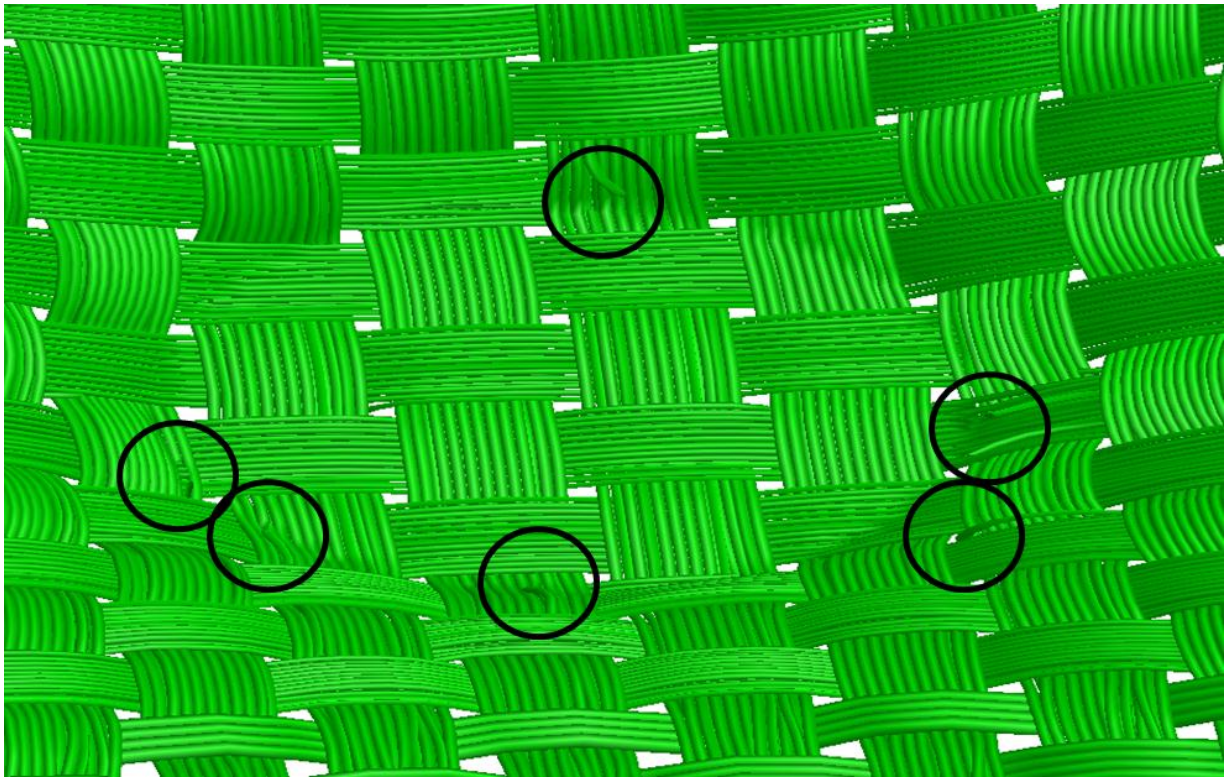

Figure 3-16: RCC early impact fiber failure under projectile.

In the blind comparison for 16 grain projectiles the low areal density numerical data and the experimental data showed separation until the areal density increased above 4-8 layers. This is because the projectile was behaving somewhere in between a spherical projectile and a sharp edged RCC. With the spherical projectile the damage is caused at the nose of the projectile due to tensile failure and this failure mode shows up in DEA in early failure analysis in digital element model. RCC failure is predominantly along the edge as seen in the above figures.

3.1.3.3 Fiber coefficient of friction and moment of inertia

As discussed above the use of 19 fibers per yarn enables full scale calculations and multi layered computer simulations. The pseudo moment of inertia for each of the 19 fibers must be designed to model physical yarn if bending moment is required in the calculations to simulate shear. The coefficient of friction now plays a role in the moment of inertia calculations because it is the

bridge between the single pin jointed fiber and the actual fibers that this single digital element represents. When moment is added the single fiber becomes much stiffer due to area moment of inertia while the true to life group of fibers allows sliding between the fibers only resisted by friction and a much lower area moment of inertia. If the normal force is high (the fibers are compressed tightly together) the collection of actual fibers behaves as a single fiber as simulated with DEA until they slip. It cannot be concluded that they will not slip and then model a group of fibers as a single fiber; however computational limitations require a realistic approach which would be to introduce a pseudo moment of inertia for the single digital fiber based on the coefficient of friction. The idea is comparable to simulating a semi-composite beam in bridge deck-structure repair. In modeling the introduction of shear pin stiffeners between the concrete bridge deck and the steel structural supports a concept of I_{eff} was introduced to give more accurate predictions to the flex of the semi composite bridge.

$$I_{eff} = I_{steel} + \sqrt{\frac{\Sigma Q_n}{C_f}} \left(I_{composite} - I_{steel}\right) \tag{3.16}$$

The sum term $\Sigma Q_n$is shear force provided by all the pin connectors and C_f is the compressive force by the concrete deck above the steel beam [46]. In the American Institute of Steel Design code this equation for effective moment of inertia for partial composite connection is stated as

$$I_{eff} = I_{bare} + \sqrt{PCC} \left(I_{tr} - I_{bare}\right) \tag{3.17}$$

PCC is the percent composite connection, a unitless percentage (25%-100%) and the other terms are the same as the above equation [47]. The equations used for calculating the moment of inertia of the digital fiber involve the coefficient of friction. Equation (3.9) was the proposed solution to the pseudo moment of inertia however after running tests for convergence it was

modified to obtain convergence and rewritten (3.18)as Equations (3.18) and (3.19). For Kevlar KM2 the variables k are assigned values: $k_1 = 2$ and $k_2 = 1$.

$$I_{digital\ fiber} = \mu^{k_1} I_1 + (k_2 - \mu^{k_1}) I_2 \tag{3.18}$$

$$I_1 = \frac{\pi {d_f}^4}{64} \; and \; I_2 = \frac{N_d}{N_a} \frac{\pi {d_f}^4}{64} \tag{3.19}$$

3.2 DEA ballistic testing

A standard model used in testing Kevlar ballistic panels is 15”x15” sized fabric and is held in a clamp with an aperature 12”x12”. So the numerical model is effectively a 12”x12” sized fabric with fixed boundaries. This paragraph will focus on this setup to present to parameters of a numerical model to determine the computational requirements. A plain weave Kevlar fabric has 34x34 yarns per 1”x1” of fabric. To accurately model a fabric in a ballistic simulation a uniform mesh of 19 fibers per yarn will be used in this numerical model. Typically the distance between nodes is ½ the fiber diameter which is effectively the element length and therefore is a direct predictor of mesh density. So to refine the DFMA mesh the original yarn or fiber is divided and the new effective cross-sectional area of the resulting fibers are each the original fiber or yarn area divided by the root of the number of new fibers. Once the new fibers are elemented the total number of elements increases by a multiple of the root of the number of new fibers and the number of new fibers. This equates to about 83 times more elements when a single fiber per yarn is re-meshed into a 19 fiber per yarn. It is possible to model a single layer of 12”x12” uniform mesh with DEA under a ballistic loading with accuracy and reasonable speed.

The modeling of layered panels cannot be realized at a mesh of 19 fibers per yarn and at full scale of 12”x12” with current computer resources. Layered panels are a unique system due to

inter layer friction which results in a non-linear property enhancement of the ballistic system. A system of layering will be examined in the development of Hybrid DFMA fabric modeling and Hybrid DEA ballistic impact discussed in the next chapter.

Chapter 4 - Hybrid mesh development

Hybrid mesh is developed to overcome obstacles to simulating standard tests in fabric ballistics. It is a viable option due to the nature of ballistic mechanics in soft fabrics. DFMA has successfully modeled fabrics and is generalized to create any weaving pattern as well as layered and 3-D fabrics. DEA has successfully simulated ballistic impact on fabrics created with DFMA. The DEA approach provides sufficient accuracy to determine the V_{50}, fabric displacement, stress and strain in the fabric and is numerically practical as detailed in previous chapters as the model mesh can be greatly reduced to simulate single layer 2-D fabrics without sacrificing accuracy. Hybrid fabric modeling of woven fabrics requires a new approach to relaxation and assembly to create a fabric within DFMA. The hybrid fabric is compared to DFMA results for identical fabrics and the results are discussed. Hybrid full scale multi layered fabrics are then created and validated against experimental results.

Variable mesh density fabric requires separate unit cells with periodic boundaries. This requires four types of unit cells in order to unite the cells at boundaries for a hybrid fabric assembly. These unit cells are differentiated by the boundaries along the edges which are fully periodic or semi-periodic or non-periodic. Assembly is such that the non-periodic and periodic boundaries connect. This requirement introduces the division of the initial hybrid unit cells into levels. Hybrid is classified under levels of assembly which would make a two mesh density fabric a 2 level system. Each periodic level is separated from the next periodic level by a non-periodic transition level. Each cell has the same dimensions so that a two level hybrid system of cells would require 25 unit cells for initial relaxation. During relaxation the periodic edge defines the shape of the connecting non periodic edge so that it makes a correct connection and will form a seamless yarn and fiber once the hybrid is assembled into a fabric. During each step

of the relaxation process the non-periodic fibers end nodes are mirrored to connect directly to the adjoining periodic end nodes.

This leads to the development of a hybrid mesh and numerical testing to determine the mesh density required to accurately simulate experimental results. There are two approaches discussed here: the area based mesh and the yarn based mesh. In the DEA full field uniform mesh (19 fibers per yarn) ballistic simulation, the modeling is only conducted on smaller scale layered fabric and single layer standard test fabric.

The Army Research Laboratory (ARL) spent considerable effort to develop ballistic test standards in the area of armor. The testing of lightweight armors for a limit to their resistance is defined as the V_{50} limit. This value is determined as a speed of the projectile where the complete penetration and partial penetration of armor are both likely events [48]. The reduction in scatter in the V_{50} data requires more rigid control of the testing environment and strict requirements on acceptable test parameters. Control of these parameters adds to the complexity and therefore costs of ballistic tests and only allows coarser range of certainty for reasonable cost to determine V_{50}. The standard for testing approved for all the departments and agencies of the Department of Defense is MIL-DTL-44050B for testing aramid ballistic cloth [49]. This standard defines the physical requirements of the ballistic panels and the physical panel dimensions and test stand criteria for a test to be accepted by the Department of Defense (DoD). A full sized panel is 15 inches by 15 inches and the test sample mount will hold the panel by its entire periphery providing a minimum test area of 121 square inches. Each test is required to have a number of layers depending on the type of ballistic test performed. The goal of simulation then for research is to meet these standards for size (the standard test) so as to produce directly comparable results.

The importance of size is apparent for optimization design. To arrive at a design it is important to have a validation from a model with the same physical dimensions and reactions to impact. Under a dynamic impact the stress is an important factor in the design and the rebound of the wave from the fixed boundaries dictates displacement profile and stress contours in the fabric. Friction of yarns from a full size fabric model will influence energy absorption by the fabric before rebound or breakage.

When the fabric is modeled down to its component yarns and fibers and each fabric panel is layered to form a three dimensional layered assembly there is a gap that will exist between each layer if the fabric is not staggered. Figure 4-1 shows the effect of directly layering the identical panels to create a layered assembly using digital fabric with coarse 4-fiber per yarn.

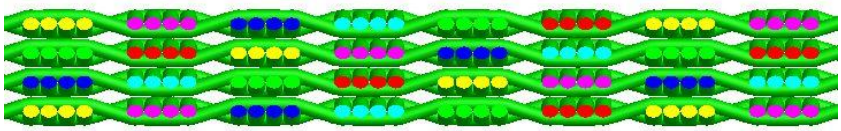

Figure 4-1 Panel layer side veiw detail directly stacked.

While the tops of the yarns touch there are gaps as seen in the figure that are not present in real fabric. A ballistic panel undergoes a process where the fabric panels are forced to interlock with each connecting layer. A physical fabric will compress to a lower energy state in a staggered layering. The DFMA software has the capability to stager the upper layer in relation to its base layer and follow this procedure for each layer pair in turn.

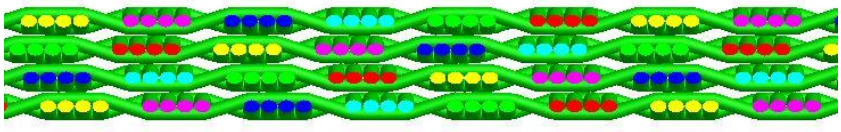

Figure 4-2: Random staggered layered fabric.

As the mesh density increases there is a more noticeable thickness in the panel assembly as shown in Figure 4-3.

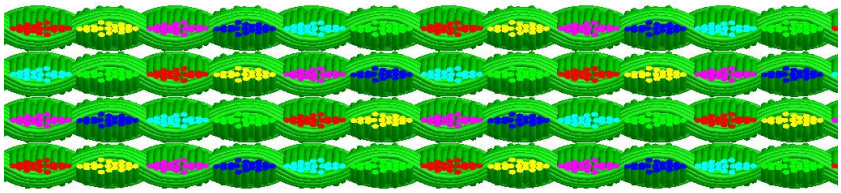

Figure 4-3: Staggered fabric layers

Novotny et al. completed a detailed theoretical study of gap effect on the early stages of bullet impact against layered fabrics. Their simulations which consists of pins and connecting elements in a true two-dimensional fabric allow them to have each fabric lay directly on top the other and add various gaps they select for their study. The conclusions were that gap weakens the layered system considerably during the stage of early impact. Their research is discussed in Chapter 2. The new capability of DFMA allows layering of panels and the capability to align the layers at offset in the horizontal junction. This lower potential energy state would be where the peaks of the underside of the top layer would align with the valley of the lower layer. Aligning the fabric correctly ensures accurate ballistic panel simulation.

The goal of this work is to simulate standard test model to enable design of ballistic panels both of the three dimensional layered panels and the three dimensional woven fabric. Create a tool to model V_{50} and displacement to determine ballistic characteristics of a design before performing physical proof tests. With this approach and accurate simulation of fabric, the designer will have tools to create a cost effective design cycle for fabrics of a required strength and displacement. For two dimensional fabrics layered into a three dimensional panel this would

enable the user to design for the required numbers of panels to arrive at a required ballistic resistance. This would also enable the user to design a standard test sized three dimensional weave for the optimal toughness and explore factors contributing to the best weave for the effective ballistic resistance.

4.1 Area based mesh

The area based mesh is based on the concept of FEM where there is a dense mesh at and surrounding the area of interaction and a coarse mesh in the far area. The yarns intersecting the area of fine mesh are discontinuous in mesh density along their length. The hybrid model involves a rectangular area of fine mesh at the impact site that transitions immediately to a coarse mesh in the area far from the impact site as show in Figure 4-4.

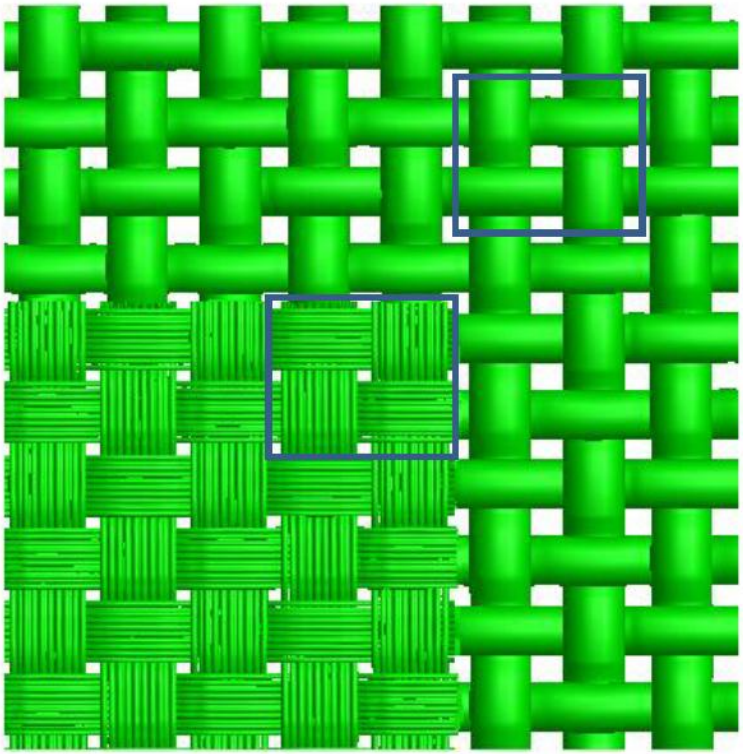

Figure 4-4: Area detail of area based mesh [37].

In order to match the thickness of uniform mesh the single fiber yarns are oval shaped. This will provide a direct connection to the fibered yarns and a smooth transition from one to the other so that the fabric remains the same thickness throughout. In Figure 4-5 both coarse and fine unit cells are detailed in a top and side view.

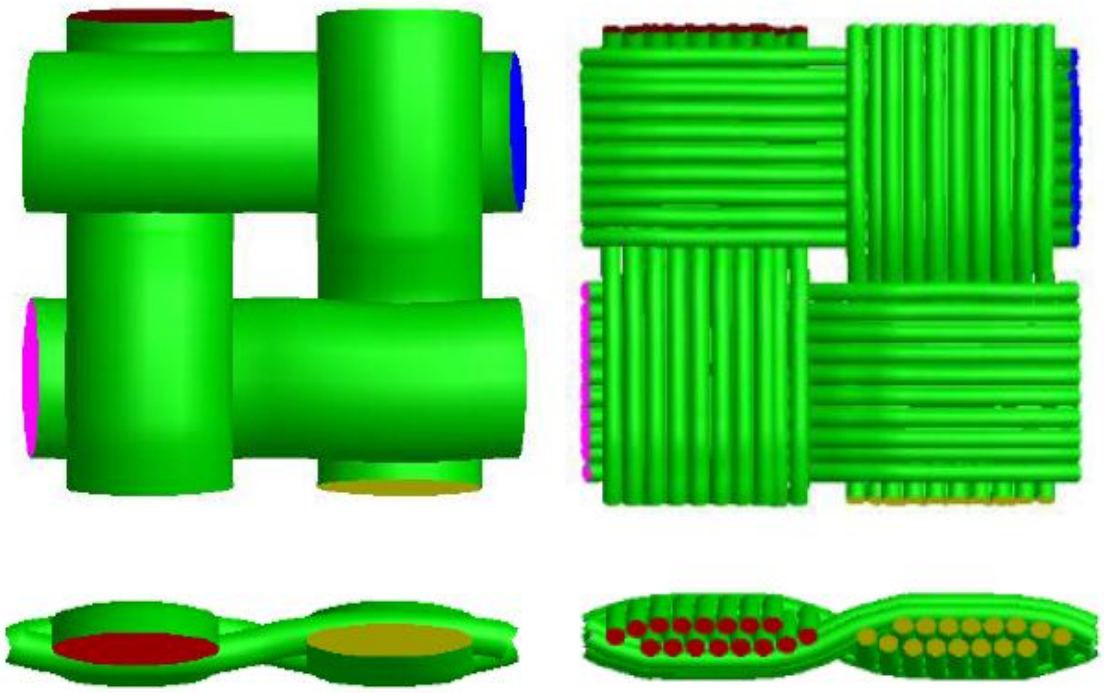

Figure 4-5 Area based mesh unit cell detail [37].

Once this fabric is created it will be subjected to numerical simulations and compared to uniform mesh DEA tests. The physical fabric modeling parameters are given in Table 4-1.

Table 4-1: Area based mesh properties and projectile information

Material	Kevlar KM-2
Weave	(34 yarn x 34 yarn) / (25.4 mm x 25.4 mm)
Areal Density	180 g/m^2
Projectile Diameter	5.51 mm
Projectile Shape	Right Circular Cylinder
Projectile Weight	16 grain

The first step in the simulation process is to run convergence simulations against full field mesh DEA tests. The obvious factor to realizing convergence is dimensions of the fine mesh area as well as the mesh density of the yarns. Past observations using DEA to simulate ballistic events have proven that there is a certain level of mesh refinement which will provide very high accuracy and use the least amount of computer resources. Since the mesh density of 19 fibers has been determined to adequately represent the 600 fiber per yarn KM2 fabric, the focus will be on determining the size of the fine mesh area.

The area based mesh showed little promise determining valid results. The problem with modeling fabric in this configuration is that artificial boundaries are present at the junction of the fine mesh and the coarse mesh and most importantly this non-uniformity causes stress wave reflections within the yarn distorting fabric ballistic strength [37]. Reflected waves at the boundary distort the stress present at the impact site. The area based mesh predicts a higher yarn tension at the impact center due to these stress wave reflections. Therefore the area based mesh is not adopted. The graphs actually appear to lie on top of each other showing that an accurate representation would only be reached when the dimensions of the area based mesh converge with those of the full field mesh, obviously opposite of the intended outcome [37]. The graphs of residual speed are higher and the graphs of residual speed show a fabric that absorbs less energy and allows the projectile to keep its velocity through the fabric pointing to a lower predicted V-50. The overall conclusions from the area based mesh are that it cannot represent the accuracy of the full field with a small fine meshed area and that the joints would have to be artificially represented with different modulus to allow full transmission of the stress wave. This complicates the design process and is not in line with the design goals.

4.2 Yarn based mesh

The yarn based mesh is more realistic yarn simulation. The experimental fabric testing reveals a grouping of principal load bearing yarns and non-principal non-impact yarns. It would be natural to distinguish these yarns into different mesh levels. In orthogonal yarns this becomes a cross-pattern and each yarn extends to the edge of the fabric. The standard test is a square boundary clamp exposing a square area of fabric subjected to displacement under ballistic impact. Yarn based mesh hybrid is developed as a square and a square assembly process. The fabric simulated in DEA is not restricted to a square area because it can be cut after assembly into a rectangle or circular pattern.

The hybrid configuration will be classified by size of the fabric and the numbers of primary yarns so that a 4" x 4" fabric with 14 primary yarns will be 4x4-14. The first step in development of this method is to add an option within DFMA to create and relax a multi-cell model which will then be meshed with variable density mesh and assembled into the final fabric. This fabric will have a unique assembly and relaxation and as mentioned will require multiple unit cells with a boundary between assembly "levels". The concept described below allows control of the mesh density of both the coarse and fine meshed areas of the fabric and also the assembly sizes of both fine and coarse mesh areas in the final fabric assembly.

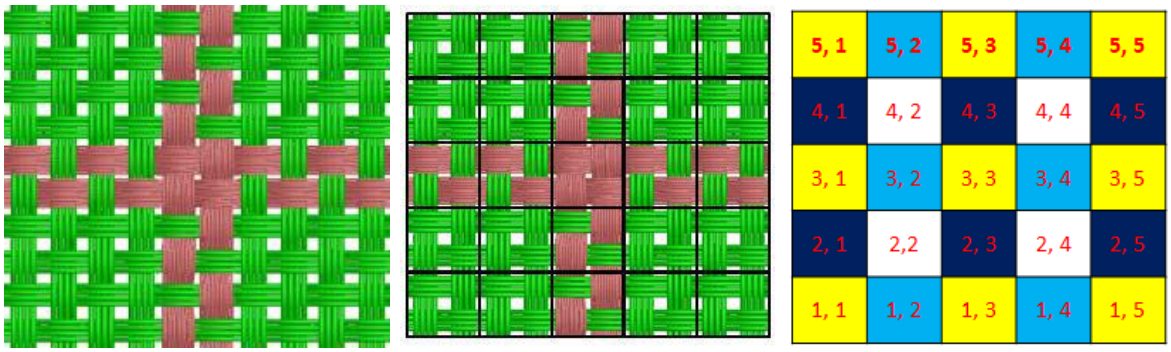

Figure 4-6: Hybrid cells [37].

Figure 4-6 left shows the hybrid unit cells with primary yarns and coarse mesh. In the center fabric of Figure 4-6 a grid is overlaid on the fabric to show the divisions of the fabric into cells. Figure 4-6 right shows a schematic of the unit cells in the fabric. The 4 colors in Figure 4-6 right depict the type of unit cell boundaries: yellow is periodic; blue and dark blue is semi-periodic and white is non-periodic. To have 2 levels of independent mesh requires that a transient level separate the periodic boundaries. The system of 25 unit cells allows the assembly of a variable two level density mesh up to any size the user wants. The fabric assembly process is shown for a small assembly in Figure 4-7.

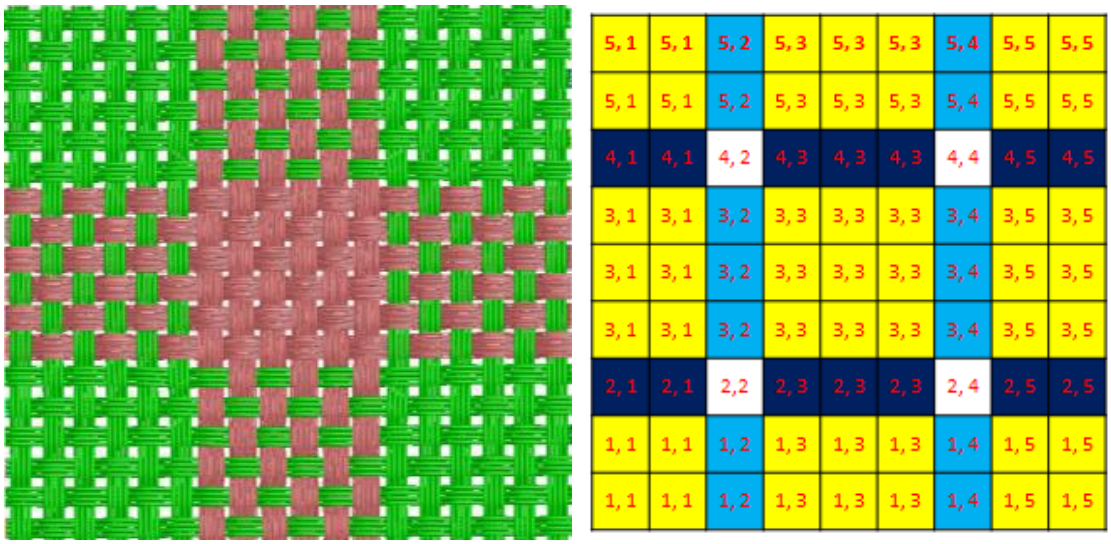

Figure 4-7: Hybrid fabric assembly [37].

The white cells cannot be assembled in any direction, the dark blue assemble right and left, the light blue assemble top and bottom and the yellow cells are fully periodic and assemble in all directions. The final fabric has continuous primary yarns and coarse mesh in the far field eliminating the artificial joints while allowing coarse mesh for most of the fabric. This mesh allows as large an assembly as computer resources allow and DFMA software allows cutting into rectangular or circular areas.

4.2.1 Yarn based numerical simulations

The following simulation and experimental tests use a fabric and projectile with the parameters given. Table 4-2 lists the hybrid numerical comparison of fabric projectile impact part 1) with standard DEA and part 2) with experimental standard tests.

Table 4-2: Validation of hybrid mesh DEA ballistics

Numerical vs Numerical Simulations			
Fabrics	***Type***	***Material***	***Yarns per inch***
	2-D	Kevlar KM2	34x34
Projectile	***Weight***	***Type***	***Material***
	4 grain	RCC	Steel
Testing Part 1	***Group***	***Layers***	***Fabric Size (inch)***
	1	1	4x4
	2	4	4x4
	3	1	12x12
Numerical vs Experimental Simulations			
Testing Part 2	***Group***	***Layers***	***Fabric Size (inch)***
	1-7	4, 8, 12, … 28	12x12

Part 1 of these tests uses data that has been generated in other research in comparison with experimental results. The comparisons will be between 1) impact forces between fabrics and projectiles 2) strike velocity and residual velocity curves 3) ballistic limit. The experimental testing in Part 2 is only comparable to the hybrid as numerical full scale does not have the computer resources to simulate these experimental results. The experimental test results for Part 2 were provided by Soldier Protection and Individual Equipment. The comparisons will be between 1) Strike velocity and residual velocity curve and 2) ballistic limit (V_{50}). It is helpful list the input data in Table 4-3.

Table 4-3: DEA input data

Yarn Strength: Weft/Warp	3.569 GPa / 2.522 GPa
Yarn Cross-Sectional Area	Based on yarn weight and specific density
Fiber Density / Fabric Areal Density	1440 g/m^3 / 180 g/m^2
Fiber Transverse Stress Strain Curve	Perdue experimental data
Weaving Pattern / unit cell size	Plain weave / 0.0015m x. 00015m
Fabric Boundary Condition	Fixed-fixed
Fabric Shape	Rectangular
Inter Fiber / Fiber Projectile Friction	0.3 / 0.3

The results from the tests listed in Table 4-2 are listed here in order by part and group.

4.2.1.1 Part 1: Comparison group 1

Four meshes are used for this comparison. Three hybrid meshes shown in Figure 4-8 are compared to uniform fine mesh. The overall outcome is to determine the number of principal yarns required to accurately capture the ballistic impact outcomes listed above. The dark circle represents the impact area of the 4 grain projectile. It is worth noting especially for the results that follow that the area of impact only covers 4 principal yarns and interacts with at least 6 yarns total when the two edge yarns are included. The term "4 principal yarns" refers to each direction separately so it refers to 8 intersecting yarns. The red colored principal center intersecting yarns are meshed with 19 fibers per yarn and the non-principal green yarns are meshed with 4 fibers per yarn.

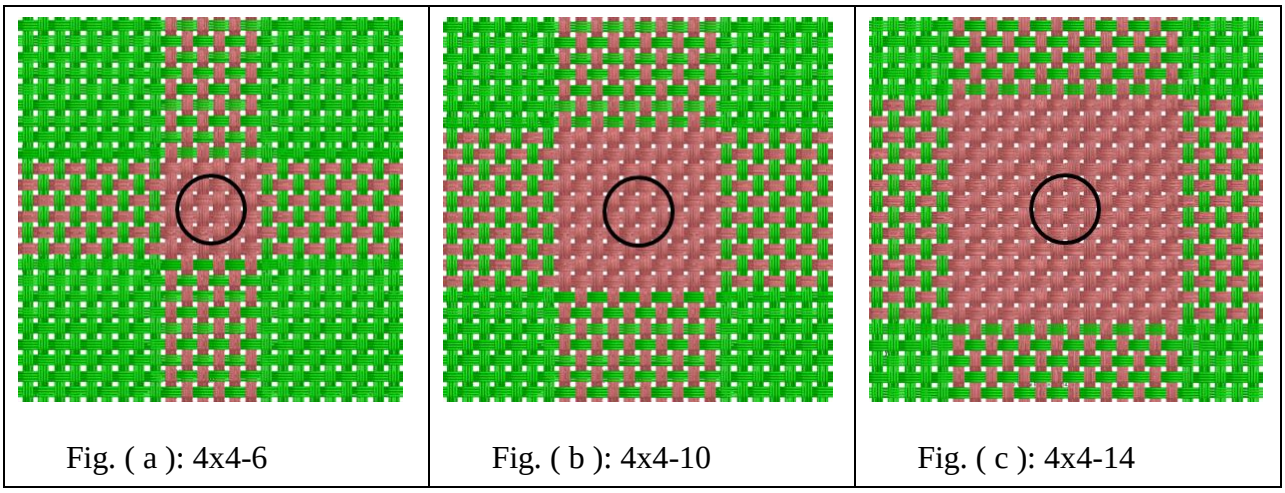

Fig. (a): 4x4-6 | Fig. (b): 4x4-10 | Fig. (c): 4x4-14

Figure 4-8: Center portion of hybrid mesh with 3 different numbers of principal yarns [37]

The tests were completed and the three different comparisons are listed graphically for a strike velocity of 250 m/s in Figure 4-9.

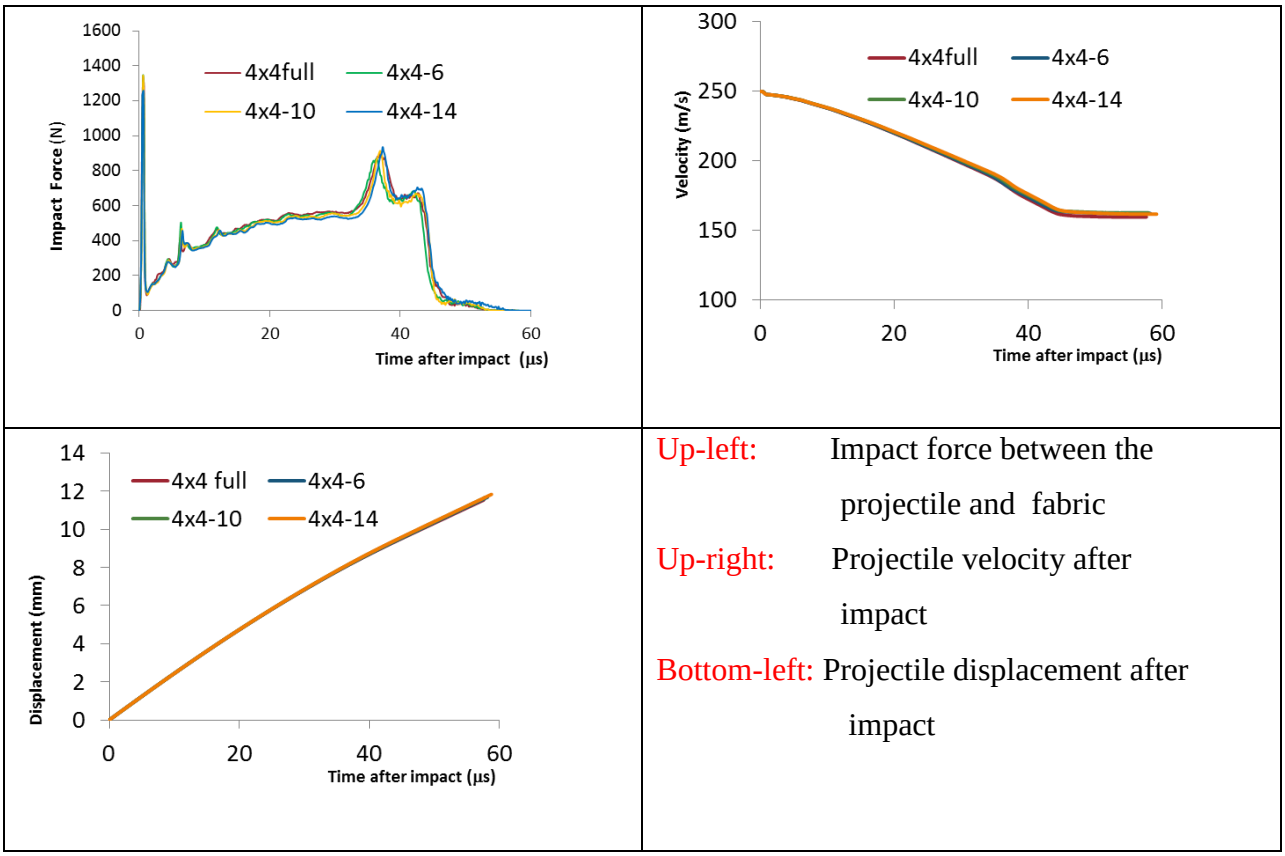

Figure 4-9: Graphical results from Part1 Group 1 [37]

The main take away from these figures is the close agreement. The 4 grain projectile is very small and only covers 4- 6 yarns. This shows in the agreement of the figures above. Figure 4-10 shows the contrast between yarns and the projectile dimensions. From this figure the relationship of projectile to principal yarns in the particular test can be seen. The 4 grain RCC is the smallest RCC projectile located on the right of Figure 4-10.

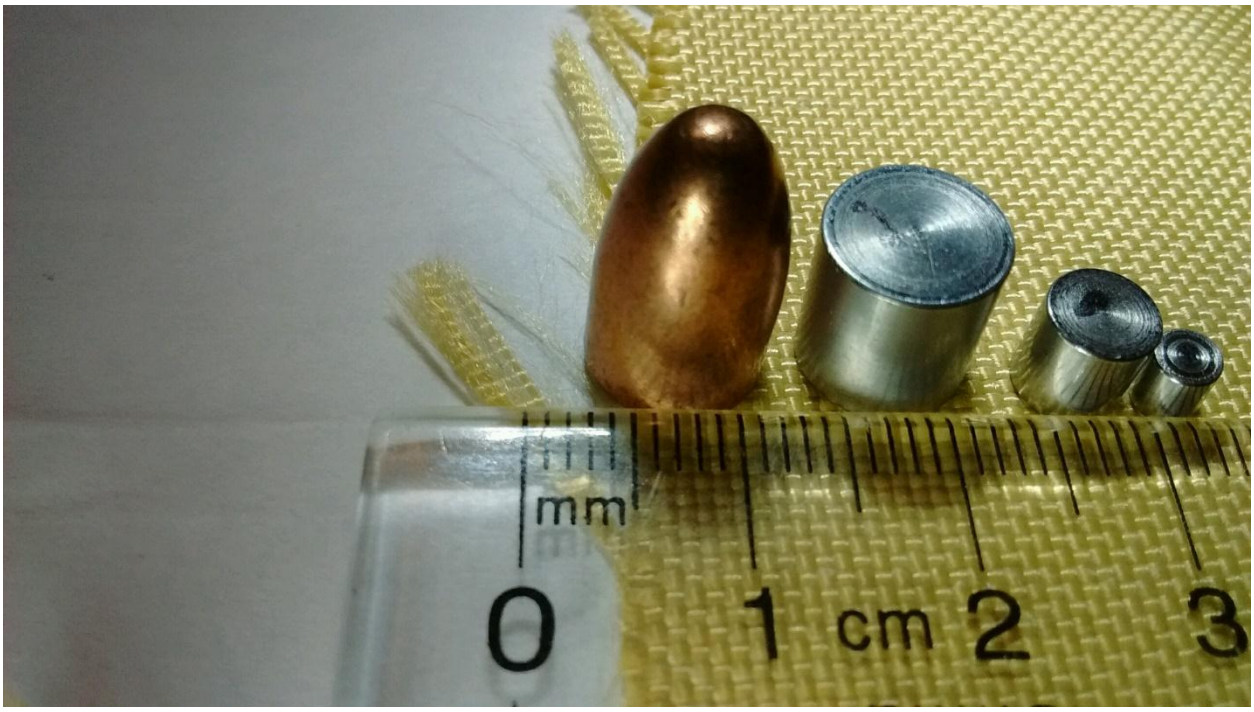

Figure 4-10: Local fabric geometry contrasted against projectile dimensions

The experimental testing is used to narrow in on a ballistic strength or V_{50} speed. The numerical simulations for this group of tests are carried out to determine this value numerically then this value is compared to the fine uniform mesh results. Figure 4-11 shows the uniform fine mesh comparisons to the three different principal yarn configurations of hybrid mesh. The agreement is the overall take away and is expected as the projectile is a 4 grain RCC which only interacts with 4-6 principal yarns.

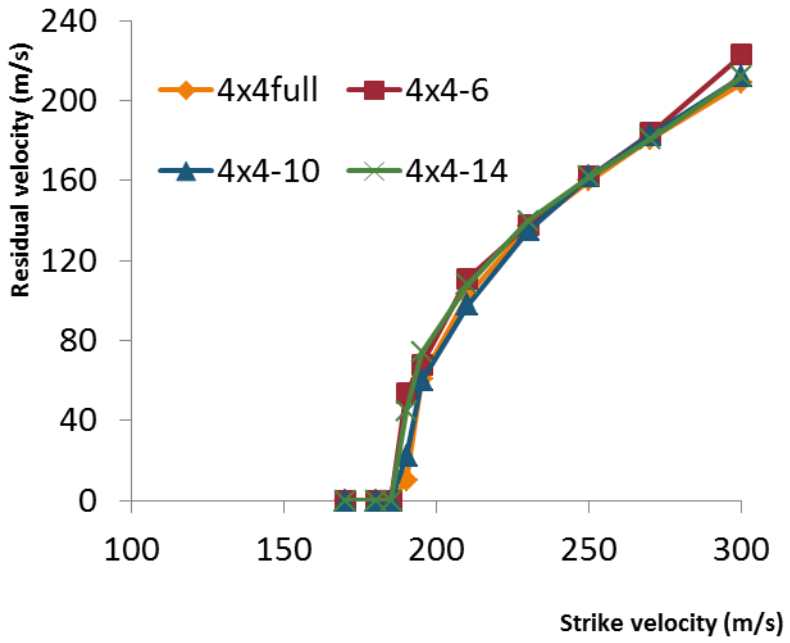

Figure 4-11: V_{50} comparison of hybrid mesh and uniform mesh [37]

The ballistic limit in experimental tests is determined by applying a normal distribution function to a set of projectile speeds near V_{50}. This method is applied to the following data in Table 4-4 from the ballistic comparison.

Table 4-4: V_{50} data single layer uniform and hybrid comparison tests [37]

V_s (m/s)	Residual Velocity (m/s)			
	4x4full	4x4-6	4x4-10	4x4-14
170	R	R	R	R
180	R	R	R	R
185	R	R	R	R
190	10	54	22	45
195	61	68	60	74
210	103	111	98	108
230	137	138	135	140
250	160	162	162	162
270	181	184	183	181
300	209	223	212	212

Then the mean and standard deviation are calculated based upon the Maximum Likelihood Estimates [50] using a software called SenTest developed by Neyer Software [51]. The V_{50} determined for the data in Table 4-4 is 185 – 190 m/s for both hybrid mesh and uniform mesh.

4.2.1.2 Part 1: Comparison group 2

The layered tests are completed in the same manner as group 1. Figure 4-12 shows the layered response of the impact force between the fabric and the 4 grain projectile.

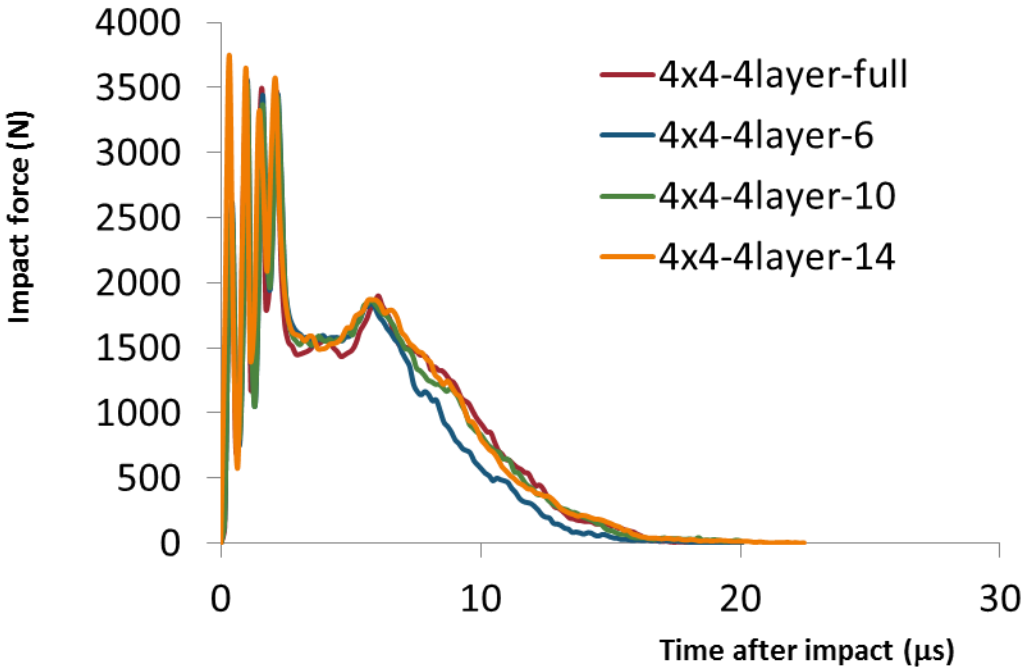

Figure 4-12: Graphical results for impact force [37]

These graphs show the force experienced by the projectile. Each layer shows gradual failure one at a time through the saw tooth pattern in the early stage of impact. There are 4 peaks showing principal yarn resistance to projectile penetration and eventual failure. The final smaller peak shows friction resistance between remaining contacting yarns (pushed out of the way or are right next to principal yarns) and the projectile as it passes through the fabric.

The ballistic limit is then determined for the layered response. Figure 4-13 shows the uniform fine mesh comparisons to the three different principal yarn configurations of hybrid layered mesh. Again the agreement for all numbers of principal yarn fine mesh of the hybrid with uniform mesh is the overall take away since the 4 grain RCC only interacts with 4-6 principal yarns.

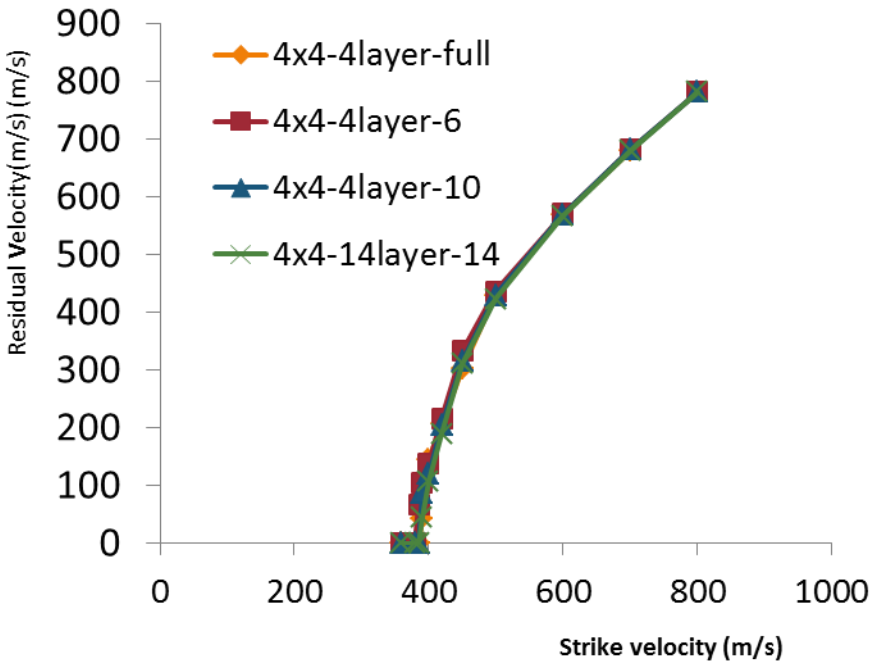

Figure 4-13: V_{50} comparison of layered hybrid mesh and uniform mesh [37]

This data for the curve in the above figure is listed in Table 4-5. It is analyzed in the same way as the data in Table 4-4 calculating mean and standard deviation based upon the Maximum Likelihood Estimates using SenTest software to determine the V_{50}. The ballistic limit for both the uniform mesh and the hybrid mesh is 383 m/s – 390 m/s.

Table 4-5: V_{50} data multi-layer uniform and hybrid comparison tests [37]

Vs	Residual Velocity (m/s)			
	4x4-4-F	4x4-4-6	4x4-4-10	4x4-4-14
360	**R**	**R**	**R**	**R**
380	**R**	**R**	**R**	**R**
383	**R**	**R**	**R**	**R**
385	**R**	**68**	**R**	**R**
390	**43**	**104**	**88**	**45**
400	**145**	**139**	**120**	**108**
420	**206**	**216**	**204**	**190**
450	**302**	**333**	**315**	**311**
500	**430**	**436**	**430**	**423**
600	**569**	**571**	**569**	**567**
700	**679**	**681**	**681**	**679**
800	**781**	**781**	**781**	**781**

4.2.1.3 Part 1: Comparison group 3

For this next comparison only the 12x12-6 and 12x12-14 shown in Figure 4-14 will be compared to the uniform mesh since the 4x4-10 was identical 4x4-14. This will save time and effort and will give the same information that can be obtained from all three sized principal mesh hybrid fabrics. This last comparison for Part 1 will be conducted the in the same manner as the group 1 and 2.

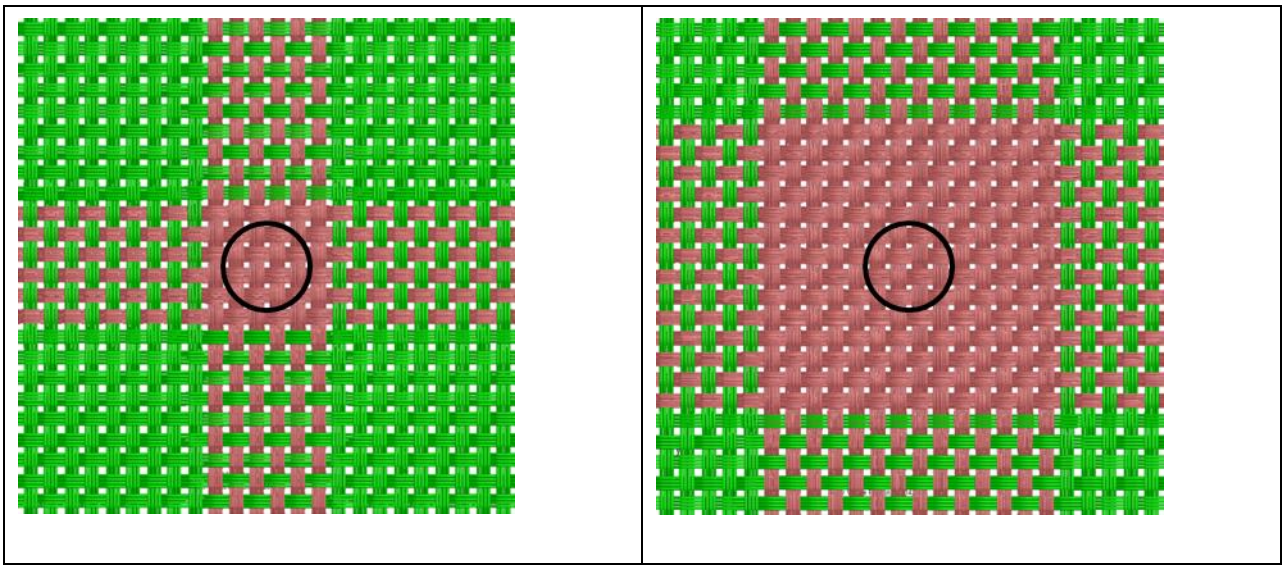

Figure 4-14: Small portion of the center of the standard sized hybrid mesh [37]

The impact force between fabric and projectile is given in Figure 4-15.

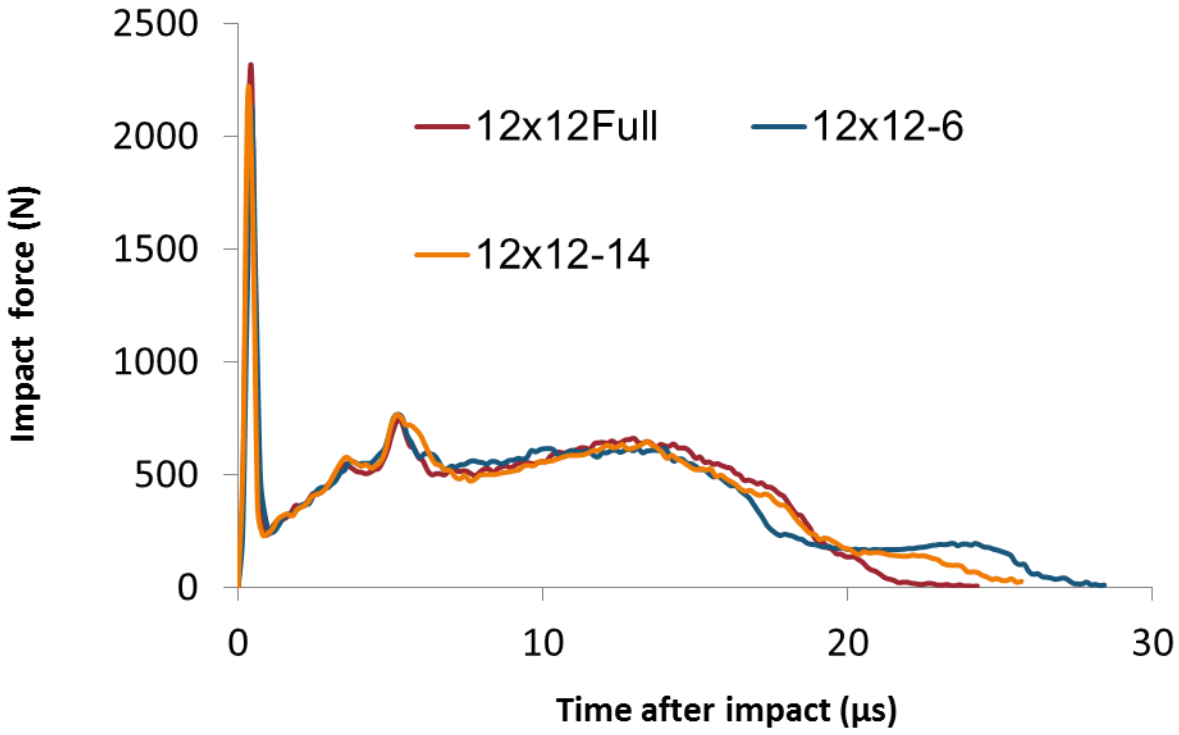

Figure 4-15: Impact force between fabric and projectile for standard single layer tests [37]

For this final comparison the agreement is very good in early impact and the 12x12-14 shows slightly more agreement in late impact. This is also the limit of the uniform mesh with the current computer resources. This is where the conclusions can be summed up that hybrid mesh can effectively represent the uniform fine mesh with nearly indistinguishable accuracy. The final graph Figure 4-16 shows the impact force between the projectile and the fabric.

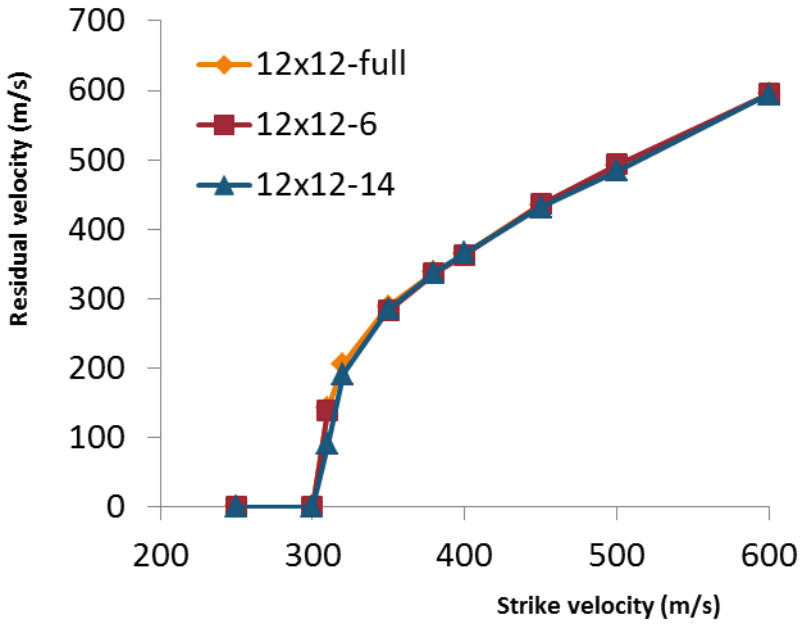

Figure 4-16: V_{50} comparison standard test hybrid mesh and uniform mesh [37]

There is good agreement between the uniform mesh for the standard test single ply uniform mesh. The tabulated data for the Vr and Vs are given in Table 4-6.

Table 4-6: V_{50}: Standard test uniform and hybrid mesh comparison [37]

Vs (m/s)	Residual Velocity (m/s)		
	12x12-full	12x12-6	12x12-14
300	**R**	**R**	**R**
310	**142**	**140**	**91**
320	**206**	**-**	**191**
350	**289**	**283**	**285**
380	**338**	**336**	**337**
400	**365**	**363**	**366**
450	**435**	**436**	**432**
500	**492**	**493**	**484**
600	**595**	**595**	**594**

The ballistic limit for both uniform and standard mesh is 300 - 310 m/s using the SenTest software for analysis.

4.2.1.4 Part 2: Comparison group 1 - 7

Now that hybrid mesh has been verified to accurately represent DEA for modeling projectile impact the following steps are taken to model experimental impact for standard layered tests. The single layer simulations with uniform mesh approached the limitations of computer resources so any layering was just not attempted at standard test size. Table 4-2 lists the fabric and projectile information and the comparison group layers and Table 4-3 lists the input data for the DEA test. The layers are compacted with staggered layering for the lowest system potential energy as described above to prevent any variance in ballistic efficiency.

Figure 4-17 includes key comparisons of layered experimental tests and layered hybrid fabric simulations. The results show the areas where there are some discrepancies of the hybrid from the experimental results. In Figure 4-17 Fig.(a) shows that the V_{50} will be higher than the

experimental and in Fig.(b) and Fig.(c) the discrepancy goes away. In Fig.(d) there is again a discrepancy this time however the V_{50} predicted is lower than the experimental. In these numerical experiments the shear is not included which means only tension failure.

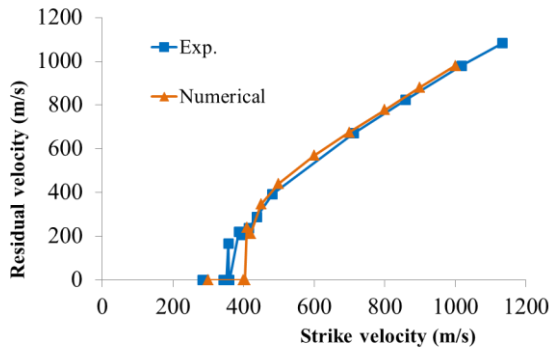

Fig.(a): 4 Piles

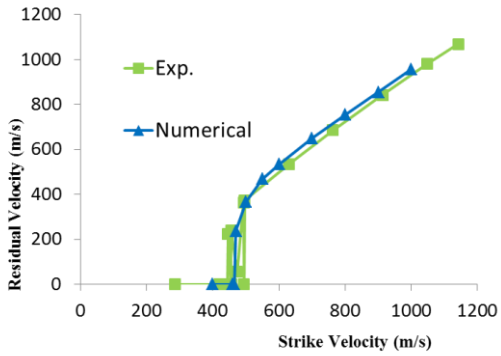

Fig.(b): 8 Piles

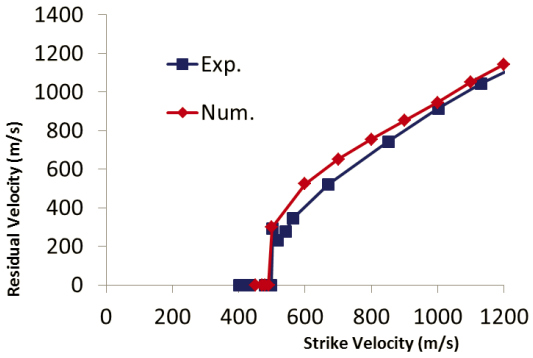

Fig.(c): 12 Piles

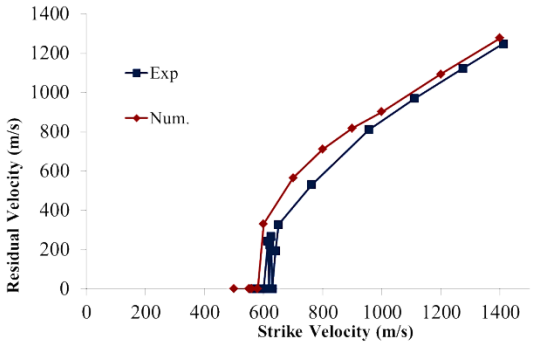

Fig.(d): 20 Piles

Figure 4-17: V_{50} comparison standard layered test hybrid mesh and experimental [37]

The data for all layered numerical simulations is analyzed by SenTest and the V_{50} results are shown compared to experimental values in Table 4-7.

Table 4-7: V_{50} data for layered fabric [37]

Number of plies	Experimental	Numerical
1	186	295
4	357	405
8	463	460
12	501	495
16	542	540
20	618	580
24	653	615
28	696	655

The information is presented graphically in the Figure 4-18 with the experimental data. The discrepancies in the low and high layered fabrics are discussed in Section 3.1.3.1. The model with bending added is shown in Figure 3-13 and a curve is fit to the data. The radius of curvature is also discussed and a single layer fabric is simulated numerically with different radius of curvatures in Figure 3-14.

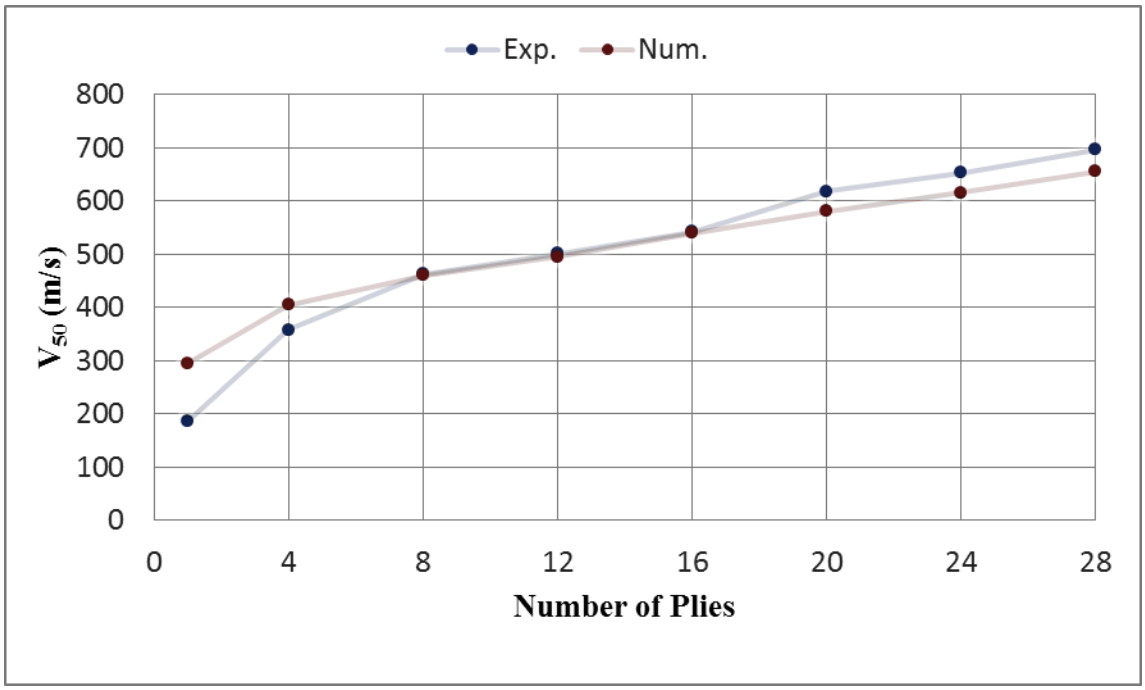

Figure 4-18: V_{50} of layered fabric [37]

4.3 Summary

A hybrid approach was developed to model ballistic fabric. The following goals were reached and these conclusions were made:

1. The hybrid area based mesh did not approach the uniform mesh results due to discontinuities along the principal yarns.
2. Hybrid yarn based mesh was introduced and described as a computer tool which can generate basic variable meshed cells to be assembled into variable density numerical fabric. This hybrid fabric shows promise of modeling standard tests with a much smaller memory foot print than uniform mesh.
3. Multiple layers of fabric can be independently modeled and variably stacked to create any weave of layered or 3D fabric.
4. Comparisons between uniform mesh showed that hybrid mesh with up to 14 yarns with a simulation of a 4 grain projectile impact produces almost identical ballistic simulation results.

For the first time standard tests are modeled with hybrid mesh and compared to experimental results. A high degree of agreement is observed for mid-range layer numbers and data separation is noted for low and high layered fabrics. The solutions for the data separation discrepancies are discussed in chapter 3.

Chapter 5 - Numerical simulation

The Hybrid model has been verified in previous chapters to produce the same impact results as the full density model. It is then used with confidence to model the full scale layered physical fabrics which is not possible with full mesh density DEA simulations. Discrepancies are noted between numerical and physical ballistic impact which is attributed to shear and moment in physical fabric which previously was not calculated numerically. In this chapter hybrid fabric is used in full scale numerical simulations with standard weight steel laboratory RCC shot which includes in addition to the 4 grain, the 16 grain projectile. The numerical simulations incorporate the modifications to the DEA calculations to include shear and moment to address the discrepancies noted in the previous chapter.

The yarns bending rigidity depends on the conditions which it is subjected to in the fabric. The DEA model has the extra complication of being modeled by digital fibers which are themselves representative of multiple physical fibers. The digital yarn being composed of the digital fibers in the simulation must be modeled to reflect the bending rigidity of actual yarn. In order to simulate the actual yarn the bending rigidity of the digital fiber must be developed to replace the physical bending rigidity of the real fibers which it represents as a single digital fiber. The two extreme situations for a digital fiber are first that the real fibers it represents do not touch and therefore do not interact having their own independent bending moment similar to no friction between fibers and the second is that these physical fibers are pressed tightly together and the digital fiber which represents these fibers acts as a single unit in bending similar to when a high friction coefficient prevents them from moving relative to each other. The first case is a yarn with higher strength where tensile failure is the main failure mechanism than the second

case where shear can play a large role and the bending rigidity is much higher with the digital fiber being more brittle. The actual case of the physical yarn is the case in between these two extremes where the friction coefficient is a factor between 1 and 0. The digital yarn's flexibility where the actual coefficient of friction is used would be dependent on the mesh density. If the mesh density is the same as the actual yarn then the actual moment of inertia would be identical whereas if the digital yarn has a density of one fiber per yarn then friction is not a factor or can be considered as high enough to prevent any movement between fibers. The solution would be therefore to select k values where the V_{50} is constant with the known coefficient of friction and with any mesh density. **Figure 5-1** shows a schematic of the cross-sectional depiction of the yarn over laid with the cross-section of the digital fibers. As can be seen in the simplified schematic each digital fiber contains multiple physical fibers and at 19 FPY the profile is possible. The actual DFMA profile is shown later in this chapter for a yarn in a digital fabric.

Digital Fiber Digital and Physical Fiber Physical Fiber

Figure 5-1: Digital and physical yarn cross-section

The intermediate case is where the digital fiber bending rigidity is influenced by fiber frictional forces where fibers may have relative movement within the digital fiber once they overcome inter fiber frictional force and this intermediate case is where the actual solution would lie. The equation for the development of the moment of inertia is given above as Equation (3.18). The relation between this moment of inertia and the k-values is given in **Figure 5-5**. With limited computer resources the equations k values are modified and simulations are run to determine where there is a convergence over a range of mesh density. The convergence determines the true digital fiber moment of inertia to represent the physical yarn.

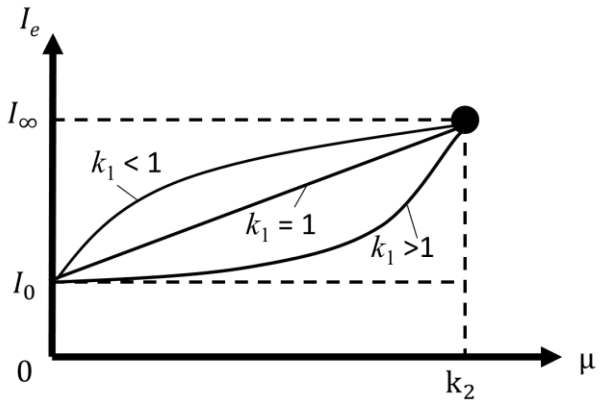

Figure 5-2: Friction related to moment of inertia

The first step in the process of developing an equation of moment of inertia for a digital fiber for a digital yarn would be the stand alone digital yarn. This allows the range of mesh density to approach the actual FPY without overusing available computer resources. As discussed before in previous chapters this standalone yarn is incapable of representing the yarn in a fabric so special conditions are placed on these simulations. This simulation is useful to develop the moment of inertia with the given resources by allowing up to actual number of physical fibers to be represented to validate a convergence solution for Equation (3.18). The goal is then to develop an effective bending rigidity solution to Equation (3.18) which represents the digital fiber accurately. The initial approach is to apply the simulation to a single yarn over a range of four fiber yarn up to a density close to actual fiber per yarn where the bending moment changes are insignificant over this mesh range with selected k values. The yarn under consideration is held flat without any undulations and without tension with the ends of the yarn connected to mass objects to represent the continuous yarn to the boundary. Without undulations this setup therefore does not represent and actual yarn within a fabric however this is not important to convergence simulations and these results will be further verified with scaled fabric. Considering the local bullet geometry discussed above the second condition applied to all fibers

would make the yarn a candidate for shearing action against this bullet edge and this would always be the case if the fibers do not spread out against bullet contact. In an independent yarn flattening happens, however in simulated yarn with boundaries, as if it were in a fabric, this spreading is limited as in real fabric. Another consideration in regards to cross-section is that the oval shape is not possible for single yarn and when impacted this shape is not held as it would be in fabric by crossing and parallel yarns. Again this is not too relevant when determining convergence as later fabric tests are planned for verification. The following models are created and convergence simulations are run to determine convergence (repeated to fix some discrepancies in previous research).

Table 5-1: Single yarn cross-sectional shapes (internal research at KSU)

		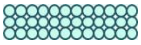				
4-d	16-d	36-d	64-d	100-d	144-d	196-d

d: digital fiber per yarn

So the individual yarn is bounded so that the yarn cannot spread and the simulation is conducted. The behavior of single yarns and yarns in fabrics are discussed in literature and the observed behavior is recorded. The methods here to represent the fabric are physical so the goal is to determine a representation of the moment of inertia of a digital fiber to represent a bundle of fibers. A similar situation discussed in bridge design. In modeling the introduction of shear pin stiffeners between the concrete bridge deck and the steel structural supports a concept of I_{eff} was introduced to give more accurate predictions to the flex of the semi composite bridge as discussed in Section 3.1.3.

The equations used for calculating the moment of inertia of the digital fiber involve the coefficient of friction. After running tests for convergence this equation was modified to obtain convergence and rewritten as Equations (3.18) and (3.19). For Kevlar KM2 the variables k are

assigned values: k_1 = 1.4 and k_2 = 1 as determined through simulating multiple mesh density fabric to determine convergence by modifying k1 and k2 in **Figure 5-3**.

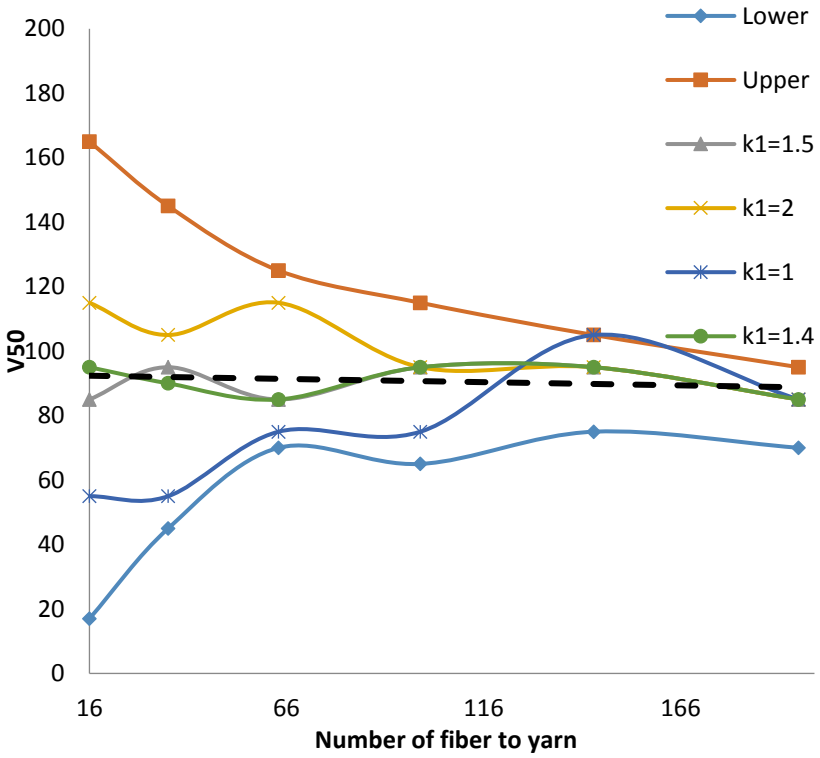

Figure 5-3: Single yarn test results

As mentioned above the yarns bending stiffness depends on the fiber interactions. With no fiber interactions the yarn bending stiffness becomes the sum result of the individual fiber moment of inertia, I_1 in Equation (3.19), while the other extreme is the fibers experience no relative movement with respect to each other and the digital fiber behaves as a continuum, I_2 in Equation (3.19) then the yarn stiffness becomes the sum of the digital fiber moment of inertia. I_1 and I_2 represent the upper and lower bounds of the moment of inertia.

Now that the k values are determined, a scaled model of the fabric is created and similar tests as the single yarn are run on this digital fabric to verify the results of the single yarn. These are both simulated with DFMA with a 4 grain RCC projectile with 95-µm local edge geometry in

impact against 4-inch fabric in multiple simulations with varying numbers of fibers per yarn (FPY). There are multiple mesh densities of the yarns as shown in **Figure 5-4**.

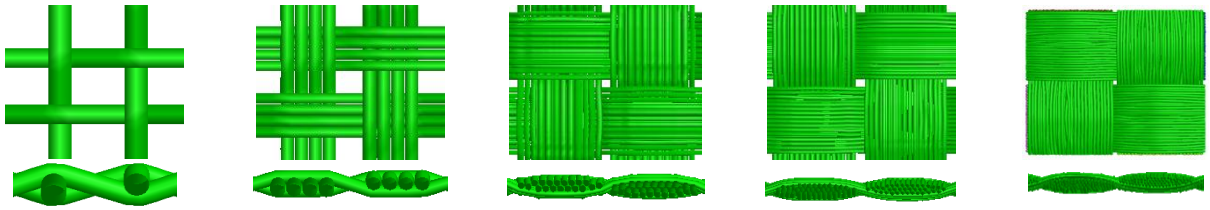

1-FYP 4-FYP 19-FYP 37-FYP 74-FYP

Figure 5-4: Close detail top and front view of the fabric

The above variable mesh densities are impacted with the 4 Gr RCC to determine the V_{50} ballistic strength. The previous standalone yarn allows mesh density approaching actual fiber per yarn however it has somewhat a limit that it is not subjected to actual boundary limitations of the actual fabric. **Table 5-2** lists the V_{50} strength of the fabric with changes in the k1 power factor in Equation (3.18). The upper and lower bounds show the fabric strength bounds between friction free fabric and the yarn continuum fabric while varying the power factors in between show the behavior of the fabric which is expected to be a constant V_{50} for some point which accurately represents the moment of the digital fiber for actual fiber simulation in a fabric. This data is displayed on a graph to visually show the data over a range of yarn fiber densities and give visual to determine the parameters where ballistic strength is constant with mesh density. When convergence occurs the values of k1 and k2 should represent an equation which represents effective digital fiber bending rigidity.

Table 5-2: Development of moment equation

K1	K2	Fiber/Yarn	1	4	12	19	24	30	37	74
							V_{50}			
Upper(μ→0)	1		0	305	305	265	265	255	255	215
Square(k1=2)	1		0	295	285	235	245	235	245	215
Linear(k1=1)	1		0	65	175	185	195	195	205	195
1.5	1		0	245	245	225	225	225	230	205
1.4	1		0	223	230	217	222	222	222	205
1.3	1		0	205	215	215	215	215	220	205
1.2	1		0	125	205	205	205	215	215	205

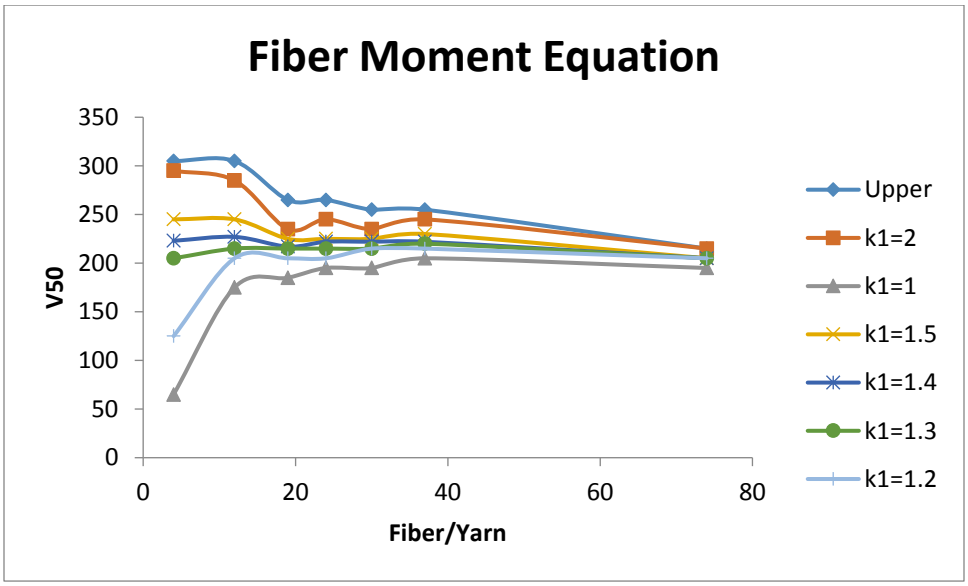

Figure 5-5: Effective digital fiber bending rigidity determination

From Table 5-2 and Figure 5-5 the k1 values that emerge as convergent are k=1.3, 1.4 since the value of V_{50} is fairly constant over the number of yarns. This verifies the values from the single yarn simulations.

Chapter 6 - Numerical results

There are two comparisons of numerical to experimental, the 4 grain and 16 grain projectiles impacting Kevlar KM2 fabric. These comparisons have been completed in Section 4.2.1. The same setup will be used and 1, 4, 8, in units of 4 up to 28 layers will be impacted. In this chapter the modified DFMA will incorporate shear and moment to answer the discrepancies from Section 4.2.1.

6.1 Numerical and experimental 4 grain projectile impact

The moment of inertia and shear are very sensitive to the cross-section interactions of the fibers within the yarn. The homogeneous yarn, which is the same as when no relative movement is allowed between the fibers, is weaker than the non-interacting fibers. These two extremes form the boundary between where the friction interacting yarn would reside.

Figure 6-1 shows a close up of the hybrid fabric with the 4 grain bullet used in the simulations where the mesh density is 19 FPY for the principal yarn. The coarser mesh density allows digital fiber movement while 19 FPY mesh density and above almost the same spacing between yarns to simulate real Kevlar fabric. On the top, front and isometric views in **Figure 6-1** the bullet is centered within the area of the fine mesh so all the impact interactions happen to the fine mesh yarns.

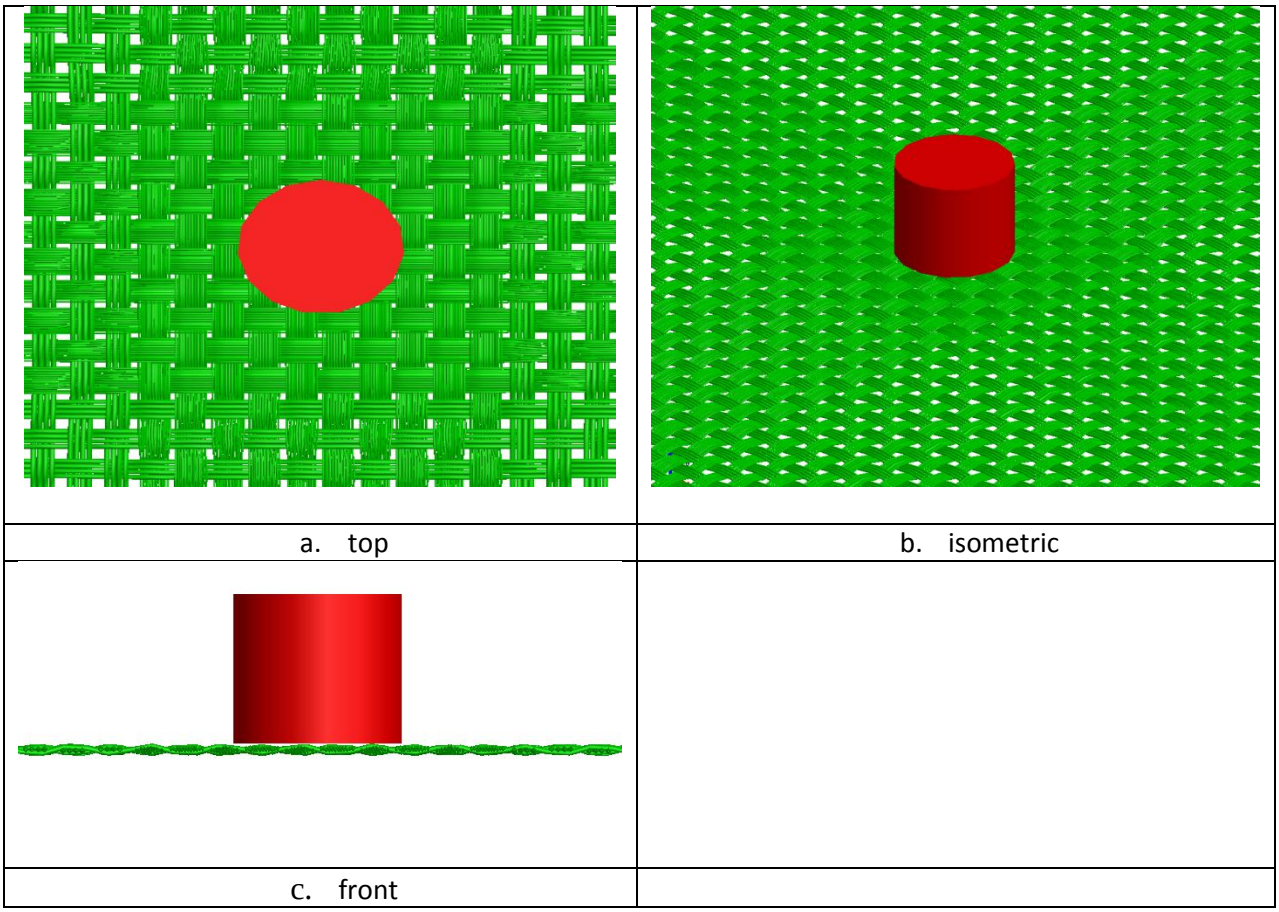

Figure 6-1: 4 grain bullet over lay on single layer hybrid fabric

This table is the data for the 4 grain RCC.

Table 6-1: Modified DFMA 4 grain projectile impact data

Number of Piles	Experimental	Numerical	Variance
1	186	205	-10.22%
4	357	465	-30.25%
8	463	495	-6.91%
12	501	530	-5.79%
16	542	565	-4.24%
20	618	605	2.10%
24	653	635	2.76%
28	696	665	4.45%

The following figure depicts the results from experimental and the numerical results fit to a trend line.

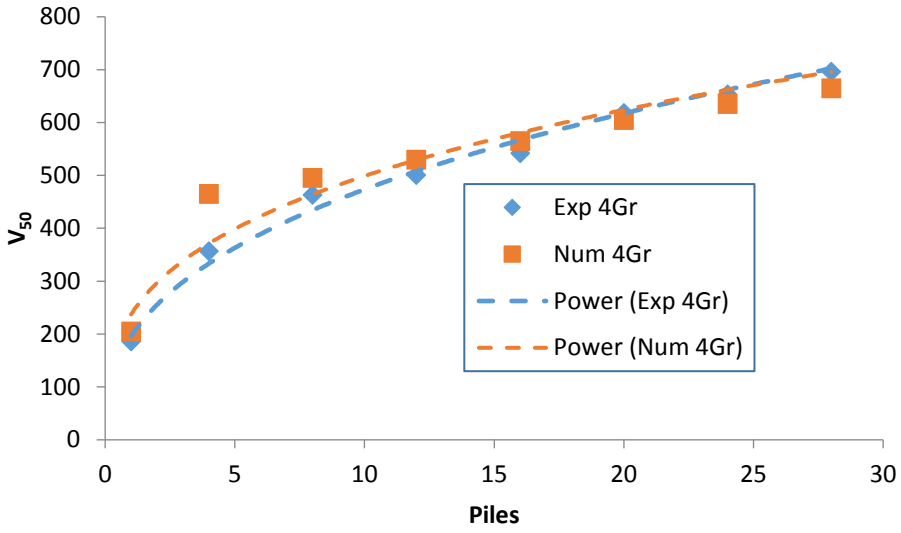

Figure 6-2: 4 grain projectile numerical vs experimental

The raw result data has some possible outliers one of which is that the 4 layer experimental results are lower than expected. There are a few reasons that this can be considered an outlier. The strongest reason is that experimental results show results that do not confirm that this is a normal data point with only the factors of shear moment and physical accuracy used in the numerical simulation. The experimental results for the 4 grain projectile impacting a 12-inch by 12-inch fabric shown in Figure 6-2 are lower than experimental results of a separate experimental ballistic test with a 4 grain projectile impacting a 4-inch by 4-inch fabric.

Table 6-2: V_{50} of square bounded fabric

4x4 size 4-pile fabric and 4 grain projectile V_{50}	12x12 size 4-pile fabric and 4 grain projectile
386 m/s	357 m/s

Table 6-2 shows that there are other factors in play. In Section 2.3 research shows that the smaller a fabric is the weaker it is as compared to a larger fabric when both are under the same conditions, with identical layering. In the case shown in Table 6-2 the smaller fabric is significantly stronger ballistically than the larger fabric which begs the question of the outlier as product of some unknown factor such as yarn spreading, projectile yaw, or some new factor not tested such as small projectile footprint and high concentrated stress could be influenced by air back pressure resisting immediate fabric movement allowing time for higher stress build up to failure under lower impact speeds. Two of these proposed factors have been tested to show a weaker ballistic strength in the tested fabric due to projectile slipping through yarns or the yaw that allows the edge to exert higher shear/wedging through the fabric.

It is of interest to note that the experimental results are performed with multiple shots into the same fabric. It is important to take into consideration that the fabric weave tightness influences strength. One of the reasons is that it prevents the yarns in the fabric from sliding from the bullet path rather than remaining under the projectile requiring breakage prior to bullet penetration and therefore resulting in much larger energy absorption. The experimental V_{50} is the obtained from statistical analysis 16 shots at the same fabric for each value of ballistic strength. For the particular set of data for these tests first shots taken were at speeds much higher than final V_{50} while the remaining shots were at or near V_{50}. For the one and four layer fabric the speeds are obviously lower. What this means is that the bullet is in contact longer than the higher layer fabrics where the speeds are much higher. This allows full development of the conical profile and more pulling of primary yarns and movement of the secondary yarns. The question that would be left is how this affects the fabric. Does it loosen the fabric separate the yarns and therefore allow the remaining shots to slip past some of the yarns?

The next reason is brought to light reviewing the 4 grain projectile and the 16 grain projectile V_{50} for 4 layer fabric. The 4 layer fabric is about the same ballistic strength for the 4-grain projectile as for the 16 grain projectile. For the rest of the layered shots the ballistic strength of the 4 grain projectile impact is much larger than the 16 grain impact. The argument for the three factors considered becomes stronger ie yaw effects would be canceled by more layers and yarn separation really cannot happen in the remaining layers of thicker fabrics and the density of the air becomes a very small factor of the fabric as layers are added as well as less deflection of thicker fabric. The yaw and yarn slippage are not give in the experimental data and the air effects are not simulated numerically so this is left open to further analysis.

In conclusion of these tests show in Figure 6-2, the trend lines added converge as the layers increase. The initial skewing of the 1-layer and 4-layer fabrics causes a little early separation of the trend lines.

Table 6-3: Original DFMA 4 grain projectile impact data

Number of plies	Experimental	Numerical	Variance
1	186	295	-58.60%
4	357	405	-13.45%
8	463	460	0.65%
12	501	495	1.20%
16	542	540	0.37%
20	618	580	6.15%
24	653	615	5.82%
28	696	655	5.89%

The problems noted in Section 4.2.1 are repeated here in **Table 6-3** with the variance added are greatly improved for layers 1 and for layers 20 through 28 while there is less but still good agreement between the middle layers. Layer 4 impact results need further analysis due to indications that the experimental 4 layer testing is an outlier. The methods of simulation are

different between experimental and the numerical in the case that the experimental is a statistical analysis of 16 shots at the same piece of fabric whereas the numerical is a single shot to the center of the fabric. The improvement of the consistency over the data range allows further experimentation into statistical analysis of multiple numerical shots over the fabric.

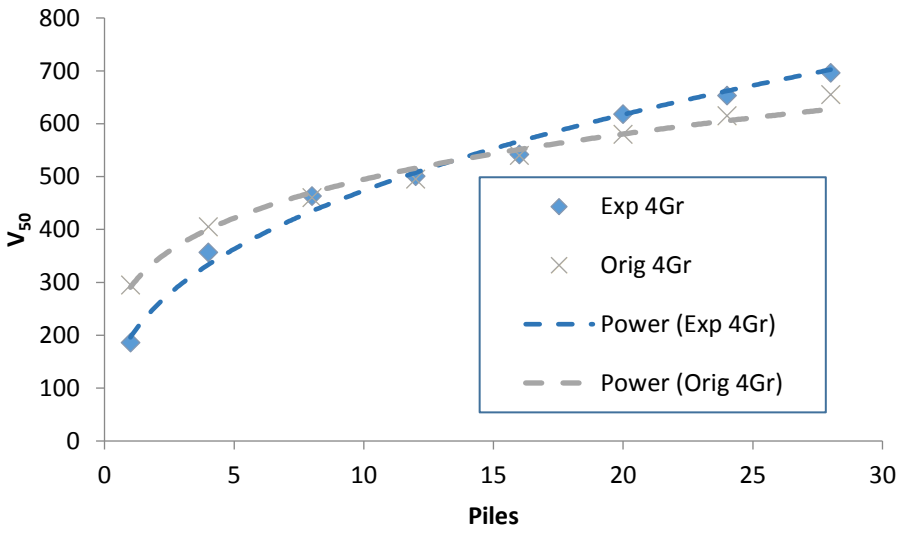

Figure 6-3: Original 4 grain impact data compared to experimental results

The improvement between old and new data is apparent when the modifications were made to DFMA numerical code. The trend line entitled Orig 4Gr and its corresponding data are taken from Section 4.2.1where the hybrid V_{50} data was generated and compared to experimental and this data is over laid on Figure 6-2. The original data is skewed at the lower layer and higher layer simulations as compared to the modified which is less skewed at the lower layer simulations and converges toward the higher layer simulations.

Adding the shear and moment and projectile geometry gives more consistent results of the entire range of layered ballistic impact. This is a positive step forward to now consider statistical analysis with multiple numerical shots to physically mimic the experimental tests. It should be considered that these shots, 16 in number per ballistic strength test, are not at the

center of the fabric. The consensus from research is that a smaller fabric is weaker and therefore extrapolating from that a shot taken closer to the boundary should be able to penetrate at a lower velocity. This also has to be taken into further consideration and tested with research to determine the actual outcomes.

6.2 Numerical and experimental 16 grain projectile impact

The 16 grain projectile impact is compared to experimental data. An over lay of the bullet on the fabric is given in **Figure 6-4**. The bullet contact is within the fine grain principal mesh yarns.

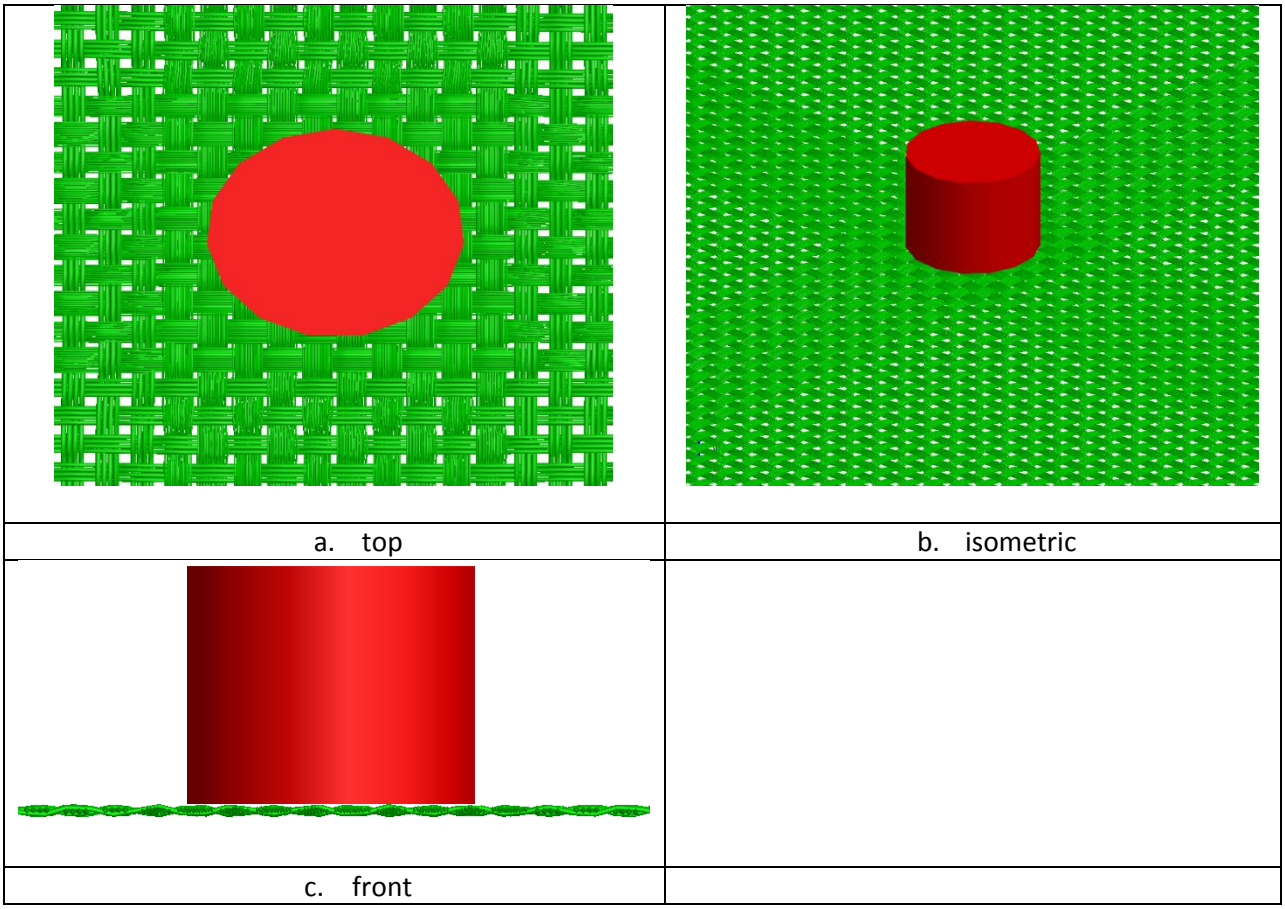

Figure 6-4: 16 grain bullet over lay on single layer hybrid fabric

As above the data is compared to the experimental results in Table 6-4 with variance percentage.

Table 6-4: 16 grain impact data

Number of Piles	Experimental	Numerical	Variance
1	197	185	6.09%
4	352	370	-5.11%
8	416	450	-8.17%
12	462	475	-2.81%
16	504	495	1.79%
20	552	525	4.89%
24	597	545	8.71%
28	628	565	10.03%

This data in the above table is presented in Figure 6-5 and trend lines are added to highlight the agreements between the trends of the data.

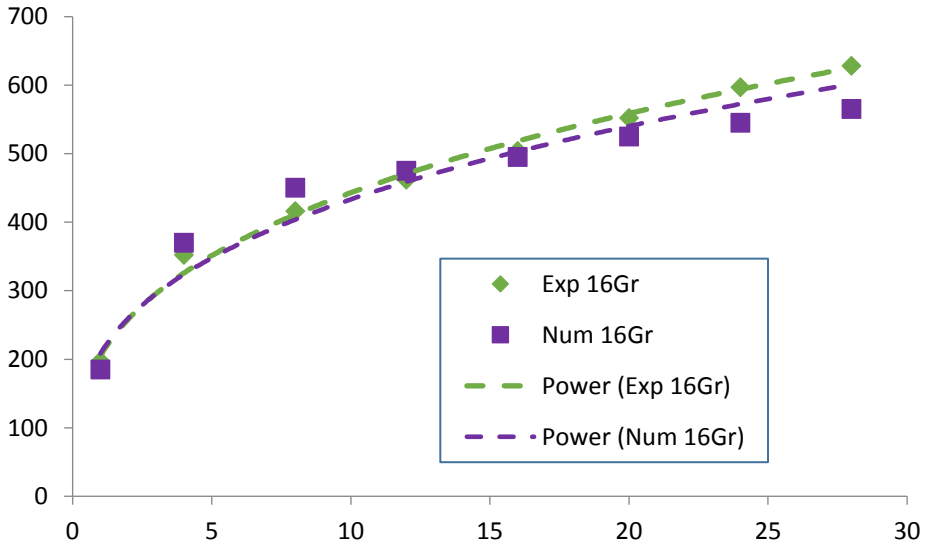

Figure 6-5: 16 grain projectile numerical vs experimental

The agreement is similar to the previous set of data for the 4 grain projectile the difference being the 4 layer has much better agreement and there is early convergence and late divergence. The modified DFMA results shown above show an improved agreement to the experimental from the original data. Numerical simulations were completed on the 16 grain projectile impact and the data and variance from experimental is presented.

Table 6-5: Original 16 grain impact data vs experimental

Number of Piles	Experimental	Numerical	Variance
1	197	128	35.03%
4	352	278	21.02%
8	416	375	9.86%
12	462	440	4.76%
16	504	471	6.55%
20	552	500	9.42%
24	597	529	11.39%
28	628		

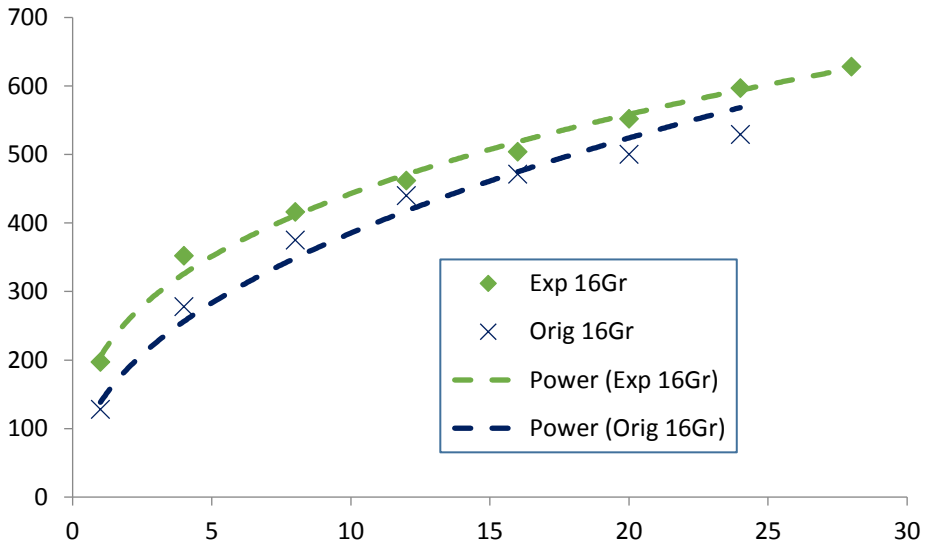

Figure 6-6: Original 16 grain impact data compared to experimental results

One of the outcomes from these additions of shear and moment modifications to DFMA is consistency between the impacts with different mass projectiles as well as reducing the variance between experimental and numerical. Both Figure 6-2 and Figure 6-5 show similar trends as related to the experimental whereas both Figure 6-3 and Figure 6-6 are not similar which demonstrates the physics was lacking to consistently simulate different mass projectiles. When comparing the latter two figures one shows higher numerical ballistic strength for lower layered fabric and lower ballistic strength for the higher layered (thicker) fabrics whereas the 16

grain impact shows consistently lower strength for the original impact strength. The former shows a somewhat consistent agreement, stronger with thinner fabrics and weaker with thicker fabrics, and variance percentages within the same ranges.

With these results it is more plausible to change the methodology of the numerical simulations. It is important to note that as discussed above that the experimental simulations involved 16 shots against one piece of fabric in order to get two clear fully penetrating shots and two lower rebound shots close to each other in order to determine V_{50}. The numerical simulations on the other hand are a single shot to the center of the fabric. While not all of the experimental shots are used in the determination of V_{50}, the rest of the shots are completed for the sake data verification and the development of the statistical analysis.

6.3 Conclusion

The objective of this research is to improve simulation of ballistic impact with a more physically accurate approach, a modified DFMA to include shear and moment, bullet local geometry as well as include defect incorporation into the digital fabrics. The bounds of this research are that the projectiles which have variable mass are only RCC and non-deformable. To develop the moment equations, single yarns are tested and the factors of the equations are determined by convergence of ballistics outcomes. These developed equation parameters are then tested in small scale layered fabrics. The following conclusions are reached:

1. Computer resources are not available to compute a physical model of a fabric. The DEA approach structurally models the physical fabric at a minimum mesh density reducing the need for computer resources. A hybrid mesh approach further reduces the fabric size with primary and non-primary yarn variable mesh density modeling. During high speed impact only contacting “primary” yarns the stress has a time to develop and therefore they bear 100% of the

ballistic loading. Hybrid fabric models the small number of primary yarns as finer mesh and the majority of the yarn, the non-primary yarn, is modeled as coarse mesh. Full scale layered fabrics are modeled and numerical impact can be completed.

2. Shear is an actual mechanism that will affect the ballistic strength due to the local projectile geometry. While this local projectile geometry is much larger than the individual fiber, and thus the fiber is not technically a candidate for projectile edge shear, the yarn itself is a candidate for shear and fiber interactions through friction are what control the moment of inertia of the yarn and thus the shear interactions with the projectile. The digital fiber moment of inertia is developed initially using a single yarn and is determined as $I_{digital\ fiber} = \mu^{1.4} I_1 + (1 - \mu^{1.4}) I_2$ then the equation is verified by simulating a small uniform fabric over a range of mesh densities. The solution for the variables of the equation are determined by convergence over a range of mesh densities which means that at any mesh density the digital yarn will physically model the actual yarn moment of inertia and produce accurate ballistic results.

3. The fibers have defects. The experimental method to determine the statistical defects affects over a specific gage length is to remove a fiber from a yarn in a fabric place it in a test apparatus then measure tensile strength. A standard ASTM single fiber tension test is designed and used to create a Weibull distribution of tensile strength over a range of fibers tested. The data is used to develop the equations using the Weibull statistical model which is $F(\sigma) = 1 - Exp\left(-\frac{l}{0.025} \times \left[\left(\frac{\sigma}{3.866e9}\right)^{10.6593} - \left(\frac{\sigma}{4.033e9}\right)^{10.6598}\right]\right)$ and then a random strength assignment is used to place defects in the numerical fiber under simulation.

4. The shear of the fiber is unknown and actual shear of a fiber at 12 μm is not easy to determine. The analytical method used here is to determine saturated strength ratio which is a

ratio of the tensile strength when shear strength is maximum to the tensile strength when shear strength is 0. When the strength ratio is equal to saturated strength ratio (0.384900179), the maximum shear strain $\gamma_u = 0.3836$ and using the shear modulus G = 2 GPa the shear strength $\tau_u = 0.3836*G = 0.7672$ GPa. This shear strength is determined experimentally by a tension twist test of a single fiber. The method is to determine the shear saturation where the fiber is twisted over increasing angles and pulled to failure. The data generated over the range of angles is modeled by a polynomial equation and the shear strength is solved from this equation.

5. The goal of this research is to modify DFMA to consistently model ballistic impact over a range of projectile masses and fabric sizes using variable mesh density physical size fabric with impact results in conformity with experimental data. When reasonable accuracy is reached that would make it possible to have a fabric design software for ballistic panels that has general modeling capabilities including the ability to model 3-d woven fabrics. A general modeling software is possible once the DEA model incorporates all the relevant physical aspects of woven fabric and incorporates all the influencing ballistic details of the experimental test.

References

[1] W. R. Novotny, A. Cepuš, A. Shahkarami, R. Vaziri and A. Poursartip, "Numerical investigation of the ballistic efficiency of multi-ply fabric armours during the early stages of impact," *International Journal of Impact Engineering*, vol. 34, no. 1, pp. 71-88, 2007.

[2] Y. Duan, M. Keefe, T. A. Bogetti and B. Powers, "Finite element modeling of transverse impact on a ballistic fabric," *International Journal of Mechanical Sciences*, vol. 48, no. 1, pp. 33-43, 2006.

[3] Y. Wang, M. Yuyang, D. Swenson and B. A. Cheesman, "Digital element approach for simulating impact and penetration of textiles," *International Journal of Impact Engineering*, vol. 37, no. 5, pp. 552-560, 2010.

[4] L. J. Huang, Y. Q. Wang, Y. Y. Miao, D. Swenson and C.-F. Yen, "Dynamic Relaxation Approach with Periodic Boundary Conditions in Determine the 3-D Woven Textile Micro-geometry," *Composite Structures*, vol. 106, pp. 417-425, 2013.

[5] M. Cheng, W. N. Chen and T. Weerasooriya, "Mechanical Properties of Kevlar KM2 Single Fiber," *Journal of Engineering Materials and Technology*, vol. 127, pp. 197-203, 2005.

[6] M. Cheng, W. N. Chen and T. Weerasooriya, "Experimental Investigation of the Transverse Mechanical Properties of a Single Kevlar KM2 Fiber," *International Journal of Solids and Structures*, vol. 41, no. 22-23, pp. 6215-6232, 2004.

[7] H. H. Yang, Kevlar Aramid Fiber, New York: Wiley, 1993.

[8] N. V. David, X. -L. Gao and J. Q. Zheng, "Ballistic Resistant Body Armor: Contemporary and Prospective Materials and Related Protection Mechanisms," *Applied Mechanics Reviews*, vol. 62, no. 5, p. 050802, 2009.

[9] D. Roylance, "Ballistisc of Transversely Impacted Fibers," *Textile Research Journal*, vol. 47, no. 10, pp. 679-684, 1977.

[10] J. C. Smith, C. A. Fenstermaker and P. J. Shouse, "Experimental Determination of Air Drag on a Textile Yarn Struck Transversely by a High-Velocity Projectile," *Journal of Research of the National Bureau of Standards*, vol. 68C, no. 3, pp. 177-181, 1964.

[11] S. Chocron, T. Kirchdoerfer, N. King and C. J. Freitas, "Modeling of Fabric Impact With High Speed Imaging and Nickel-Chromium Wires Validation," *Journal of Applied Mechanics*, vol. 78, no. 5, p. 051007, 2011.

[12] S. Chocron, T. Kirchdoerfer, N. King and C. Freitas, "Modeling of Fabric Impact with High-Speed Imaging and Nickel-Chromium Wires Validation," in *26th International Symposium on BALLISTICS*, Miami, FL, 2011.

[13] D. Roylance, A. Wilde and G. Tocci, "Ballistic Impact of Textile Structures," *Textile Research Journal,* vol. 43, no. 1, pp. 34-41, 1973.

[14] D. Roylance and S.-S. Wang, "Influence of Fibre Properties on Ballistic Penetration of Textile Panels," *Fibre Science and Technology,* vol. 14, pp. 183-190, 1981.

[15] P. M. Cunniff, "An Analysis of the System Effects in Woven Fabrics under Ballistic Impact," *Textile Research Journal,* vol. 62, no. 9, pp. 495-509, 1992.

[16] V. P. W. Shim, V. B. C. Tan and T. E. Tay, "Modelling deformation and damage characteristics of woven fabric under small projectile impact," *International Journal of Impact Engineering,* vol. 16, no. 4, pp. 585-605, 1995.

[17] R. Dent and J. G. Donovan, "Projectile Impact with Flexible Armor-Model with Crimp Interchange," U.S. Army Natick Research, Development and Engineering Center, Natick, MA, technical report NATICK/TR-88/080L, 1988.

[18] D. C. Prevorsek, Y. D. Kwon, G. A. Harpell and H. L. Li, "Spectra® Composite Armor: Dynamics of Absorbing the Kinetic Energy of Ballistic Projectiles.," in *34th International SAMPE Symposium, pp.1780-1789*, Reno, Nevada, 1989.

[19] D. Roylance, P. Chammua, J. Ting, H. Chi and B. Scott, "Numerical Modeling of Fabric Impact," in *Proceedings of the National Meeting of the American Society of Mechanical Engineers (ASME)*, San Francisco, 1995.

[20] Ting, Carina, J. Ting, P. Cunniff and D. Roylance, "Numerical Characterization of the Effects of Transverse Yarn Interaction on Textile Ballistic Response," in *30th International SAMPE Technical Conference 57-67*, San Antonio, 1998.

[21] D. A. Shockey, J. H. Giovanola, J. W. Simons, D. C. Erlich, R. W. Klopp and S. R. Skaggs, "Advanced Armor Technology: Application Potential for Engine Fragment Barriers for Commercial Aircraft," U.S. Department of Transport and Federal Aviation Administration Report, 1997.

[22] Y. Duan, M. Keefe, T. A. Bogetti and B. A. Cheeseman, "Modeling Friction Effects on the Ballistic Impact Behavior of a Single-ply High-strength Fabric," *International Journal of Impact Engineering,* vol. 31, no. 8, pp. 996-1012, 2005.

[23] Y. Duan, M. Keefe, T. A. Bogetti, B. A. Cheeseman and B. Powers, "A numerical investigation of the influence of friction on energy absorption by a high-strength fabric subjected to ballistic impact," *International Journal of Impact Engineering,*

vol. 32, no. 8, pp. 1299-1312, 2006.

[24] M. . G. Northolt and J. J. van Aartsen, "On the crystal and molecular structure of poly-(p-phenylene terephthalamide)," *Journal of Polymer Science,* vol. 11, no. 5, pp. 333-337, 1973.

[25] M. G. Northolt, "X-ray diffraction study of poly(p-phenylene terephthalamide) fibres," *European Polymer Journal,* vol. 10, no. 9, pp. 799-804, 1974.

[26] K. Tashiro, M. Kobayashi and H. Tadokoro, "Elastic moduli," *Elastic Moduli and Molecular Structures of Several Crystalline Polymers, Including Aromatic Polyamides,* vol. 10, no. 2, pp. 413-420, 1977.

[27] J. Kim, W. G. McDonough, W. Blair and G. A. Holmes, "The modified-single fiber test: A methodology for monitoring ballistic performance," *Applied Polymer Science,* vol. 108, no. 2, pp. 876-886, 2008.

[28] K. Krishnan, S. Sockalingam, S. Bansal and S. D. Rajan, "Numerical simulation of ceramic composite armor subjected to ballistic impact," *Composites Part B: Engineering,* vol. 41, no. 8, pp. 583-593, 2010.

[29] B. Song and W. Lu, "Effect of twist on transverse impact response of ballistic fiber yarns," *International Journal of Impact Engineering,* vol. 85, pp. 1-4, 2015.

[30] B. D. Sanborn and T. T. Weerasooriya, "Effect of Strain Rates and Pre-Twist on Tensile Strength of Kevlar KM2 Single Fiber," Army Research Laboratory, Aberdeen Proving Ground, 2013.

[31] Y. Q. Wang and X. Sun, "Determining the Geometry of Textile Performs Using Finite Element Analysis," in *Proceedings of the American Society for Composites, 15th ASC Technical Conference on Composite MaterialsMaterials, Vol 9, September 24-27*, College Station, TX, 2000.

[32] X. Sun and Y. Q. Wang, "Geometry of 3-D Braiding Rectangular Perform with Axial Yarns," in *Proceedings of the 46th International SAMPE Symposium, Vol 46, p 2455-2464*, Long Beach Convention Center, CA, 2001.

[33] Y. Q. Wang and X. Sun, "Digital Element Simulation of Textile Process," *Journal of Composite Science and Technology,* vol. 63, pp. 311-319, 2001.

[34] L. Huang, "Determining Micro- and Macro-Geometry of Fabric and Fabric Reinforced Composites," Kansas State University, Manhattan, 2013.

[35] N. I. o. Justice, *Selection and Application Guide to Ballistic-Resistant Body Armor for Law Enforcement, Corrections and Public Safety,* Washington, DC: U.S. Department of

Justice, 2014.

[36] H. Talebi, S. V. Wong and A. M. S. Hamouda, "Finite element evaluation of projectile nose angle effects in ballistic perforation of high strength fabric," *Composite Structures,* vol. 87, no. 4, pp. 314-320, 2009.

[37] M. M. Dippolito, Y. Wang, Y. Ma, C.-F. Yen, J. Zheng and V. Halls, "Real Scale Simulation of Ballistic Tests for Multi-Layer Fabric Body Armors," in *ASME 2014 International Mechanical Engineering Congress and Exposition*, Montreal, 2014.

[38] T. I. Zohdi and D. Powel, "Multiscale construction and large-scale simulation of structural fabric undergoing ballistic impact," *Computer Methods in Applied Mechanics and Engineering,* vol. 195, no. 1-3, pp. 94-109, 2006.

[39] M. Grujicic, A. Hariharan, B. Pandurangan, C.-F. Yen, B. A. Cheeseman, Y. Q. Wang, Y. Y. Maio and J. Q. Zheng, "Fiber-Level Modeling of Dynamic Strength of Kevlar® KM2 Ballistic Fabric," *Journal of Materials Engineering and Performance,* vol. 21, no. 7, pp. 1107-1119, 2012.

[40] F. Figucia, "Energy Absorption of Kevlar Fabrics Under Ballistic Impact," U. S. Army Natick Research & Development Command, Natick, Massachusetts, 1980.

[41] G. Zhou, X. Sun and Y. Q. Wang, "Multi-chain digital element analysis in textile mechanics," *Journal of Composite Science and Technology,* vol. 64, no. 2, pp. 239-244, 2004.

[42] Y. Y. Miao, E. Zhou, Y. Q. Wang and B. A. Cheeseman, "Mechanics of Textile Composites: Micro-Geometry," *Journal of Composite Science and Technology,* vol. 68, no. 7-8, pp. 1671-1678, 2008.

[43] Y. Y. Miao, Y. Q. Wang, J. Yu, C.-F. Yen, D. Swenson and B. A. Cheeseman, "Energy Loss Due to Transverse Plastic Deformation of Fibers in Textile Fabric Impact Process," in *Technical Conference of the American Society for Composites; the 2nd Joint US-Canada Conference on Composites*, Red Hook, NY, 2011.

[44] K. Goda and H. Fukunaga, "The evaluation of the strength distribution of silicon carbide and," *Journal of Material Science,* vol. 21, pp. 4475-4480, 1986.

[45] Leica Microsystems, "Leica Microsystems," Leica Microsystems, 2011. [Online]. Available: www.leica-microsystems.com. [Accessed 1 June 2016].

[46] J. Nie and C. S. Cai, "Steel-Concrete Composite Beams Considering Shear Slip Effects," *Journal of Structural Engineering,* vol. 129, no. 4, pp. 495-506, 2003.

[47] A. I. o. S. Construction, *AISC-ASD89 Design of Compression Member,* Chicago, IL: American Institute of Steel Construction, 1989.

[48] A. L. Chang and B. A. Bodt, "JTCG/AS Interlaboratory Ballistic Test Program: Final Report," Army Research Laboratory, Aberdeen Proving Ground, 1997.

[49] U. S. D. o. Defense, *MIL-DTL-44050B, Detailed Specification Cloth, Ballistic, Aramid,* Washington DC: U. S. Department of Defense, 2008.

[50] M. G. Kendall and A. Stuart, The Advanced Theory of Statistics 2, New York: Hafner Publishing Company, 1967.

[51] B. Neyer, "A D-optimality based sensitivity test," *Technometrics,* vol. 36, no. 1, pp. 61-70, 1994.